Exploring the 49-kDa Subunit as Part of the Catalytic Core of Complex I (NADH:Ubiquinone Oxidoreductase) from *Yarrowia lipolytica*

Dissertation
zur Erlangung des Doktorgrades
der Naturwissenschaften

vorgelegt beim Fachbereich Biochemie

der Johann Wolfgang Goethe Universität

in Frankfurt am Main

von

Ljuban Grgić

aus Osijek, Kroatien

Frankfurt am Main 2004

(DF1)

vom Fachbereich Biochemie, Pharmazie, Lebensmittelchemie der

Johann Wolfgang Goethe Universität als Dissertation angenommen.

Dekan :   Prof. Schwalbe

Gutachter: Prof. Ludwig

                    Prof. Brandt

Datum der Disputation: 15. Juli 2004

Table of Contents:

1 INTRODUCTION

1.1 Mitochondrial Respiratory Chain

The metabolic degradation of nutrients, e.g., glucose or fat, enables the formation of strong reducing agents like NADH and $FADH_2$ from which the respiratory chain transfers electrons through a redox potential span of about 1.1 V to O_2. The free energy of this electron transfer is used for vectorial proton translocation across the inner mitochondrial membrane into the intermembrane space. ATP-synthase uses this proton gradient for the synthesis of ATP which serves as universal energy supplier in cellular metabolism. The fundamental principle of this energy conversion was proposed by Peter Mitchell and is known as the chemiosmotic hypothesis (Mitchell, 1961).

The mitochondrial respiratory chain is an assembly of approximately 20 discrete electron carriers of which not all function independently in the membrane. The only mobile electron carriers are ubiquinone in the mitochondrial inner membrane and cytochrome *c* in the intermembrane space. When treated with certain detergents in low concentrations the mitochondrial respiratory chain can be fractionated into four multi-polypeptide complexes named complexes I-IV. Three of these complexes (I, III and IV) act as redox-driven proton pumps. There are now detailed crystal structures available for three of these complexes (complex II (Yankovskaya *et al.,* 2003), complex III (Hunte *et al.,* 2000; Iwata *et al.,* 1998), complex IV (Iwata *et al.,* 1995; Ostermeier *et al.,* 1997)); only for complex I there is no high resolution structure available. As recently shown in bovine and *Saccaromyces cerevisiae* mitochondria (Schägger and Pfeiffer, 2000) these complexes do not diffuse randomly in the mitochondrial membrane; instead they are probably part of supra-molecular assemblies (supercomplexes) with defined stoichiometries that can be called '*respirasomes*'.

The mitochondrial respiratory chain is not only the major site for production of ATP. Recently it was recognised that it plays an important role in apoptosis (Green and Reed, 1998; Kroemer and Reed, 2000; Wang *et al.,* 2001) which involves the release

1

of several proapoptotic regulators including cytochrome *c* (Du *et al.,* 2000). Defects of mitochondrial metabolism are associated with a wide spectrum of disease. Significant part of this spectrum is caused by mutations in the mitochondrial DNA (*mt*DNA).

1.2 Mitochondrial Complex I

Mitochondrial complex I is the first component of the respiratory chain coupling electron transfer from NADH to ubiquinone to proton translocation across the inner mitochondrial membrane. Low resolution electron microscopic 2D and 3D analysis of complex I from various sources (*Y. lipolytica,* Djafarzadeh *et al.,* 2000; *N. crassa,* Guenebaut *et al.,* 1997; *E. coli,* Guenebaut *et al.,* 1998; *Bos taurus* heart, Grigorieff, 1998) have yielded L-shaped structures consisting of a membrane arm and peripheral arm extending to the mitochondrial matrix. A so called 'horse shoe' conformation of *E. coli* complex I was also described under conditions of zero ionic strength (Böttcher *et al.,* 2002). However, this alternate shape could not be reproduced by another group under the same conditions working with the same organism (Sazanov, 2002). Therefore, the relevance of this extraordinary structure is still a matter of debate.

Enzymes from fungi and mammals are very similar in terms of protein and prosthetic group composition, structure and function. Complex I contains a high number of polypeptide subunits of dual genetic origin. In prokaryotes, complex I is formed with a minimal set of 14 subunits, while in eukaryotes the number of subunits is increased significantly by accessory subunits. Mitochondrial complex I from mammals is composed of 46 subunits (Carroll *et al.,* 2003; Skehel *et al.,* 1998), from plants and fungi of at least 35 subunits (Weiss *et al.,* 1991; Djafarzadeh *et al.,* 2000). In eukaryotes, seven of the 14 (so called 'central') subunits which are also present in prokaryotes are nuclear coded and bear all known redox prosthetic groups. The remaining seven ND subunits are highly hydrophobic proteins encoded by the mitochondrial genome in eukaryotes. The function of the remaining accessory subunits is largely unknown.

Dissociation of complex I into fragments has been observed with purified complex I. In *E. coli* a subcomplex containing the 75-, 51- and 24-kDa subunit can be generated (Leif *et al.,* 1995). When bovine complex I is treated with chaotropes it releases a so called 'flavoprotein' (FP) (Galante and Hatefi, 1979). FP contains the 51-, 24- and 10-kDa subunits. This fragment is the electron input domain of the enzyme and transfers electrons from NADH to artificial acceptors like hexa-ammine-ruthenium or ferricyanide (Gavrikova *et al.,* 1995). Complex I subcomplexes are also generated by sucrose gradient centrifugation (Finel *et al.,* 1994) and by ion exchange chromatography in the presence of non-denaturating detergents (Finel *et al.,* 1992; Sazanov *et al.,* 2000).

Complex I subunit			Coding[a]	Prosthetic groups	Subcomplex	
Bovine	*Y. lipolytica*	*E. coli*			*E. coli*	bovine
75-kDa	NUAM	NuoG	nuclear	N1b, N1c, N4, N5	DF	Iα
51-kDa	NUBM	NuoF	nuclear	FMN, N3	DF	Iα
49-kDa	NUCM	NuoD[b]	nuclear	-	CF	Iα
30-kDa	NUGM	NuoC[b]	nuclear	-	CF	Iα
24-kDa	NUHM	NuoE	nuclear	N1a	DF	Iα
TYKY	NUIM	NuoI	nuclear	N6a, N6b	CF	Iα
PSST	NUKM	NuoB	nuclear	N2	CF	Iα
ND1	ND1	NuoH	mtDNA	-	MF	Iγ
ND2	ND2	NuoN	mtDNA	-	MF	Iγ
ND3	ND3	NuoA	mtDNA	-	MF	Iγ
ND4	ND4	NuoM	mtDNA	-	MF	Iβ
ND5	ND5	NuoK	mtDNA	-	MF	Iβ
ND6	ND6	NuoL	mtDNA	-	MF	Iγ
ND4L	ND4L	NuoJ	mtDNA	-	MF	Iγ

Table 1.1 Central subunits of complex I and its subcomplexes

Abbrevations: DF, dehydrogenase fragment; CF, connecting fragment; MF, membrane fragment; FP, flavoprotein
[a]Coding for complex I in eukaryotes
[b]In *E. coli* both subunits are fused (NuoCD)

As shown in Table 1.1, bovine complex I is fragmented into subcomplexes Iα, Iβ and Iγ. Subcomplex Iα contains about 23 mostly hydrophilic subunits, that probably

represent the peripheral arm of complex I, and also bears all the redox centres of the enzyme (Finel *et al.,* 1994). Iα shows NADH:ferrycyanide oxidoreductase activity as well as NADH:Q_1 oxidoreductase activity. However, the observed NADH:Q_1 oxidoreductase activity cannot be inhibited with the typical complex I inhibitor rotenone. Subcomplex Iβ contains about 13 mainly hydrophobic subunits and is derived from the membrane arm of complex I. It has neither known prosthetic groups nor biochemical activity. Two mitochondrially coded subunits, ND4 and ND5, are part of subcomplex Iβ. Subcomplex Iγ contains 5 subunits, from which four are the hydrophobic mitochondrially coded subunits, namely ND1, ND2, ND3, ND4L and one nuclear coded subunit KFYI. Two more hydrophilic subunits, 42- and 39-kDa, might be loosely associated with other proteins in the Iγ fraction. The 39- and 15-kDa subunits are found both in the Iα and in the Iγ fragment (Finel *et al.,* 1992). Size-exclusion chromatography showed that fragment Iα can be altered into the smaller subcomplex Iλ (Sazanov *et al.,* 2000). The Iβ subcomplex dissociates further into two parts, namely IβL and IβS. IβL contains as major subunits ND4 and ND5, whereas IβS contains the rest of the Iβ fraction.

Complex I comprises a number of redox active cofactors (Table 1.1). A non-covalently bound FMN is involved in the oxidation of NADH. Up to nine iron-sulphur clusters transfer electrons through the protein to the ubiquinone reducing catalytic core. Only six iron-sulphur clusters are visible in EPR spectra of bovine heart complex I. On the basis of the terminology introduced by Ohnishi's group, N1a and N1b are binuclear clusters and N2, N3, N4, and N5 are tetranuclear clusters. Complex I of certain bacteria contains an additional tetranuclear cluster (designated N1c). Clusters N1a and N1b are located in the 24-kDa and 75-kDa subunits, respectively. Cluster N3 is located in the 51-kDa subunit. Clusters N4, N5, N1b and N1c are present in the 75-kDa subunit. The EPR silent clusters N6a and N6b (2[4Fe-4S]) are coordinated by the TYKY subunit. Despite all the evidences for a prominent function of cluster N2 (see 1.2.2) its assignment to a specific complex I subunit and its ligation are a matter of controversial discussion. Albracht and colleagues still consider the TYKY subunit as the most likely candidate for harbouring cluster N2 (Albracht and Hedderich, 2000). New evidence suggests that cluster N2 resides in the PSST subunit (Rasmussen *et al.,* 2001; Duarte *et al.,* 2002; Ahlers *et al.,* 2000b) at the interface to the 49-kDa subunit (Kashani-Poor *et al.,* 2001b).

Although the peripheral arm of complex I bears all known prosthetic groups, FMN and [FeS] clusters, this part alone is unable to reduce quinones or quinone analogous substrates with the exception of reduction of Q1 by bovine subcomplex Iα. Therefore, it was assumed for a long time that the quinone reduction site is localised in the membrane arm. A point mutation in the ND1 subunit of *Paracocus denitrificans* that showed a higher K_M- value for Q_1 (Zickermann *et al.,* 1998) was considered as a hint that this subunit bears the quinone reduction site. So called 'Fisher-Rich' quinone binding motifs were found in the ND4 and ND5 subunits (Rich and Fisher 1999). These two findings supported the idea that the quinone reduction site is in the membrane arm.

The discovery of a mutation in 49-kDa subunit of *Rh. capsulatus* that leads to inhibitor resistance (Darrouzet *et al.,* 1998) and the observation that the PSST subunit is labelled covalently with a photoreactive derivative of the quinone analogous inhibitor pyridaben (Schuler *et al.,* 1999), led to the conclusion that the interface between the 49-kDa and PSST subunits is part of the catalytic core of complex I. Brandt and co-workers have found in inhibitor-competition experiments that bovine heart complex I has only one binding domain for numerous structurally different inhibitors (Okun *et al.,* 1999). Mutants in the 49-kDa subunit that show either complex I inhibitor resistance or lower complex I activity also support the hypothesis that catalytic core resides at the interface between the 49-kDa and PSST subunits (Dupuis *et al.,* 1998; Kashani-Poor *et al.,* 2001b).

It is natural to assume that the active site of complex I should be placed in a hydrophobic environment. As a part of the active site the 49-kDa subunit was assumed to reside in or very close to the connecting part of complex I between membrane and peripheral arm. Recently, Zickermann *et al.* (2003) have labelled 49-kDa subunit of complex I from the yeast *Y. lipolytica* with monoclonal antibodies and 2D-structure analysis by electron microscopy revealed that the 49-kDa subunit is located at the tip of the peripheral arm, significantly distant from the membrane part (Figure 1.1).
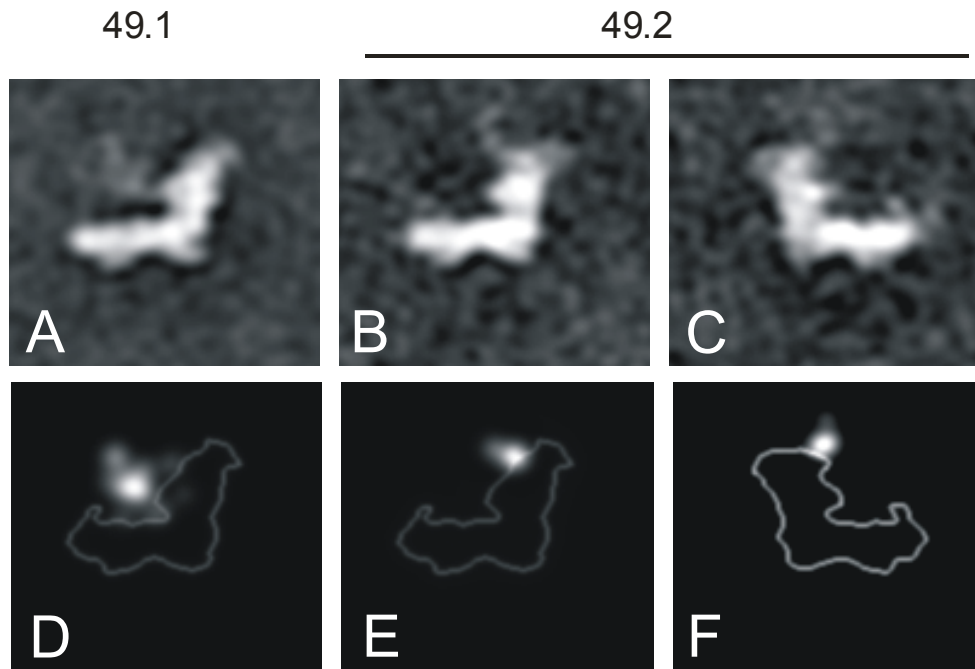
Figure 1.1 Two-dimensional averages of single particles decorated with antibodies[1]

A) Average of 60 complex I particles decorated with antibody 49.1 in flip view. B) and C) average of 60 complex I particles decorated with antibody 49.2 in flip(B) and flop (C) view. D), E) and F) Student's *t* test of the averages shown in *panels* A-C. Light areas indicate a statistical difference between labelled and unlabelled particles (confidence level >95%). The contour lines of the unlabelled averages (not shown here) were superimposed over the Student's *t* test images.

---

[1] From Zickermann *et al.*, *J. Biol. Chem.*, (2003), **278,** 29072-29078.

1.2.1 Evolutionary Origin of Complex I

Complex I is built from three different structural modules namely the NADH dehydrogenase module that represents the electron input site located in the peripheral arm, the proton pump module that is still largely unknown but is probably located in the membrane arm and the quinone reduction module (catalytic core) proposed to reside at the interface between the PSST and 49-kDa subunits. The proposal that during evolution complex I was formed from these pre-existing structural modules was very useful for structural modelling especially in the case of the homology of several subunits of complex I to hydrogenases (Friedrich and Scheide, 2000; Finel, 1998). The different homologies are summarised in Table 1.2.

The electron input domain of complex I is related to the NAD^+ reducing hydrogenase from *Alcaligenes eutrophus* (Pilkington *et al.,* 1991). The 24-kDa and 51-kDa subunits are homologous to HoxF and the first 200 residues of the 75-kDa subunit are homologous to HoxU. HoxF and HoxU together form the NADH oxidoreductase part of this hydrogenase.

Membrane bound type-3 hydrogenases, for example those that are encoded by the *hyc* operon in *E. coli* or the *ech* operon in *Methanosercina barkeri* show not only homologies to the 49-kDa and PSST but also to the 30-kDa, TYKY and ND1 subunits. The complex I subunits ND2, ND4 and ND5 show weak homology to each other and also to Na^+/H^+ antiporters of the type encoded by the *mrp* operon in *Bacillus subtilis* and the corresponding *mnh* operon in *Staphylococcus aureus* (Mathiesen and Hägerhäll, 2002; Steuber, 2001).

The type-4 hydrogenase in *E. coli* that is encoded by the *hyf* operon contains the same homologues to complex I genes already found in type-3 hydrogenase (Andrews *et al.,* 1997). Additionally it also contains genes for two more proteins of the Na^+/H^+ or K^+/H^+ antiporter family type that are homologous to ND2, ND4 and ND5.

The 49-kDa and PSST subunits are homologous to the large and small subunits of water soluble [NiFe] hydrogenases. The homology between the large subunit of water soluble [NiFe] hydrogenases and the 49-kDa subunit of complex I is too poor to unambiguously align the sequences. However, the corresponding subunit from the

membrane-bound Ech [NiFe] hydrogenase from *Methanosarcina barkeri* exhibits significantly higher homology to the complex I 49-kDa subunit than to the large subunit of its water soluble counterpart (Künkel *et al.,* 1998).

```
           120                                  456
 Y.l. 49-kDa  HRGTEKLIEYKTYMQALPYFDRLDYVSMMTN    TMDLVFGEVDR
 M.b. EchE    HRGLETFINTKDFNQTTYVCERICGICSAHL    TIDPCVSCTER
 D.f. LS      FRGLEIILKGRDPRDAQHFTQRACGVCTYVH    AFDPCIACGVH
           49                                  539
```

Figure 1.2 Partial alignment of sequences of the [NiFe] containing subunit of hydrogenases and the 49-kDa subunit of complex I.

Y.l. 49-kDa = *Y. lipolytica* complex I, 49-kDa subunit; *M.b.* EchE = *Methanosarcina barkeri* hydrogenase, EchE subunit; D. f. LS = *Desulfovibrio fructosovorans* hydrogenase, large subunit. In yellow: [NiFe] ligating cysteins replaced by in red highly conserved residues in complex I.

This allowed a reliable alignment of the regions around the [NiFe]-ligating cysteines that are arranged in two pairs located near the N-terminus and the C-terminus. Interestingly, the inhibitor resistance mutation V407M in the 49-kDa subunit of *Rh. capsulatus* corresponds to one of the cysteine residues that ligate the [NiFe] site in water soluble [NiFe] hydrogenases (Darrouzet *et al.,* 1998).

To test this hypothesis site directed mutagenesis of residues in the 49-kDa subunit of complex I from *Y. lipolytica* was undertaken. Highly conserved residues D143, V460 and E463 (shown in red in the alignment in Figure 1.2) that correspond to the cysteine ligands of the [NiFe] site in [NiFe] hydrogenases were mutated into asparagine, alanine and glutamine, respectively. Mutations D143N, V460A and E463Q resulted in strong reduction or complete loss of catalytic activity. Mutant D458A had a dramatically increased I_{50} value for DQA and rotenone (Kashani-Poor *et al.,* 2001b). These findings strongly suggest that domains around the hydrogen active [NiFe] site of hydrogenases have been conserved and play a crucial role in the catalytic process of complex I. They also strongly support the hypothesis that the quinone reduction site of complex I has evolved from the hydrogen active [NiFe] site

of [NiFe] hydrogenases. In our group a structural model based on the known crystal structure of the water soluble [NiFe] hydrogenase from *D. gigas* (Volbeda *et al.,* 1995) was constructed (Kashani-Poor *et al.,* 2001b). Residues from the large subunit from this water soluble [NiFe] hydrogenase were simply replaced with the corresponding residues of the 49-kDa subunit (Figure 1.2). From this structural model it could be derived that the catalytic core of complex I resides at the interface between the PSST and the 49-kDa subunits.

Complex I subunit	Homologous subunits in related enzymes				
	NAD$^+$ reducing hydrogenase *A. eutrophus*	Water soluble [NiFe] hydrogenase e.g. *D. fructosovorans*	Membrane bound type-3 hydrogenase (*FHL-1*) *E. coli* (Ech) *M. brakeri*	Membrane bound type-4 hydrogenase (*FHL-2*) *E. coli*	Antiporter e.g. *B. subtillis*
75-kDa	HoxU	-	-	-	-
51-kDa	HoxF	-	-	-	-
49-kDa	-	large subunit	EchE/HycE	HyfG	-
30-kDa	-	-	EchD/HycE	HyfG	-
24-kDa	HoxF	-	-	-	-
TYKY	-	-	EchF/HycF	HyfH	-
PSST	-	small subunit	EchC/HycG	HyfI	-
ND1	-	-	EchB/HycD	HyfC	-
ND2	-	-	EchA[a]/HycC[a]	HyfB,D,F[a]	MrpD[a]
ND3	-	-	-	-	-
ND4	-	-	EchA[a]/HycC[a]	HyfB,D,F[a]	MrpD[a]
ND4L	-	-	-	HyfE?	-
ND5	-	-	EchA[a]/HycC[a]	HyfB,D,F[a]	MrpA[a]
ND6	-	-	-	-	-

Table 1.2 Homologies of complex I subunits to subunits of other bacterial enzymes

[a]The ND2, 4 and 5 subunits are weakly homologous to each other, an assignment of the individual subunits to other proteins is ambiguous.

1.2.2 Cluster N2 and Its Role in the Mechanism of Proton Translocation in Complex I

One of the main reasons why the catalytic mechanism of complex I is poorly understood lies in the characteristics of its prosthetic groups, the iron-sulphur clusters [FeS]. Iron-sulphur clusters cannot be studied by optical spectroscopy but instead require the more difficult technique of low temperature EPR for characterisation and assessment of their redox state.

Reaction catalysed by complex I:

$$\mathrm{NADH} + \mathrm{Q} + \mathrm{H}^+ + \boldsymbol{n}\mathrm{H}^+_{\mathrm{in}} \rightleftharpoons \mathrm{NAD}^+ + \mathrm{QH}_2 + \boldsymbol{n}\mathrm{H}^+_{\mathrm{out}}$$
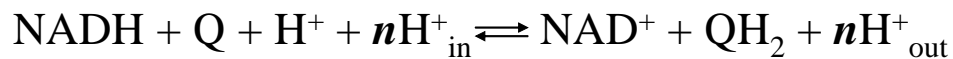
Knowledge of the exact value of n is absolutely necessary to make any assumptions about the enzyme catalytic mechanism. For bovine heart mitochondria $n = 4$ was measured (Wikström, 1984). Over the years many proposals have been made regarding how mitochondrial complex I might pump protons (Brandt, 1997). There are three basic types of mechanism, all present in the oxidative phosphorylation system that could serve as a model for complex I:

- directly redox linked proton pump (cytochrome *c* oxidase)

- redox linked ligand conduction mechanism (*bc₁* complex)

- conformational energy transfer (ATP synthase)

It is assumed that FMN ($E_{m,7.5} = -336$ mV) together with cluster N3, which is located in the same subunit, functions as an electron input device, whereby FMN and its semiflavin are the mediators between the two electron donor NADH and the one electron transferring iron-sulphur clusters (Sled *et al.,* 1994). The coupling mechanism between redox reactions and proton translocation in complex I is still unknown but there are several experimental data which support a key role for cluster N2 in quinone reduction and proton translocation. This cluster has the most positive redox midpoint potential ($E_{m,7} = -150$ mV) which is pH-dependent (–60 mV/pH for bovine heart complex I) (Ingledew and Ohnishi, 1980) and N2 features magnetic

interactions with semiquinone radicals as shown by EPR spectroscopy (Magnitsky *et al.,* 2002).
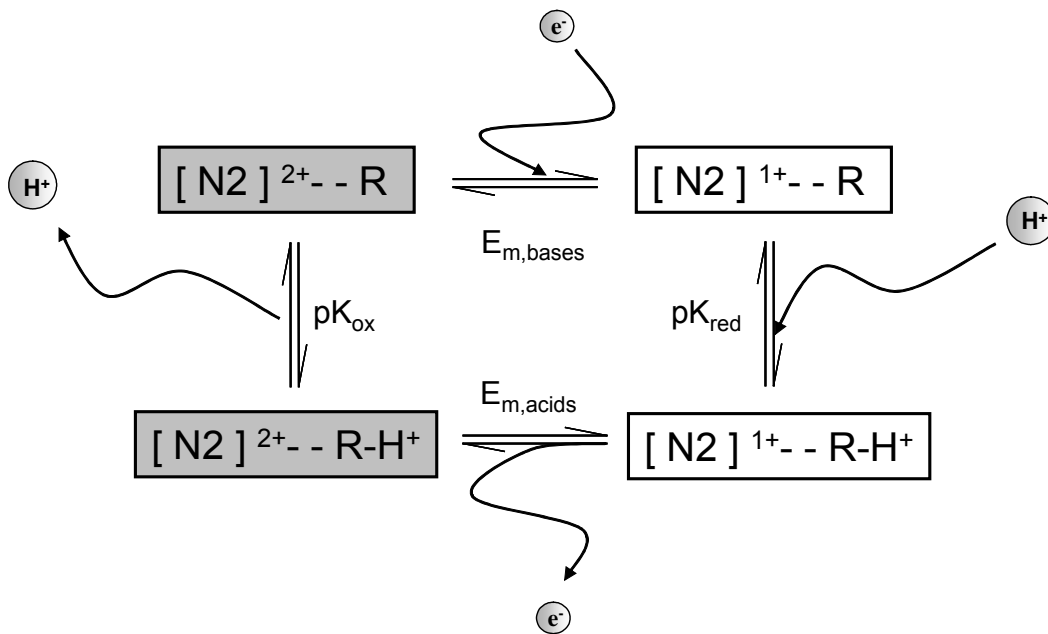
Figure 1.3 Proton translocation associated with a Redox-Bohr Group

Redox- and protonation states of the iron sulphur cluster N2 associated redox-Bohr group (R) in complex I. Upon reduction, the basicity of the center is increased and R becomes protonated. After reoxidation and deprotonation the initial state is restored again. To accomplish a 1:1 stoichiometry in proton/electron transport, the pK values have to be at least 2 units apart from each other and the pK of the reduced forms should be >8.

These are consistent with the hypothesis that N2 is the immediate electron donor to the quinone and that it might be directly involved in a proton pumping mechanism via an associated redox-Bohr group (Figure 1.3). Such a group would become protonated upon reduction of N2 and deprotonated again when the centre becomes reoxidised. Provided that the proton donor and the final proton acceptor are different groups, this process would result in a one proton per one electron stoichiometry.

The recent finding that the 49-kDa subunit and thus the catalytic core comprising cluster N2 is clearly separated from the membrane (Zickermann *et al.,* 2003) places the site of quinone reduction into the hydrophilic domain. Therefore at this point the most likely scenario is that the redox chemistry of quinone reduction around cluster N2 induces specific conformational changes. These changes are then transmitted to

the hydrophobic subunits in the membrane that have been derived from Na^+/H^+ or Na^+/K^+ antiporters and act as ion pumps.

1.2.3 Complex I and Disease

Mitochondrial disorders occur in humans with a frequency of around 1:10.000 live births (Bourgeron *et al.,* 1995). Most disorders are caused by the malfunction of one or more enzyme complexes of the oxidative phosphorylation system (OXPHOS). Isolated complex I deficiency is one of the most frequently observed deffects in the OXPHOS system.

Dysfunction of complex I causes 3 different problems: (1) lack of NAD^+ when NADH is not reoxidised by complex I, (2) decrease of ATP level due to complex I inability to pump protons and (3) production of reactive oxygen species (ROS).

Mutations in both the mitochondrially and nuclear encoded genes are known to cause complex I deficiencies (Loeffen *et al.,* 2000). Mutations in mitochondrially encoded genes lead to a variety of neuromuscular syndromes, including myoclonic epilepsy associated with ragged red fibers (MERRF); mitochondrial encephalomyopathy, lactic acidosis and stroke-like episodes (MELAS); Chronic Progressive External Ophthalmoplegia (CPEO); Kearns-Sayre syndrome (KSS). Many cases of Leber's hereditary optic neuropathy (LHON), appear to be associated with a defect in complex I. The defect identified in many cases is a single nucleotide change in the mitochondrial DNA converting arginine-340 in the ND4 subunit of complex I into histidine. Leigh syndrome is a severe progressive neurodegenerative disorder that may be caused not only by mutations in *mt*DNA but also in nuclear DNA, as exemplified by mutations in *NDUFS7,* encoding the homologue of the PSST subunit (Triepels *et al.,* 1999) and *NDUFS8,* encoding the homologue of the TYKY subunit (Loeffen *et al.,* 1998). Recently, researchers at the Nijmegen Center for Mitochondrial Disorder (Nijmegen, The Netherlands) found mutations in the *NDUFS2* gene, encoding the 49-kDa subunit in four patients (from three families) with cardiomyopathy and encephalomyopathy (Loeffen *et al.,* 2001). The three distinct mutations are described later in the text (see 1.4.1.2)

In addition, the compound, 1-methyl-4-phenylpyridium ion (MPP^+), the active metabolite of the parkinsonism toxin N-methyl-4-phenyl-1,2,3,6-tetrahydropyridine

(MPTP), acts as an inhibitor of complex I (Gluck *et al.,* 1994). Association of pesticides and environmental toxins are believed to be the most likely cause of Parkinson's disease (PD). It was found that chronic exposure of rats to the commonly used complex I inhibitor rotenone also reproduced features of Parkinson's disease (Betarbet *et al.,* 2000). The mechanism of rotenone toxicity in rats is still unknown. Recent studies suggest that it is neither due to ATP depletion nor NADH accumulation in the mitochondrial matrix but rather due to oxidative damage caused by ROS produced most likely by complex I (Sherer *et al.,* 2003).

1.3 *Yarrowia lipolytica* a Model Organism

Compared to the other respiratory enzymes there is not much experimental data available about complex I structural organisation, composition, catalytic core and especially about the mechanism of electron transfer from NADH to ubiquinone and its coupling to proton translocation. These problems are not only due to the size or complexity of this extraordinary enzyme, but also due to the lack of an appropriate system for systematic research at the molecular level. The most commonly used eukaryotic model system with the most complete set of genetic tools, the yeast *Saccharomyces cerevisiae,* does not bear complex I. Complex I has therefore been most extensively characterised in *Bos taurus* and *Neurospora crassa*. However, genetic manipulation in these organisms is rather difficult and time consuming at the moment. Different bacteria such as *E. coli* and *Rh. capsulatus* have very well elaborated possibilities for genetic manipulation. However, complex I from these sources is instable and therefore protein handling and characterisation is not trivial.

Yarrowia lipolytica strains have been found in many dairy products such as cheese and yoghurts. It is a strictly aerobic non pathogenic yeast. Its optimum growth temperature is about 28°C. *Y. lipolytica* can use a variety of compounds as a carbon source: glucose (2 %), sodium acetate (up to 0.4 %), ethanol (up to 3 %) as well as n-, l-alkanes and fatty acids. Most genetic tools such as replicative plasmids and strains with stable mating types and different auxotrophies for positive and negative selection as well as genome sequence are available. All this makes *Y. lipolytica* an excellent model organism for structural and functional studies of different biochemical processes.

1.3.1 Respiratory Chain from the Yeast *Yarrowia lipolytica*
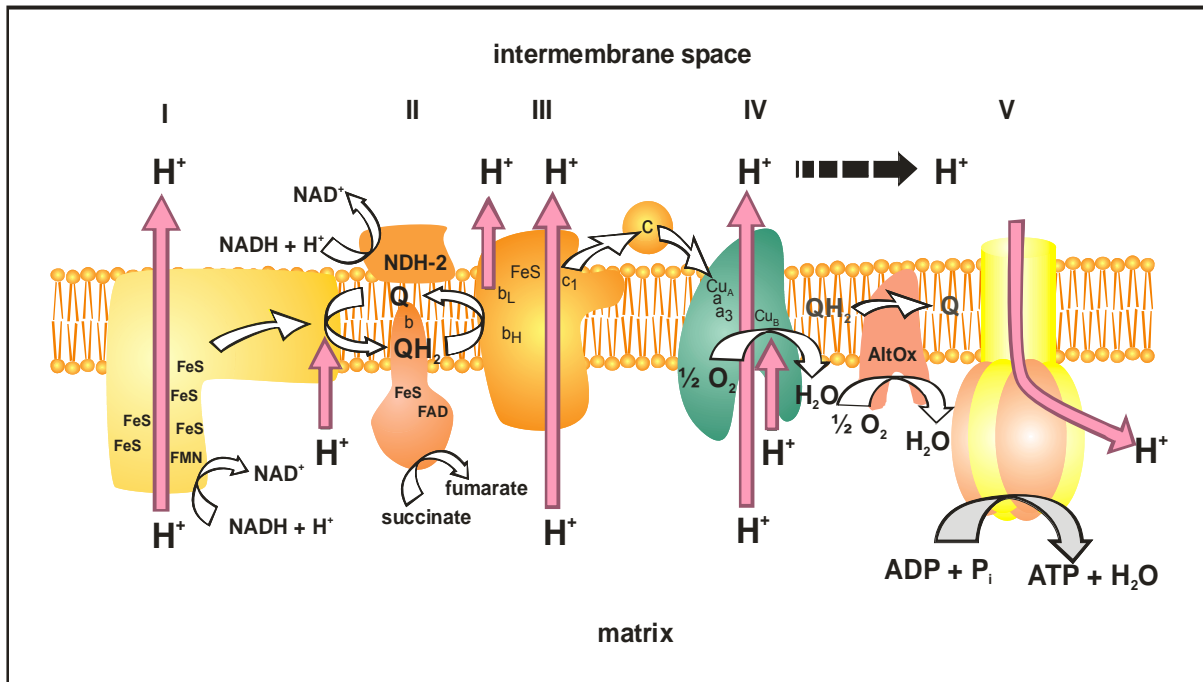
Figure 1.4 Mitochondrial respiratory chain from *Yarrowia lipolytica*

Four electron transferring respiratory complexes are labelled as: I (NADH:ubiquinone oxidoreductase); II (succinate:ubiquinone oxidoreductase); III (cytochrome *c* reductase); IV (cytochrome *c* oxidase). Compared to the mammalian respiratory chain, *Y. lipolytica* has an extra external alternative NADH dehydrogenase labelled as (NDH-2) and one alternative ubihydroquinone oxidase (Alt-Ox).
The electron flow is shown with white arrows, whereas proton translocation is shown with red arrows.
FeS: iron-sulphur centre; FMN: flavin mononucleotide; FAD: flavin - adenine dinucletide; NAD^+: nicotinamide-adenine dinucleotide; NADH: hydronicotineamide–adenine dinucleotide; Q: ubiquinone; QH_2: ubihydroquinone; *b*: heme *b*; b_H: high potential heme *b*; b_L: low potential heme *b*; a_3: heme a_3; *c*: cytochrome *c*; c_1: cytochrome c_1; Cu_A and Cu_B: copper centres.

The respiratory chain of *Y. lipolytica* is very similar to the mammalian respiratory chain. It consists of four multisubunit enzymes (complex I-IV). Additionally, *Y. lipolytica* has a hydrophilic alternative non proton pumping NADH dehydrogenase (NDH-2) (de Vries and Marres, 1987; Rasmusson *et al.,* 1998) which is usually found in yeast and plants. NDH-2 consists of one polypeptide which carries one non-covalently bound flavine adenine dinucleotide (FAD) as a prosthetic group. How this water soluble NDH-2 is anchored on the inner membrane and how it interacts with

14

hydrophobic ubiquinone is still unknown (Kerscher, 2000). *Y. lipolytica* carries only one gene copy for NDH-2 (Kerscher *et al.,* 1999). NDH-2 is located in the intermembrane space and therefore cannot contribute to the oxidation of NADH from the mitochondrial matrix. Therefore complex I is essential for survival (Ahlers *et al.,* 2000a). To delete complex I subunits and at the same time avoid lethality, NDH-2 was redirected into the mitochondrial matrix using the mitochondrial import signal from the 75-kDa subunit of complex I. This way, NDH-2 was able to compensate for complex I defects (Kerscher, 2000) and is called NDH-2i.

Furthermore *Y. lipolytica* has one alternative ubihydroquinone oxidase (Kerscher *et al.,* 2002), that transfers electrons directly from ubiquinone to oxygen without pumping protons. This alternative oxidase is cyanide insensitive and it is induced if cytochrome electron transfer via the cytochrome bc_1 complex and cytochrome *c* oxidase is inhibited.

1.4   Goals of this Study

1.4.1   Site Directed Mutagenesis in the 49-kDa Subunit of Complex I

The yeast *Yarrowia lipolytica* is a well worked out as a genetic model organism. Due to easy handling of this organism and stable complex I (Djafarzadeh *et al.,* 2000) it is one of the best and fastest systems to study structure and function of complex I. The composition of complex I from *Y. lipolytica* is very similar to that of complex I from *Neurospora crassa.* 32 hydrophilic and 7 hydrophobic subunits of complex I have been detected by isoelectric focusing and 2D PAGE (Abdrakhmanova, unpublished data). NDH-2i is able to compensate complex I disfunction caused by assembly defects or any other defect such as specific mutations. The C-terminal His-Tag on the 30-kDa subunit allows for the purification of complex I via Ni-NTA affinity chromatography in milligram amounts. This system also allows characterisation of site-directed mutations in complex I. The complex I mutants were characterised with BN-PAGE for assembly, specific complex I dNADH:DBQ activity normalised to NADH:HAR activity as a measure for the amount of complex I in membranes. Iron-sulphur cluster were investigated using EPR spectroscopy that was carried out by Dr. Klaus Zwicker. Proton pumping was investigated by reconstitution of complex I into proteoliposomes measured with ACMA dye fluorescence.

1.4.1.1   Mutations Selected on the Basis of the Hydrogenase Structural Model

Based on sequence analysis it had been proposed that the [NiFe] hydrogenase structural fold was conserved during evolution and that the [NiFe] site evolved to form a significant part of the active site of complex I. It was found that mutants D458A, V460M, D143E and D143C, which affect residues that correspond to three cysteines that ligate the [NiFe] active centre in [NiFe] hydrogenase, not only lower activity and inhibitor sensitivity but also influence the properties of cluster N2 (Kashani-Poor *et al.,* 2001b). Therefore residue S146 that is not conserved in complex I and corresponds to the fourth cysteine in [NiFe] hydrogenases was mutated and mutants were investigated. It was also found that mutations of the additional specific residues in the 49-kDa subunit that are either conserved among complex I from different species or among [NiFe] hydrogenases, or both have a strong influence on cluster

16

N2 which resides in the PSST subunit. These findings brought to attention that one ligand of cluster N2 could be located in the neighbouring 49-kDa subunit. As it is known that nitrogen from the imidazole ring of histidine is ligand of the Rieske iron-sulphur cluster in the bc_1-complex it seemed possible that also one of the ligands of complex I cluster N2 could contain a nitrogen-atom. Therefore conserved arginines and histidines that could serve as ligand to N2 were mutated. In the structures of water soluble [NiFe] hydrogenases it can be seen that the residues corresponding to histidine 226 and arginine 141 (*Y. lipolytica* numbering, see Figure 4.1) in the *Y. lipolytica* 49-kDa subunit are very close to the proximal iron-sulphur cluster. According to the hydrogenase model histidine 226 and arginine 141 both are in a distance within 7 Å from cluster N2. Therefore it was necessary to carry out a more detailed analysis of these residues. Also other residues such as histidine 91, histidine 95 and arginine 466 were mutated and investigated although these residues according to the hydrogenase model are not as close to cluster N2.

1.4.1.2 Reconstruction of Human Pathogenic Mutations

Loeffen *et al.* (2001) identified mutations in the NDUFS2 (49-kDa) gene in 3 families with isolated complex I deficiency:

- G-to-A transition at nucleotide 683, resulting in an arginine-to-glutamine substitution at codon 228 (human R228Q corresponds to R231Q in *Y. lipolytica*). This arginine is conserved among complex I from different species (see Figure 4.1A).

- C-to-A transition at nucleotide 686, resulting in a proline-to-glutamine substitution at codon 229 (human P229Q corresponds to P232Q in *Y. lipolytica*). This proline is not strictly conserved among complex I from different species; in *E. coli* it is replaced by isoleucine (see Figure 4.1A).

- T-to-C transition at nucleotide 1237, resulting in a serine-to-proline substitution at codon 413 (human S413P corresponds to S416P in *Y. lipolytica*). This serine is not strictly conserved among complex I from different species; in *Rh. capsulatus* it is replaced by alanine (see Figure 4.1A).

One of the goals was to investigate these mutations that were lethal at very young age. Mutants R231Q, P232Q and S416P and additional site-directed mutations at these positions (*Y. lipolytica* nomenclature) were generated in the yeast *Y. lipolytica* and complex I properties were studied.

1.4.2 Mitochondrial Expression of eYFP

GFP (Green Fluorescent Protein) is found in coelenterates such as the pacific jellyfish *Aequoria victoria* (Morin and Hastings, 1971). It transduces, by energy transfer, the blue chemiluminiscence of another protein, aequorin, into green fluorescent light. GFP is a small protein comprised of 238 amino acids and can be fused to virtually any protein of interest. DNA constructs encoding such fusions can then be introduced into living cells to express the GFP fluorescent tag on the chosen protein. GFP is an extremely attractive tool mainly because the protein functions without the need for any additional co-factors. This allows expression of GFP in an array of living organisms and subcellular departments such as mitochondria, resulting in autocatalytic maturation and a fluorescent signal.

Several GFP chromophore mutations have been described (Cormack *et al.,* 1996). eYFP (enhanced Yellow Fluorescent Protein) is one of the variants of GFP and has more than 30 times higher fluorescence than wtGFP (Ormo *et al.,* 1996). The eYFP gene contains four amino acid substitutions (S65G, V68L, S72A and T203Y). The fluorescence excitation maximum of eYFP is 513 nm and the emission spectrum has a peak at 527 nm.

In the present work, eYFP was used to label the mitochondria of *Y. lipolytica* and visualise to the mitochondrial network. Mutant R228Q in human cells caused fragmentation of the mitochondrial network. In cooperation with NCMD we intend to study whether this mutation has the same effect in *Y. lipolytica.*

2 MATERIALS AND METHODS

2.1 Materials

2.1.1 Chemicals

Ethanol (J.T. Baker, Deventer-Netherlands); bovine serum albumin (BSA) (Biolabs, New England); n-Dodecyl-β-D-maltoside (Biomol Feinchemikalien GmbH, Hamburg-Germany); DEAE Bio-Gel A Agarose (Biorad Laboratories GmbH, München-Germany); Chelating Sepharose (Pharmacia Biotech AB, Uppsala-Sweden); Agar; bacto™ yeast extract, Trypton, selected peptone 140 (Gibco BRL Life Technologies, Paisley-United Kingdom); YNB (Difco Laboratories, Sparks, MD, USA); boric acid phenol developer, fixer and fixing buffer for X-ray films and X-ray films X-OMAT AR (BioMax MR (Kodak) Rochester-New York); acetone, ammonium peroxosulfate, chloroform acetic acid, Folin-Ciocalteus-Phenol reagent, isoamyl alcohol, isopropanol, $MgSO_4$, HCl, trichlorine acetic acid (Merck, Darmstadt-Germany); ammonium sulphate, EDTA, glas perls (0.25 – 0.5 mm), KCl, KOH, KH_2PO_4, sodium acetate, sodium citrate, NaCl, NaOH, $NiSO_4$, NaH_2PO_4, saccharose, X-Gal (Carl Roth GmbH & Co, Karlsruhe-Germany); ATP, nucleotides, Ni-NTA Fast Flow Sepharose (Pharmacia); acrylamide, bisacrylamide, Coomassie-Blue G-250, urea, polyethylene glycol (PEG) 4000, dodecylsulphate Na-salt (SDS), tricine, agarose, amino caproic acid, amino acids, ampicilline, DMSO, ethidium bromide, glucose, glycerine (Pharmacia); hexaammine ruthenuim(III) chloride (HAR), hepes, KCN, lithium acetate, mercapto ethanol, mops, d-NADH, NADH, NaN_3, nystatine, PMSF, TEMED, tris, asolectin, oligonucleotides (Sigma Chemie GmbH, Deisenhofen-Germany), Bio-Beads SM-2 (Bio-Rad), asolectin (Fluka); oligonucleotides (ARK Scientific GmbH Biosystems, Darmstadt-Germany) or MWG-Biotech Ebersberg-Germany).

2.1.2 Inhibitors

2-decyl-4-quinazolinyl amine (DQA) was a generous gift from Aventis CropScience, Biochemical Research, Frankfurt am Main, Germany; rotenone was purchased from Sigma Chemie GmbH, Deisenhofen, Germany.

2.1.3 Media and Solutions

Media for *Escherichia coli*:

LB-media: 1 % NaCl, 0.5 % Yeast Extract, 1 % Bactotryptone, pH 7.5 (1.5 % agar for plates)

SOC-media: 0.5 % Yeast Extract, 2 % Bactotryptone, 10 mM NaCl, 2.5 mM KCl, 10 mM $MgCl_2$, 10 mM $MgSO_4$, 20 mM glucose

Media for *Yarrowia lipolytica*:

Sporulation medium (CSM): 0.7 % Yeast Nitrogen Base w/o $(NH_4)_2SO_4$ and amino acids, 0.5 % $(NH_4)_2SO_4$, 50 mM sodium citrate

YPD-medium: 2 % Bacto™Pepton, 1 % Yeast Extract, 2 % glucose

Permanent culture medium: YPD-media + 40 % glycerine

Minimal synthetic medium (S): 1.7 % Yeast Nitrogen Base w/o $(NH_4)_2SO_4$ and amino acids, 5 % $(NH_4)_2SO_4$, pH 5.0 were prepared as a 10 × stock solution and sterile filtrated. Carbon source (0.4 % acetate or 2 % glucose) were prepared as 2 × stock solution, autoclaved and added to 10 × S-media. Depending of the type of selection one or several of the following components were added: 130 µM histidine, 200 µM lysine, 460 µM leucine, 180 µM uracil.

Buffers and solutions:

10 × TAE-buffer: 400 mM tris / acetate, 10 mM EDTA, pH 8.3

TE: 10 mM Tris / HCl, 1 mM EDTA, pH 8.0

20 × SSC-buffer: 3 M NaCl. 0.3 M sodium citrate, pH 7.0

One step buffer (freshly prepared): 45 % PEG4000, 0.1 M lithium acetate pH 6.0, 100 mM dithiothreitol, 250 µg/ml salmon sperm DNA as carrier

IPG Buffer (Sigma)

Rehydratation Buffer: 8 M Urea, 1.5 % Triton X-100, 10 mg/ml DTE 0.5 % IPG Buffer and a trace of bromphenol blue

SDS equilibration Buffer: containing 50 mM Tris-HCl pH 8.8, 6M Urea, 30 % glycerol, 4 % SDS, 10 mg/ml DTE and a trace of bromphenol blue

20

2.1.4 Strains

Escherichia coli competent cells

strain	genotype
XL1-Blue	*recA*1 *endA1yrA*96 *thi*-1 *hsdR*17 *supE*44 *relA*1 *lac* [F'*proAB lacI*ᵠ*ZΔM*15 *Tn*10 *(Tet*ʳ)]
XL10-Gold	*recA*1 *endA*1 *gyrA*96 *thi*-1 *hsdR*17 *supE*44 *relA*1 *lac* [F'*proAB lacI*ᵠ*ZΔM*15 *Tn*10 (Tetʳ)]

Table 2.1 *Escherichia coli* strains

Yarrowia lipolytica

strain	genotype
E129	*Mat*A *lys11-13 ura3*-302 *leu2*-270 *xpr2*-322
E150	*Mat*B *his-1 ura3*-302 *leu2*-270 *xpr2*-322
NK2.1	*nucm::URA3 Mat*A *ndh2i lys11-23 ura3*-302 *leu2*-270 *xpr2*-322
GB12	3*0Htg2 Mat*B *ndh2i his*-1 *ura3*-302 *leu2*-270 *xpr2*-322
Δnugm GH1	*nugm::URA3 Mat*A *ndh2i ura3*-302 *his*-1 *xpr2*-322
KL6	*nukm::LEU2 Mat*B *ndh2i leu2*-270 *lys11*-23 *xpr2*-322 *ura3*-302
PIPO	30 Htg pop-in-pop-out *Mat*A, *lys*-1, *ura3*-302, *leu2*-270

Table 2.2 *Yarrowia lipolytica* strains

2.1.5 Plasmids

name	property	source
pCR2.1	see product's description	Invitrogen, Groningen, The Netherlands
pBluescript SK($\pm$)	see product's description	Stratagene, Heidelberg, Germany
pSK-/NUAM	pBluescript SK($\pm$) with genomic DNA coding for 75 Da subunit from complex I	Dr. Stefan Kerscher, Frankfurt/Main, Germany
pINA240	*Yarrowia lipolytica* "shuttle"-vector containing 2,3 kb fragment with *LEU*2 gene	Prof. Gaillardin, Paris, France
pUB4	*Yarrowia lipolytica* "shuttle"-vector containing 1 kb fragment with *Hyg* B^R gene	Dr. Stefan Kerscher, Frankfurt/Main, Germany
pUB26	modified pUB4 base changed in ARS68 (T737A)	Dr. Stefan Kerscher, Frankfurt/Main, Germany
pINA240/30-Htag2	pUB26 with 2.1 kb *Sal* I fragment of 30 kDa subunit with modified C-terminus (6xA + 6xH) from complex I	Dr. Stefan Kerscher, Frankfurt/Main, Germany
pEYFP	see product's description	BD Biosciences, Clontech, Heidelberg, Germany

Table 2.3 Plasmids

2.1.6 Instruments

Centrifuges:

Heraeus Biofuge A (Osterode, Germany)

Heraeus Labofuge 400 (Osterode, Germany)

Heraeus Minifuge GL (Osterode, Germany)

Heraeus Cryofuge 8500i (Osterode, Germany)

Cool centrifuge J2-21, Beckman Instruments GmbH (München, Germany)

Ultracentrifuge L7-65 and L8-70M, Beckman Instruments GmbH (München, Germany)

Rotors:

Cooled centrifuge: JA-10, JA-20, JS13.1 Beckman Instruments GmbH (München, Germany)

Ultracentrifuge: Ti 45, Ti 50.38, Ti 70.1, Beckman Instruments GmbH (München, Germany)

Photometer:

UV 300 Shimadzu (Düsseldorf, Germany)

U-3210 Hitachi (Düsseldorf, Germany)

MultiSpec-1501, Shimadzu (Düsseldorf, Germany)

SPECTRAmax PLUS[384], Molecular Devices GmbH (Ismaning, Germany)

Fluorometer:

Hoefer[®]DyNA Quant[®]200, Pharmacia Biotech (San Francisco,USA)

RF-5001 Shimadzu, (Düsseldorf, Germany)

Thermo cycler:

DNA Thermal Cycler 480, Perkin Elmer (Weiterstadt, Germany)

GeneAmp[®] PCR System 2400, Perkin Elmer (Weiterstadt, Germany)

cyclone[®] gradient, Peqlab, Biotechnologie GmbH (Erlangen, Germany)

Electroporation:

E. coli Pulser Bio-Rad (Hercules, USA)

DNA Sequencer:

ABI PRISM™ 310 Genetic Analyzer, Perkin-Elmer (Weiterstadt, Germany)

Sonifier:

B 15 Sonifier / Cell Disrupter, Branson (Danbury, UK)

EPR-Spectrometer:

ESP 300 E, Bruker (Rheinstetten, Germany) with continuous flow cryostat ESR 900,

Tubney Woods Abingdon (Oxon, UK) and liquid helium cooler, Messer-

Griesheim (Griesheim, Germany)

EPR-tubes:

Quartz glass Nr.: 707-SQ-250M (length: 250 mm, diameter: 4 mm), Spintec (Remshalden, Germany)

Other instruments:

10 l Fermenter, Biostat E; Braun (Melsungen, Germany)

Bead-Beater glass pearls mill, Biospec (Bartlesville, USA)

Cell-Desntegrator-C, Bernd Euler (Frankfurt/Main, Germany)

BioSys 2000 Workstation®, Beckman Instruments

GmbH (München, Germany)

BioLogic HR Workstation, Bio-Rad Laboratories GmbH (München, Germany) with TSKgel G 4000 SW column (21.5 mm × 600 mm), TosoHaas GmbH (Stuttgart, Germany)

Photo camera MP4 land camera, Polaroid

GelSystem MINI, Biostep (Jahnsdorf, Germany)

Hybridisations oven HB-1D, Techne (Wertheim, Germany)

Laser Scanning Microscope (LSM) 510 META (Carl Zeiss, Jena, Germany)

Microscope, Leitz (Wetzlar, Germany)

Ultrafree - 20 Centrifugal Filter Unit® with Biomax™ - 30 High Flux Polysulfone

Membrane, Millipore GmbH (Eschborn, Germany)

UV-Transiluminator TF 20M, 312 nm, Herolab

IPGphor Amersham Pharmacia Biotech (Freiburg, Germany)

2.1.7 Software

DNA and Protein Analysis software:

Mac Vector 3.5, IBI

HIBIO DNASIS™ for Windows® Version 2, Hitachi Software Engineering Co., Ltd.

Sequence Navigator, Applied Biosystems

Husar, DKFZ, Heidelberg, Germany

Enzfitter Version 2.0.16.0, Biosoft, Cambridge (UK)

Swiss-PdbViewer v3.7b2, Glaxo Wellcome Experimental Research

(http://www.expasy.ch/spdbv/mainpage.html)

RasWin molecular Grafics, Windows Version 2.7.1, Copyright R. Sayle 1992-1999.

SOFTmax PRO, Molecular Devices GmbH (Ismaning, Germany)

Other software:

Zeiss LSM Image Browser Version 3,2,0,70 Carl Zeiss GmbH (Jena, Germany)

Microsoft Office Package

2.2 Methods of Molecular Biology / Gene Technology

2.2.1 *Yarrowia lipolytica* Δnucm CL1 Strain

Y. lipolytica haploid strain Δnucm CL1 (*nucm::URA3*, *Mat*A, *30Htg2, ndh2i, lys11*-23, *ura3*-302, *leu2*-270, *xpr2*-322) was made by mating strain NK2.1 (*nucm::URA3*, *Mat*A, *ndh2i, lys11*-23, *ura3*-302, *leu2*-270, *xpr2*-322) (Kashani-Poor *et al.,* 2001a) with GB12 (*30Htg2 Mat*B, *ndh2i, his*-1, *ura3*-302, *leu2*-270, *xpr2*-322), followed by sporulation of the resulting diploid and selection of a haploid strain carrying the appropriate markers. To exclude the possibility of aneuploidy the absence of the wild type *NUCM* gene was checked by Southern Blotting.

2.2.2 DNA Gel Electrophoresis

DNA was separated according to standard procedures (Sambrook *et al.,* 1989) in the presence of 0.5 µg/ml of ethiduim bromide. Depending on the DNA fragment length agarose concentration from 0.6 – 2.0 % in 1×TEA buffer were used. If the DNA fragments were extracted from the gel TEA buffer with extra additive was used (UV-safe TAE, MWG-Biotech, Ebersberg). Used DNA molecular weight standards: 1 kb Ladder, 100 bp Ladder plus (MBI Fermentas, St. Leon-Rot).

2.2.3 Fill-in Reaction of 5`-Overhang

DNA blunt-ends were made with large fragment of *E. coli* DNA-polymerase I (Klenow-polymerase, New England Biolabs GmbH, Schwalbach/Taunus) described by (Sambrook *et al.,* 1989).

2.2.4 DNA-Vector Dephosphorylation

To avoid self-ligation of empty vectors the DNA ends were dephosphorylated with SAP (Shrimp Alkaline Phosphatase, Boeringer Mannheim, Mannheim).

2.2.5 Phosphorylation of PCR-Products

To enable the ligation of PCR products it was necessary that both fragment ends were phosphorylated. The phosphorylation was made by T4 polynucleotide kinase (New England Biolabs) as described by (2000). Alternatively to the phosphorylation of DNA fragments, primers could be phosphorylated before PCR.

2.2.6 DNA Extraction from Agarose Gels

DNA extractions from agarose gels were made with "Easy Pure Kit" (Biozym Diagnostic GmbH, Hess. Oldendorf) or with QIAprep® Gel Extraction Kit (Qiagen).

2.2.7 Ligation

T4 DNA-ligase and provided buffer (Gibco BRL Life Technologies) were used to ligate DNA fragments. Ligation was usually carried out over night at 14°C.

2.2.8 Making of Electro-Competent *Escherichia coli* Cells

Electro competent *E. coli* cells were made according the procedure from Current Protocols (2000). Transformation efficiency was up to 2×10^9 colonies/µg DNA.

2.2.9 Transformation into *Escherichia coli* (electro-competent cells)

The transformation of plasmids (with Amp^R gene) into *E. coli* electro competent cells took place in *E. coli* Pulser (Biorad) as described in Current protocols (2000). Transformants were successively grown over night on LB solid medium in the presence of ampicillin (50 µg/ml).

2.2.10 Preparation of Plasmid-DNA from *Escherichia coli*

Plasmid-DNA was prepared according to (Zhou *et al.,* 1990) from small amount of cultures (1.5-3 ml). Plasmid DNA for sequencing was prepared using the QIAprep$^®$ Spin Miniprep Kit (Qiagen).

2.2.11 DNA Sequencing

Double-strand DNA was used as template for sequencing. The sequencing reaction was made with "ABI Prism dye terminator cycle sequencing kit" (Perkin Elmer, Weiterstadt). Sequencing was performed in an ABI Prism Automated Sequencer type ABI 310.

2.2.12 Polymerase Chain Reaction (PCR)

10 ng of plasmid-DNA resp. 100 ng genomic DNA, 5 µl of both oligonucleotides (5 µM), 5 µl of provided 10X reaction buffer were combined in a total reaction volume of 50 µl. To avoid dimerisation of oligonucleotides as well as non-specific binding of oliogonucleotides to matrix DNA manual "hot-start" was used. Used polymerases were: *Taq* DNA polymerase, *Taq*2000^{TM} DNA polymerase, *Pfu* DNA polymerase and *Pfu*Turbo^{TM} DNA polymerase from Stratagene (Heidelberg) as well as *Taq* DNA polymerase from Sigma Chemie GmbH (Deisenhofen).

2.2.13 Generation of Point Mutations

The shuttle-vectors pINA240 or pUB4 with 2.87 kb insert coding for the *NUCM* gene was used as template for site directed mutagenesis. Point mutation was introduced by PCR with the "QuikChange^{TM} site-directed mutagenesis kit" (Stratagene, Heidelberg).

2.2.14 Southern Blot

Digested DNA (genomic DNA: 500 ng; plasmid DNA: 50 ng) was separated using agarose gel (1 %) electrophoresis. The DNA was transferred over night on Hybond N^+-membrane (Amersham, Braunschweig). To covalently crosslink DNA to the membrane UV-light radiation from Stratalinker (Stratagene, Heidelberg) was used.

2.2.15 ^{32}P DNA Labelling

DNA fragments were labelled with $[\alpha$-^{32}P] dCTP (25 µCi for 25 ng DNA) using the "Random primer labelling – Prime-It$^®$II" Kit (Stratagene, Heidelberg). Efficiency check of radioactive labelling was done by pipetting 3 µl of 1:100 diluted reaction mixtures onto two filter sheets (Whatman DE 81 ion exchange paper, Whatman International Ltd., Maidstone, England). One of the filters was washed two times for 5 minutes with $2 \times$ SSC buffer and subsequently washed for 5 minutes in cold ethanol. To estimate incorporation of the radioactive label, count rates of both filters were controlled after drying using a Geiger counter.

2.2.16 Hybridisation of Radio Active Labelled DNA Probes

Hybridisation took place in a glass tube in a hybridisation oven (HB-1D, Techne). A pre-hybridisation was made for 15 minutes at 68°C and the main hybridisation for 60 min at 68°C with "QuikHyb$^®$" hybridisation solution (Stratagene, Heidelberg). For the main hybridisation, ^{32}P-labelled DNA fragment was used in the presence of 100 µl (10 mg/ml) salmon sperm DNA. Subsequently, blots were washed four times (2×15 min with $2 \times$ SSC, 0.1 % SDS; 2×15 min with $0.1 \times$ SSC, 0.1 % SDS) to remove non-specifically bound radioactive probe. Blots were exposed to Kodak X-Omat AR films with an amplifier-sheet over night at –80°C.

2.2.17 Transformation of *Yarrowia lipolytica*

Yarrowia lipolytica cells were transformed according to the method of (Chen *et al.,* 1997). A single colony was taken from a fresh plate or cells from 0.5 ml of an over night culture in complete medium was spun down and dispersed by vortexing for 1 min in 100 µl of freshly prepared one step buffer (45 % PEG4000, 0.1 M lithium acetate pH 6.0, 100 mM dithiothreitol, 250 µg/ml salmon sperm DNA as carrier). Subsequently the mixture was incubated for 1 h at 39°C and was spread on well

28

dried selection plates. Transformants could be observed after 3 days incubation at 28°C.

2.2.18 Conjugation, Sporulation and Random Spore Isolation

Strains of opposite mating type were separately inoculated into 10 ml of YPD and grown overnight. 0.1 ml of these cultures were transferred into fresh 10 ml YPD and grown for 18 - 21 h. Cell were centrifuged (6000 g for 3 minutes) and resuspended in 1 ml YM (about 2 - 10 X 10^8 cells/ml). One ml of each strain of opposite mating type was mixed together with 8 ml YM in a flask, shaken at 28°C for 16 - 24 h and plated on selective medium to isolate diploid cells. A single colony from the plate was inoculated into 10 ml YPD and grown overnight. Cells were centrifuged and resuspended in CSM with a concentration around 2 - 5 X 10^7 and sporulated for 4 days in flasks at 220 rpm and 23°C. After 4 days the culture was stored at 4°C for 1 day. 5 ml of the culture were centrifuged and cells resuspended in 10 ml YPD and shaken for 2 h at 28°C. The pH was adjusted to 4.5-5.0 and 0.25 ml of a 1 mg/ml nystatin solution was added. The incubation at 28°C was continued for another 1.5 h. Cells were washed twice with water, resuspended in SD and portioned into 6 aliquots. Aliquots were incubated with 0.5 ml of a 12.5% ethanol solution and incubated for a series of different times (0-120 minutes). After each incubation time, cells were washed and plated on selective medium.

2.2.19 Isolation of Total DNA of *Yarrowia lipolytica*

Total DNA isolation was according to the "rapid isolation of yeast chromosomal DNA" protocol (2000). Plasmid DNA was obtained by transformation of 150 ng of total DNA into *E. coli* competent cells.

2.3 Methods of Protein Chemistry

2.3.1 Growth of *Yarrowia lipolytica*

Yarrowia lipolytica parental strains were grown in YPD medium at 28°C in rotatory flasks. A clone of *Y. lipolytica* from an agarose YPD plate was taken for a pre-culture and shaken in a flask between 18 - 24 hours. Subsequently, 200 - 400 ml were put in

a 10 l fermenter (Biostat E; Braun, Melsungen). The fermentation lasted for 14 - 18 hours. The yield was up to 90 g cells / l (wet weight).

Mutant strains were grown by fermentation in 10 l of YPD medium. Pre-culture medium depended on the plasmid used in *Y. lipolytica.* Minimal media SD+lysine was used if pINA240 plasmid was present or YPD media with Hygromycin B^R if pUB4 plasmid was present. The fermentation was inoculated with 1/10th of fermentation volume of pre-culture. Pre-cultures were shaken in flask for 24 hours and fermentation also took 24 hours. Even when omitting selective pressure during fermentation, no substantial loss of plasmid was observed.

2.3.2 Preparation of Mitochondrial Membranes

Mitochondrial membranes were prepared from freshly harvested cells or from cells that had been shock frozen in liquid nitrogen and kept at –80°C. To break the cell walls 0.5 mm glass beads (Bend Euler Biotechnologie, Frankfurt) were used in a cell disintegrator. 300 – 500 g of cells were suspended in the same amount of buffer (600 mM saccharose, 20 mM Na/MOPS, 1 mM EDTA, pH 7.2). Cell breakage was carried out for at least 2 hours in the presence of 2 mM PMSF (protease inhibitor). Centrifugation for 25 min. at 2000 $\times$ g was used to separate cell debris (pellet) from mitochondrial membranes (supernatant). To collect mitochondrial membranes this supernatant was ultracentrifuged for 1 hour at 100,000 $\times$ g. The homogenised membranes were resuspended in the same buffer as above but without EDTA, shock frozen and stored at –80°C.

Membrane quality was checked by recording absorption spectra (530-630 nm) of the reduced minus oxidised forms of the heme groups contained in the respiratory chain. Mitochondrial membranes were oxidised by addition of dithionite and reduced by addition of ferricyanide. Content of heme groups *b* and *aa*$_3$ was measured at 562 nm (oxidised minus reduced form) and at 605 nm, respectively. Their concentration was usually around 1-10 µM and the ratio heme *b*: heme *aa*$_3$ around 3:1.

2.3.3 Preparation of Mitochondrial Membranes in Small Amounts

Freshly harvested cells (4 - 8 g) were used at 1:1:1 ratio of cells to buffer (same as in 2.3.2) to glass beads. The cell breakage was due to vortexing in a falcon tube for

10 × 1 min and intermittent cooling in ice for one minute. Centrifugations and further steps were the same as in 2.3.2.

2.3.4 Protein Quantitation

Protein determination was conducted after the procedure of (Lowry *et al.,* 1951) modified after (Helenius and Simons, 1972). Calibration was carried out with bovine serum albumin (BSA), in a dilution series from 0.1 – 2.0 mg/ml.

2.3.5 Blue-Native Polyacrylamide Gel Electrophoresis (BN-PAGE)

Blue-native polyacrylamide gel electrophoresis was used to separate the components of the mitochondrial respiratory chain in membranes of *Y. lipolytica* (Schägger, 2003). 500 µg of total protein was solubilised with 1 g/g dodecyl maltoside and 500 mM amino caproic acid and the resulting solubilised mitochondrial membranes were placed on 4 / 4 → 13% gradient gels.

2.3.6 SDS-Polyacrylamide Gel Electrophoresis (SDS-PAGE)

Tricine SDS-PAGE was used to check the composition and purity of complex I preparations (Schägger and von Jagow, 1994;Schägger and von Jagow, 1987)

2.3.7 Isoelectric Focusing

For IEF-separation as first dimension was used the IPGphor (Amersham Pharmacia Biotech) and 13 cm immobilised pH gradient (IPG) strips (pH 3-10). The samples of Complex I (400 µg/ml) was rehydrated in the solution containing 8 M Urea, 1.5% Triton X-100, 10 mg/ml DTE, 0.5% IPG Buffer and a trace of bromphenol blue for 12 h at 20 °C. Focusing was carried out by 50µA per IPG strip using the following steps: pH 3-10 gel, 500Vh (max 500V), 1000 Vh (max 1000 V) and 30000 Vh (max 8000V). After focusing strips were equilibrated using buffer containing 50mM Tris-HCl pH 8.8, 6M Urea, 30% glycerol, 4 % SDS, 10 mg/ml DTE and a trace of bromphenol blue. The second dimension gel consisted of Tricin-SDS 16% polyacrylamide gel.

2.3.8 Western Blot

To investigate protein expression, the semidry immunoblotting procedure was followed using a polyvinylidendifluorid membrane (Immobilon [TM]P, Millipore). The

primary antibody Anti His-Tag or Anti-GFP and a secondary Anti-Rabbit antibody (mouse).

2.3.9 Measurement of NADH:HAR Activity

Detergent- and inhibitor-insensitive NADH:HAR [HAR: hexa-ammine-ruthenium(III) chloride] activity was measured using a Shimadzu MultiSpec-1501 or a Molecular Devices SPECTRAmax PLUS[384] spectrophotometer by following NADH-oxidation at 340 - 400 nm (ε=6.22 mM^{-1}cm^{-1}). Assays were performed in the presence of 200 µM NADH and 2 mM HAR, 2 mM NaN$_3$ in 20 mM Na$^+$/Hepes, pH 8.0 at 30°C (Sled *et al.,* 1993). This activity depends only on the FMN and probably Fe-S cluster N3 (Gavrikova *et al.,* 1995). The reaction was started by the addition of 50 µg (total protein) of unsealed mitochondrial membranes.

2.3.10 Measurement of catalytic activity, K_M, I_{50}

To assay complex I activity dNADH was used as electron donor, whereas the ubiquinone analogue DBQ was used as electron acceptor. dNADH:DBQ activity at 60 µM DBQ and 100 µM dNADH was measured using a Shimadzu MultiSpec-1501 or a Molecular Devices SPECTRAmax PLUS[384] spectrophotometer by following dNADH-oxidation at 340 - 400 nm (ε=6.22 mM^{-1}cm^{-1}) at 30°C in 20 mM Na-MOPS pH 7.2 buffer containing 50 mM NaCl and 2 mM KCN. The reaction was started by adding mitochondrial membranes equivalent to 30 to 50 µg of protein/ml. Michaelis-Menten and I_{50} parameters were determined using microtiter plates in a Molecular Devices SPECTRAmax PLUS[384] spectrophotometer. The obtained data were fitted using "Enzfitter" (Version 2.0.16.0 Biosoft 1999, Cambridge).

2.3.11 pH Dependence of dNADH:DBQ Activity

The pH dependence was measured using a Molecular Devices SPECTRAmax PLUS[384] spectrophotometer by following dNADH-oxidation at 340 - 400 nm (ε=6.22 mM^{-1}cm^{-1}) in a buffer containing 30 mM of each MES, MOPS, sodium acetate, tris, glycine, 50 mM NaCl and 2 mM KCN at pH 5-10. The reaction was started with mitochondrial membranes equivalent to 50 µg of protein/ml.

Data were fitted according to the following equation (Brandt and Okun, 1997),

$$Rate = C \times \frac{1}{1+\dfrac{[H^+]}{K_A}} \times \frac{1}{1+\dfrac{K_B}{[H^+]}} \qquad \text{(Eq. 1)}$$

where *Rate* is the observed catalytic rate in the presence of saturating substrate concentrations (100 µM dNADH, 60 µM DBQ), $[H^+]$ is the concentration of protons, K_A and K_B are the dissociation constants of the two protonable groups A and B, and C is the optimal catalytic rate that would be observed if group A was deprotonated and group B was protonated in all enzyme molecules.

2.3.12 Purification of Complex I

Complex I was purified from isolated mitochondrial membranes that were solubilised with n-dodecyl-β-D-maltoside as described (Kashani-Poor *et al.,* 2001a). Purification was via Ni^{2+}-affinity with a modest reduction of the imidazole concentration from 60 mM to 55 mM in the equilibration and washing buffer followed by gel filtration on a TSK4000 column. Protein content was determined according to a modified Lowry protocol (Lowry *et al.,* 1951). Blue native polyacrylamide gel electrophoresis was performed as described (Schägger, 2003).

2.3.13 Reactivation of purified complex I

To reactivate purified complex I it is necessary to add lipids. In its natural environment, complex I is embedded in a lipid bilayer and most of these lipids are lost during protein purification. To reactivate complex I dNADH:DBQ activity, asolectin was added (total soy bean extract with 20 % lecithin) in a 1:1 (w/w) protein-to-lipid ratio. The asolectin solution was 10 mg/ml solubilised with 1.6 % OG in 1 mM KP_i and 25 mM K_2SO_4 pH 7.2.

2.3.14 Reconstitution of complex I

Reconstitution was performed by the method described in (Dröse, in preparation) using sodium-cholate as detergent. The final concentration of lipids was 10 mg/ml in buffer containing 20 mM K^+-MOPS, 50 mM KCl, pH 7.2, solubilised with sodium-cholate at a 1:2 (w/w) ratio lipid-to-detergent. 200 µg of purified complex I in 1 ml

buffer was usually added at a protein-to-lipid ratio of 1:50 (w/w). Detergents were removed by adding a 20 fold amount of BioBeads SM2 (pre-treated according to Holloway 1973), following the guidelines detailed by Rigaud and co-workers (Rigaud *et al.,* 1995).

2.3.15 Fluorometric measurements of H$^+$ transport via ACMA dye

Fluorimetric measurements were carried out at a Shimadzu RF-5001 fluorometer. Different quantities of proteoliposomes were diluted under stirring in 2 ml buffer 20 mM K$^+$-MOPS pH 7.2 containing 50 mM KCl. Proton translocation was measured with ACMA that was added to a final concentration of 0.5 µM. The fluorometer settings (integration time 1s) were: excitation wavelength 430 nm; emission wavelength 475 nm; band pass 5 nm in both cases. H$^+$-translocation was started by the addition of 60 µM DBQ and subsequently 100 µM NADH. Inhibitors and ionophores were added at following final concentration: 5 µM valinomycin; 12.5 µM nigericin; 1 µM FCCP; 1 µM DQA.

2.3.16 EPR-Spectra

Low temperature EPR spectra were obtained on a Bruker ESP 300E spectrometer equipped with a liquid helium continuous flow cryostat, ESR 900 from Oxford Instruments. Samples were mixed with NADH in the EPR tube and frozen in liquid nitrogen after 30 seconds reaction time. Spectra were recorded at 12 K or at 40 K with the following instrument settings: microwave frequency 9.475 GHz, microwave power 1 mW, modulation amplitude 0.64 mT. Under these conditions spectra show contributions from clusters N1, N2, N3 and N4. Spectra were recorded and analysed by Dr. Klaus Zwicker.

2.3.17 Redox titrations

For redox titrations mitochondrial membranes (~200 mg protein) were sedimented by centrifugation for 1 h at 48,000 X g. The pellet was suspended in 30 ml of buffer containing 30 mM each of sodium-acetate, Mes, Mops, Tris, glycine, pH 7.0, 100 mM NaCl and 1 mM EDTA and centrifuged as before. After one additional washing step the resulting pellet was suspended in 4–5 ml of the above buffer yielding a final protein concentration of 25–30 mg/ml. The following redox mediators were added to a final concentration of 30 µM each: tetramethyl-phenylenediamine, phenazine-

methosulfate, methylene blue, menadione, resorufin, indigotrisulfonate, 1,2-naphthoquinone, 2-hydroxy-1,4-naphthoquinone, phenosafranine, benzyl viologen, and methyl viologen. Redox titrations were performed anaerobically as described in (Dutton, 1978). The membrane suspension was poised at appropriate potential values by small additions of freshly prepared 50 mM dithionite. Aliquots were anaerobically transferred into an EPR tube, frozen rapidly in cold isopentane/methylcyclohexane (5:1), and stored in liquid nitrogen. Cluster N2 reduction rates in the frozen samples were then determined by recording EPR spectra at 12 K from samples poised at redox potentials between +100 and -500 mV. After subtraction of the oxidised spectrum recorded at redox poise between +30 and -30 mV, to eliminate signal contributions from components with higher redox potential, the intensity of the N2 EPR signal was calculated by scaling it to a simulated N2 spectrum. The resulting N2 reduction rates were fitted to the Nernst equation using PSI Plot (Poly Software International, Salt Lake City, UT, USA).

2.4 Confocal Laser Scanning Microscopy (CLSM)

Yarrowia lipolytica strain described in 2.2.1 with a 30kDa-eGFP/pUB26 plasmid was grown overnight in YPD media with Hygromycin B^R at 28°C in a flask. Cells were washed with a TE buffer and subsequently fixed in 1 % agarose. CLSM was performed on LSM 510 META (Carl Zeiss, Jena, Germany).

3 RESULTS

3.1 *Yarrowia lipolytica* Strains

3.1.1 Strain Δnucm

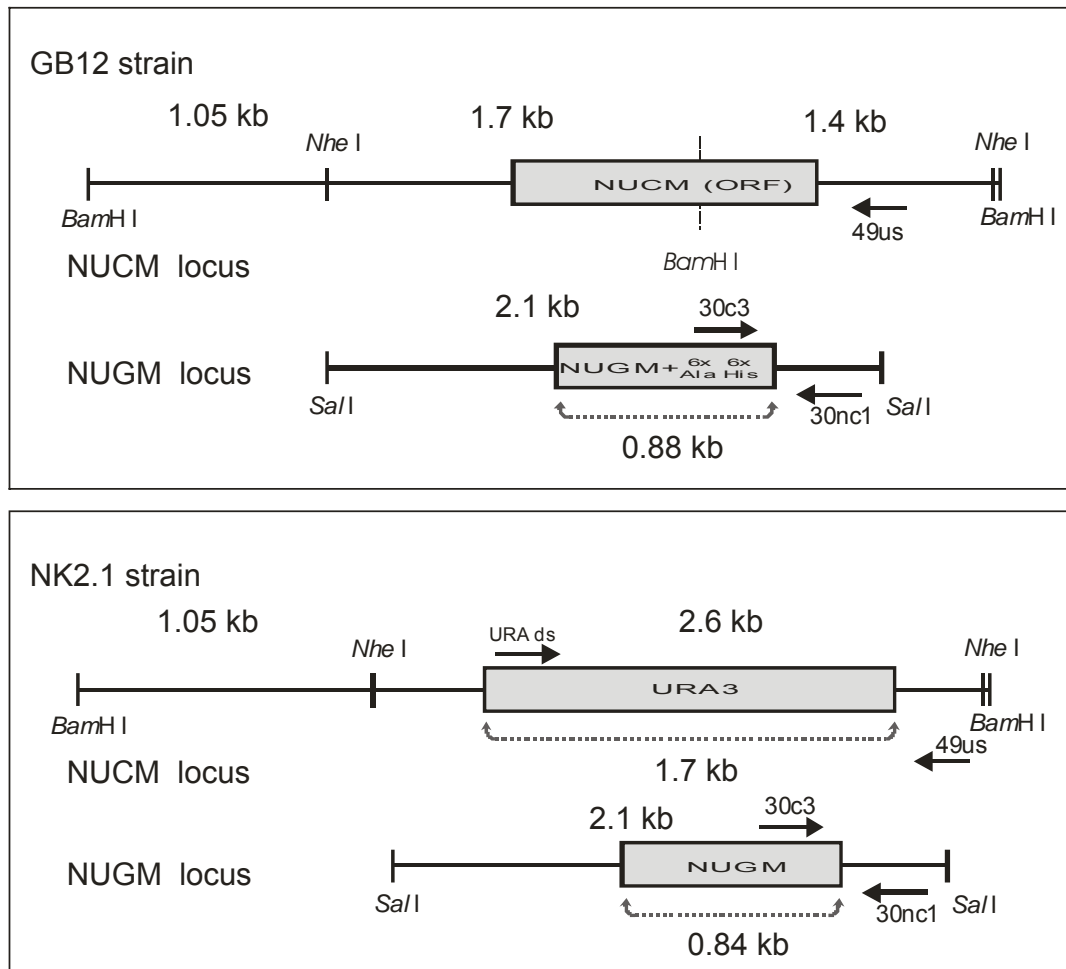**Figure 3.1 Strategy for generation of strain Δnucm with His-Tag on 30-kDa subunit**

Strains NK2.1 and GB12 were mated and sporulated. The desired spore should contain the *NUGM* allele with C-terminal His-Tag from strain GB12 and the *nucm::URA*3 allele from strain NK2.1. PCR products from primer pairs (URAds, 49us) and (30c3, 30nc1) and Southern Blots were used for checking. (see Figure 3.2 and Figure 3.3).

To obtain a strain that allows to purify complex I from 49-kDa mutants via His-Tag affinity chromatography two haploid *Y. lipolytica* strains, NK2.1 (*nucm::URA3*, *Mat*A, *ndh2i*, *lys11*-23, *ura3*-302, *leu2*-270, *xpr2*-322) (Kashani-Poor *et al.,* 2001b) and GB12 (*30Htg2 Mat*B, *ndh2i*, *his*-1, *ura3*-302, *leu2*-270, *xpr2*-322) were mated, followed by sporulation and selection of haploid strains carrying the appropriate genetic markers (see Figure 3.1). Strain GB12 carries a His-Tag on the C-terminus of the 30-kDa subunit and strain NK2.1 has a genomic deletion of the *NUCM* gene (*nucm::URA3*). Both strains have a copy of *ndh2i* integrated randomly into their genomes and it was not determined which of these *ndh2i* allele was incorporated in the final strain.

Gel A) *lys⁻* spores

Gel B) *lys⁻* spores
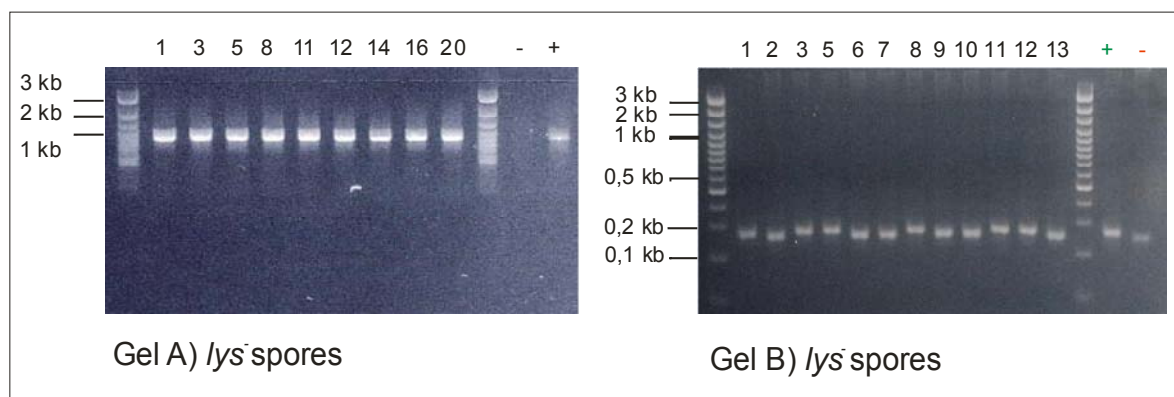
Figure 3.2 A) PCR proof for deletion of the *NUCM* gene. B) PCR checking for His-Tag[1]

A) PCR product generated with primer pair URAds and 49us. As a negative control a DNA (-) from strain GB12 and as positive control (+) genomic DNA from strain NK2.1 was used a template for PCR.
B) PCR product generated with primer pair 30c3 and 30nc1. The negative control (-) shows a 252bp PCR product generated from strain NK2.1 genomic DNA. The positive control (+) shows a 264 bp PCR product generated from strain GB12 genomic DNA.

---

[1] Data from *his⁻* spores not shown.
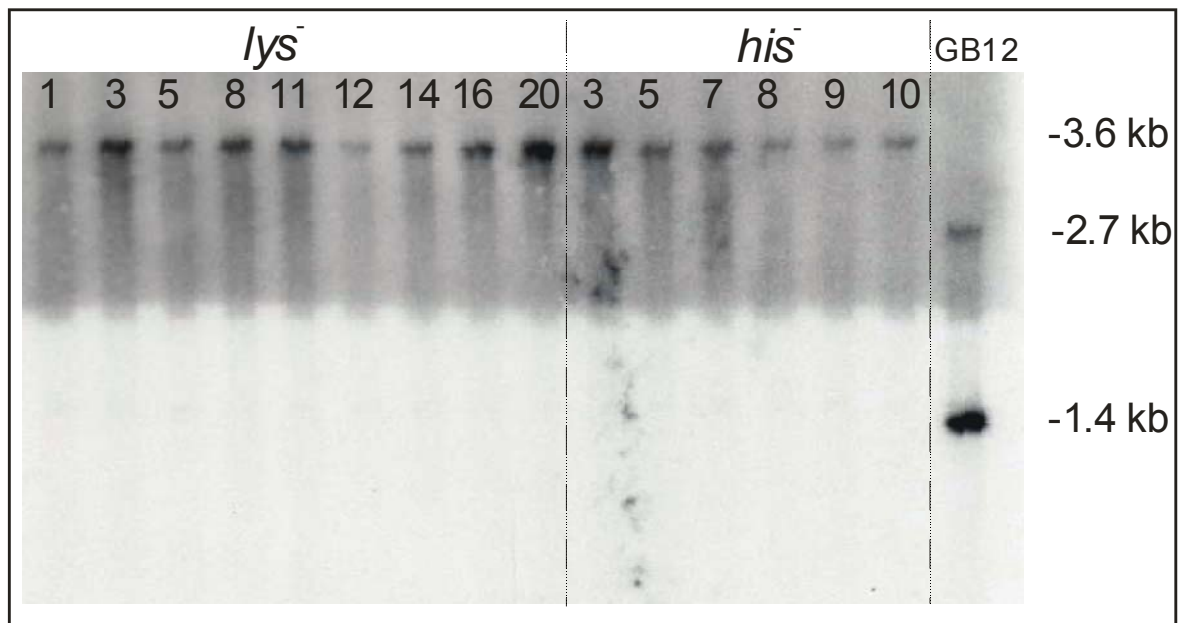
Figure 3.3 Southern Blot proof for deletion of *NUCM* gene

Genomic DNA from spores was extracted and digested with *Bam*HI. The Southern Blot Probe used is the *Nhe* I fragment from the *NUCM* locus of strain GB12 as shown in Figure 3.1. The spores that contain the *NUCM* allele have a *Bam*HI site in the ORF of the *NUCM* gene and therefore 2 bands should be visible and the spores that have the *nucm::URA3* allele are missing this *Bam*HI site and show only one band.

Two different phenotypes were observed after sporulation, strains that were *lys⁻* or *his⁻* with either *Mat*A or *Mat*B. To check for the presence of the *NUGM* His-Tag allele a PCR using primer pair 30c3 and 30nc1 was performed (see Figure 3.2 Gel B). To exclude the possibility of aneuploidy the absence of the wild type *NUCM* gene was checked by Southern Blotting (see Figure 3.3. The probe is the *Nhe* I fragment from the *NUCM* locus of strain GB12, as shown in Figure 3.1) and also a PCR check using primer pair URAds and 49us was done (see Figure 3.2 Gel A).

CL-Strains *(lys⁻)*: *nucm::URA3, 30Htg2, ndh2i, **lys11-23**, ura3-302, leu2-270, xpr2-322*

CH-Strains (*his⁻*): *nucm::URA3, 30Htg , ndh2i, **his-1**, ura3-302, leu2-270, xpr2-322*

38

Strain CL1 was used for all preparations of *Y. lipolytica* mitochondrial membranes and complex I. CL1 is named "Δnucm" in the following.

3.1.2 Complementation of strain Δnucm with plasmids bearing wild type or mutant versions of the *NUCM* gene

To have higher yields and faster growth of *Y. lipolytica* it was necessary to switch from pINA240/*NUCM* to pUB4/*NUCM*. The latter plasmid enables cells to grow on YPD complete medium with HygB^R as selection marker instead of SD minimal medium with *LEU*2 as selection marker. Firstly, the *Bam*HI site in the *NUCM* gene in pINA240/*NUCM* was removed by the introduction of a silent mutation. The GGA codon for glycine-298 was changed into the glycine codon GGC. The modified *NUCM* gene was cut from pINA240/*NUCM* using restriction enzymes *Bam*HI and *Eco*RI. The 3.1 kb *Bam*HI / *Eco*RI fragment was ligated into pUB4 (7.6 kb) which had also been cut with *Bam*HI and *Eco*RI and its ends were dephosphorylated to prevent self ligation. Complex I properties from *Y. lipolytica* Δnucm strains when transformed with the newly generated plasmid pUB4/*NUCM* were the same as when transformed with plasmid pINA240/*NUCM*. Plasmid pUB4/*NUCM* was used as template for site directed mutagenesis in the *NUCM* gene. Complemented strain CL1 with plasmid pUB4/*NUCM* is named 'parental' in the following.

3.2 Mutagenesis of Conserved Histidines and Arginines in the 49-kDa Subunit

3.2.1 Mutagenesis of Histidine 226

His-226 is invariant in all known complex I 49 kDa subunit sequences (Figure 4.1). It corresponds to a highly conserved histidine in water soluble [NiFe] hydrogenases that forms a hydrogen bond to the proximal iron-sulphur cluster of the small subunit (Volbeda *et al.,* 1995). His-226 was mutagenised into alanine and the potential iron-sulphur cluster ligands glutamine, cysteine and methionine. As judged by BN-PAGE (not shown) and NADH:HAR activity, complex I was fully assembled to normal expression levels in all His-226 mutants (Table 3.1)

Strain	Complex I		K_M (μM)	I_{50}	
	content (%)	activity (%)		DQA (nM)	rotenone(nM)
Parental	100	100	11	13	600
H226M	120	80	9	9	300
H226Q	112	56	9	13	600
H226C	122	43	5	13	600
H226A[1]	100	20	n.d.	18	770

Table 3.1 Activity tests, K_M for DBQ and I_{50} for DQA and rotenone measured on mitochondrial membranes of H226 mutants

Complex I content, activity, and inhibitor sensitivity in mitochondrial membranes of site-directed *Y. lipolytica* mutants in the 49-kDa subunit are compared to the plasmid complemented *nucm::URA3* deletion strain (parental). Complex I content is given as specific NADH:HAR oxidoreductase activity in mitochondrial membranes (100% = 1.0 μmol min^{-1}mg^{-1}), dNADH:DBQ oxidoreductase activity was normalised for complex I content (100% = 0.3 μmol min^{-1}mg^{-1}). I_{50}, concentration needed for 50 % inhibition of the inhibitor-sensitive fraction of the dNADH:DBQ oxidoreductase activity; *n.d.*, not determined.

---

[1] Data from Dr. Noushin Kashani-Poor

Only mutation H226A had a pronounced effect on specific ubiquinone reductase activity, reducing it by 80 %. Mutants H226Q and H226C had retained 56 % and 43 % activity, respectively. Membranes from mutant H226M were only slightly less (about 20 %) active than those from the parental strain. Hardly any changes were observed in the Michaelis-Menten constant K_M. A slight hypersensitivity of mutant H226M and a minor resistance of mutant H226A towards the complex I inhibitors DQA and rotenone was observed. For mutants H226C and H226Q, the I_{50} values for DQA and rotenone were unchanged (Table 3.1).

3.2.2 Mutations of Histidine 226 Affect the Properties of Iron-Sulphur Cluster N2
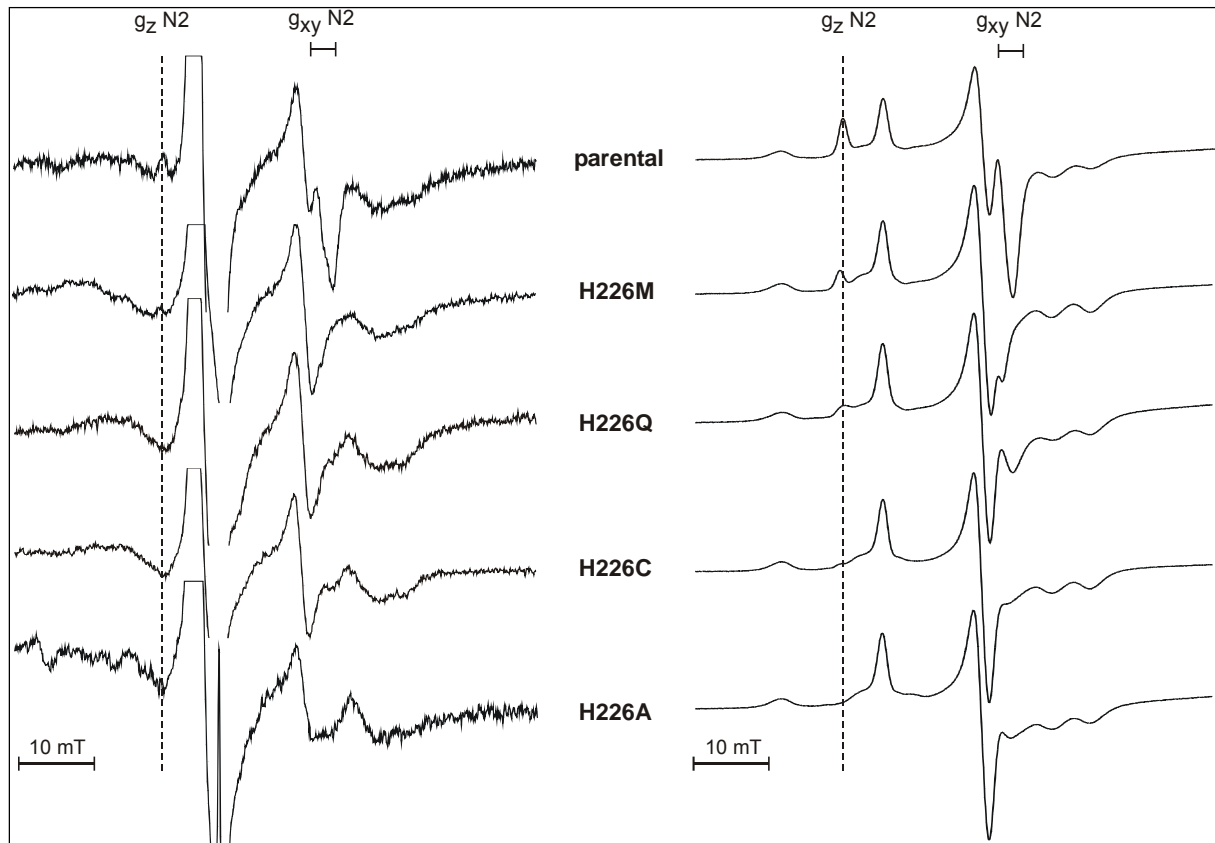
Figure 3.4 EPR spectra of H226 mutants in the 49-kDa subunit. A) Spectra of mitochondrial membranes. B) Spectra of purified complex I.

A) EPR spectra of H226 mutants from mitochondrial membranes. The EPR spectra of mitochondrial membranes were recorded at a temperature of 12 K, a microwave frequence of 9.48 GHz, a microwave power of 2 mW, and modulation amplitude of 0.8 mT. Membranes were reduced with NADH. The line represents the g_z signal of cluster N2. B) EPR spectra of purified complex I from H226 mutants. EPR spectra of complex I reduced with NADH were recorded at a temperature of 12 K, a microwave frequency of 9.48 GHz, a microwave power of 2 mW, and a modulation amplitude of 0.8 mT. Under these conditions spectra show contributions from clusters N1, N2, N3 and N4 (Djafarzadeh *et al.,* 2000). The dashed lines indicate the position of the g_z signal of cluster N2. The N2 g_z signal in H226M shows a shift to lower field values and the signal is reduced. H226Q, H226C and H226A show no shift but a very significant reduction of the g_z signal, which is comparable to the reduction in dNADH:DBQ activity.

In EPR spectra recorded from both mitochondrial membranes and purified complex I, marked effects on iron-sulphur cluster N2 but not on the other EPR detectable iron-

42

sulphur clusters resulted from all four mutations (Figure 3.4). The quality of the spectra obtained with purified complex I was much higher, because of markedly increased protein concentrations and the exclusion of interference from other paramagnetic components of the mitochondrial respiratory chain. However, the analysis of EPR spectra of mitochondrial membranes was critical to decide whether iron-sulphur clusters were lost during the purification procedure and allowed a direct comparison with the functional data summarised in Table 3.1. Again, mutation H226A had the most drastic effect resulting in complete loss of iron-sulphur cluster N2 signals. These were not even observed upon reduction of the sample with NADH/ dithionite ($E_h \cong$ -450 mV).

Similar results were obtained for mutants H226C and H226Q, but residual signals from cluster N2 corresponding to less than 10 % of wild-type level were observed in EPR spectra of purified complex I and - in the g_{xy} region - of mitochondrial membranes. In membrane preparations from mutant H226M, the g_z signal of cluster N2 was reduced by about two thirds compared to enzyme from the parental strain. An approximate N2 EPR spectrum of mutant H226M could be obtained by calculating the difference spectrum from a spectrum recorded at 45 K (N1 spectrum) and one recorded at 25 K (contributions from N1 and N2) (Figure 3.5). The resulting spectrum still had an axial line shape but with significantly shifted g_z=2.053 and g_{xy}~1.930 (N2$_{parental}$: g_z=2.051, g_{xy}=1.925, as determined from experimental spectra). The analysis of the power saturation behaviour at 12 K of the cluster N2 signal intensity also revealed a significant change of the half saturation parameter $P_{1/2}$. In the mutant $P_{1/2}$ was decreased to ~1 mW, which means only about one tenth of the value which could be determined in the parental sample. The spin concentration of cluster N2 in isolated NADH reduced complex I from H226M was estimated from EPR spectra recorded under non-saturating conditions to be ~67 % of the parental N2 intensity. These results indicate that H226 is in close proximity of N2 and the exchange of this residue had direct effects on EPR spectroscopic properties of the cluster.
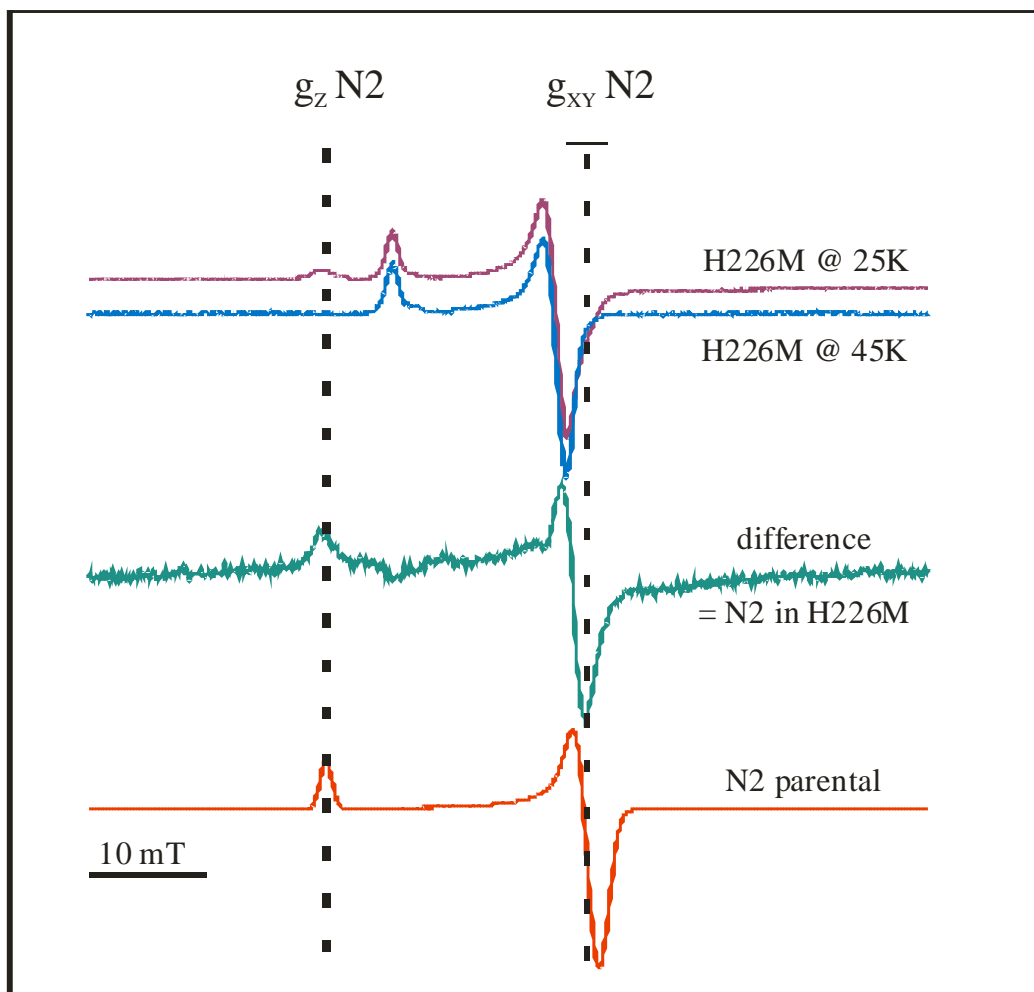
Figure 3.5 Difference EPR spectra at 25 K and 45K of mutant H226M compared to wild type

At 25 K the cluster N2 is visible whereas at higher temperature at 45 K because of much faster relaxation time cluster N2 is not detectable. This fact can be used to extract EPR signal that comes only from cluster N2. Red spectrum presents simulated spectrum of parental cluster N2.

The redox titrations of mitochondrial membranes from H226M at pH 7.0 revealed a highly diminished midpoint potential for cluster N2 of −218 mV (Figure 3.6). The dramatic effect of this mutation indicated that H226 is close enough to increase the electron affinity of N2 by its positive charge and hence a mutation in this position affects the redox properties of the centre.

Figure with axes: y-axis "Fraction N2 reduced" (0.0 to 1.0), x-axis "E_h [mV]" (-400 to 100). Annotations: $E_{m,7} = -139\,mV$ and $E_{m,7} = -218\,mV$.
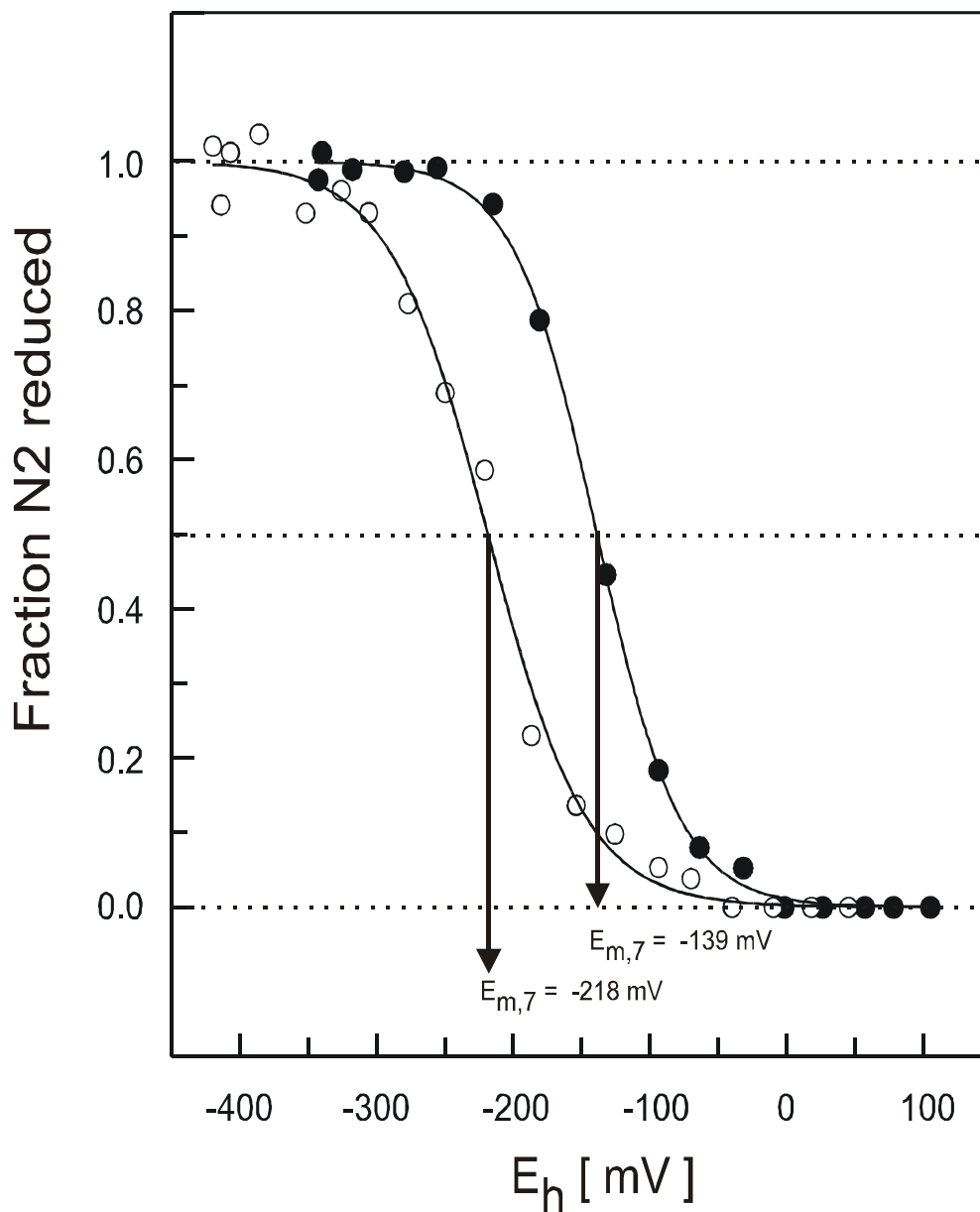
Figure 3.6 Redox behaviour of cluster N2 in parental and mutant H226M strain at pH 7.0

The reduction rate of cluster N2 was monitored by EPR spectroscopy at 12 K. (●) parental; (○) H226M. Data points were fitted according to the Nernst equation resulting in the indicated Em-values and n-values close to 1 (n = number of transferred electrons, mean = 0.9 ± 0.1 for all redox titrations of cluster N2 performed during this study). Redox-Titrations were performed by Dr. Klaus Zwicker.

The pH-dependence of the cluster N2 redox midpoint potential, detected in complex I from bovine heart (Ingledew and Ohnishi, 1980), was an important argument to claim a prominent function of this redox group in the coupling of electron transfer and proton pumping. Therefore the pH-dependence of the N2 midpoint potential in *Y. lipolytica* mitochondrial membranes was monitored between pH 5.0 to pH 9.0. At pH 7.0 the N2 midpoint potential of *Y. lipolytica* complex I was $E_{m,7}$ = -139 mV (Figure 3.6), a value very similar to those reported for complex I from other sources (Sled *et al.,* 1993).

In the physiological pH-range the midpoint potential of N2 was clearly pH-dependent with a slope of –36 mV/pH-unit (calculated between pH 5.7 and 8.0). This value differed significantly from the theoretically expected –60 mV/pH-unit (Dutton, 1978) which was found in membrane preparations from bovine heart mitochondria and in membrane particles from *Paracoccus denitrificans* (Sled *et al.,* 1993).

If we assume an amino acid side chain in close proximity of N2 which functions as redox-Bohr group, dependent on the redox state of N2, this group is characterized by specific pK values. The calculation of pK values resulted in pK_{ox} = 5.7 and pK_{red} = 7.3. The value for pK_{red} was well defined by the experimental data but there was some uncertainty for pK_{ox} because there was only one data point (at pH 5.4) representing the pH-independent region. In model calculations with fixed pK_{ox} values from pH 4.0 to pH 6.0 the slope in the pH-dependent region did only slightly change and the resulting pK_{red} values changed only half a unit from pH 7.0 (pK_{ox} =4.0) to 7.5 (pK_{ox}= 6.0).

Hence the small difference of the pK values and especially the low pK for the reduced species, which means that under physiological conditions only about half the concentration of the redox-Bohr group becomes protonated upon reduction, make a proton transfer reaction which is coupled to an electron transfer in a one to one stoichiometry unlikely.

Even more striking than the shift of the N2 midpoint potential was the complete loss of its pH-dependence as determined in the range of pH 6.0 to 8.0 (Figure 3.7). It can be concluded that protonation of H226 at low pH increases the midpoint potential of cluster N2. When the pH becomes more basic, H226 becomes deprotonated and E_m of N2 decreases.

46
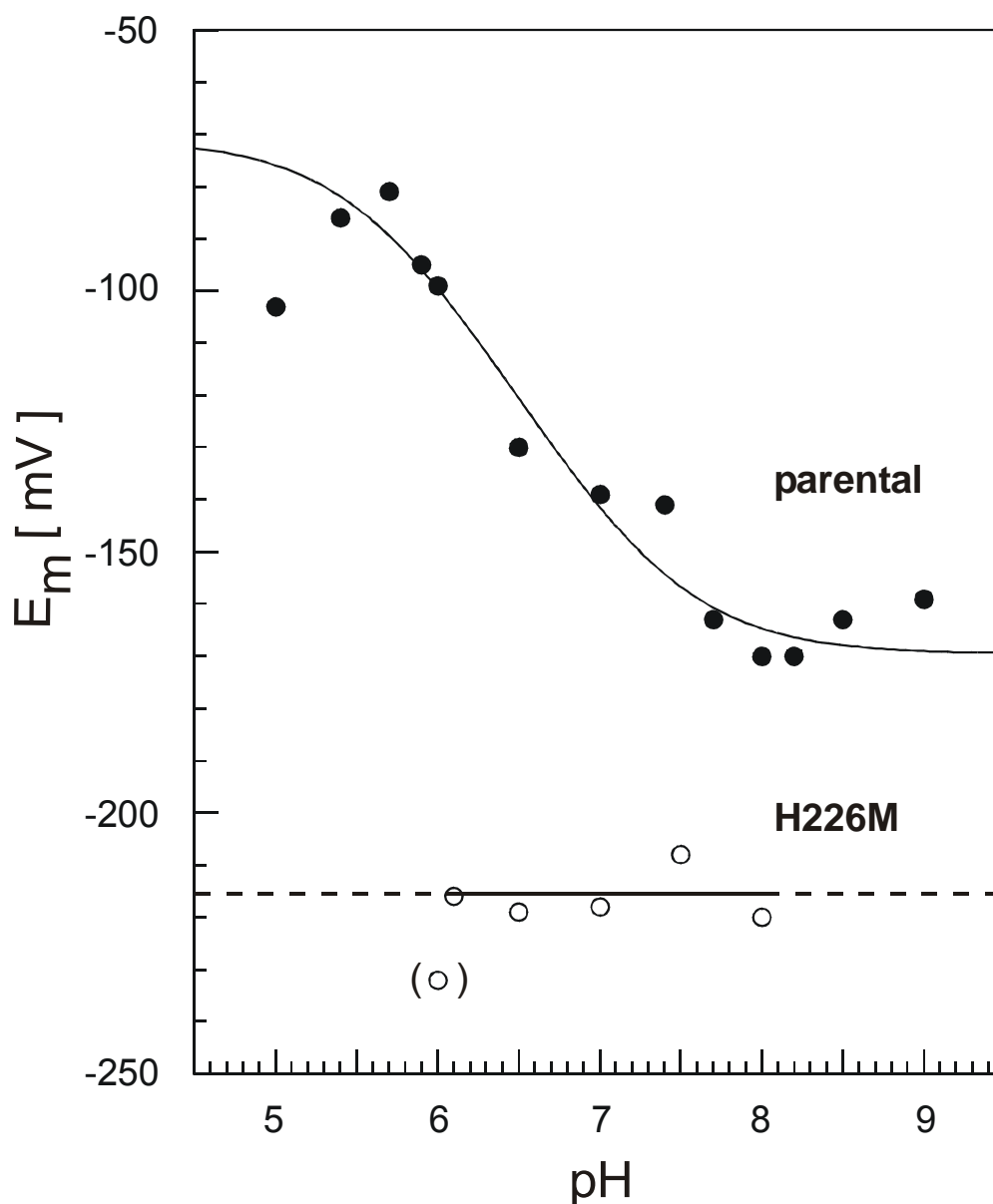
Figure 3.7 Redox behaviour of cluster N2 in H226M

pH-dependence of redox midpoint potentials of cluster N2 in mitochondrial membranes prepared from parental (●) and mutant H226M strain (○). The pH-dependence of E_m was completely lost in membranes from the mutant and the midpoint potentials were shifted by 50 - 120 mV to the negative when compared to the potential of parental membranes at the same pH. Redox-Titrations were performed by Dr. Klaus Zwicker.

These results confirm our structural model that iron-sulphur cluster N2 is located at the interface of the PSST and 49-kDa subunits. H226 of the 49-kDa is in close proximity to iron-sulphur cluster N2, close enough to modulate its electron affinity, and consequently the redox midpoint potential of this centre.
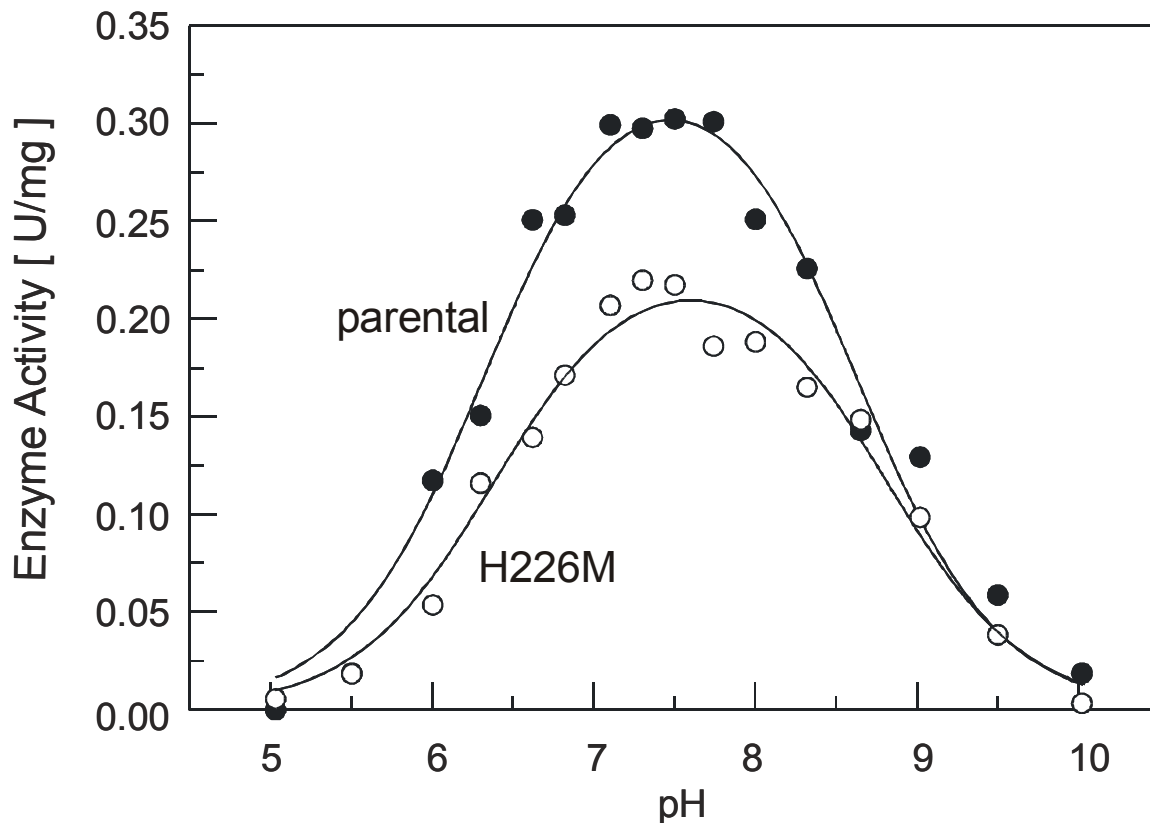
Figure 3.8 pH dependence of specific activity

The steady-state rates of dNADH:DBQ oxidoreductase activity were measured covering pH range from 5.0 to 10.0 using mitochondrial membranes (50 µg/ml total protein) at saturating substrate concentrations as described in 2.3.10. The parameters used to plot the fitted curve are listed in Table 3.2. ●, parental strain; ○, mutant H226M.

Despite these significant changes of N2 properties in the mutant H226M the pH dependence of enzymatic activity was essentially the same as for the parental membrane preparation (Figure 3.8). Both profiles showed a steep increase between pH 5.5 and 7.0, where a broad maximum between pH 7.0 to pH 8.0 was reached, followed by decay with half maximal activity between pH 8.5 and 9.0. The

characteristic pK values which can be obtained from these pH-dependencies did not change in the mutant membranes.

The maximal dNADH:DBQ activity for wild type and for mutant H226M was almost at the same pH range between 7.4 and 7.7 (Figure 3.8). pK values for wild type and for mutant H226M did not show any significant shift (Table 3.2).

	pK_A	pK_B	C
parental	6.3 ± 0.1	8.6 ± 0.1	0.347 ± 0.015
H226M	6.4 ± 0.1	8.8 ± 0.1	0.236 ± 0.009

Table 3.2 pK values controlling dNADH:DBQ activity

pK values were determined by fitting pH dependent activities to Equation 1 (see 2.3.10).

3.2.3 Reactivation and Reconstitution of Mutant H226M

During the purification of enzymes that are imbedded in the membrane bilayer at first enzymes need to be solubilised with detergents. With each subsequent chromatographic step more of the phospholipids attached to the enzyme are lost. Due to loss of lipids that are absolutely essential for activity, enzymes become 'deactivated'. To reactivate enzymes after purification it is necessary to add specific (phospho)lipids. Purified complex I was fully reactivated by the addition of asolectin (mixture of soybean phospholipids) (Kashani-Poor *et al.,* 2001a; Dröse *et al.,* 2002). Purified H226M complex I could be also reactivated to the same degree as the wild type enzyme. For purified H226M complex I the NADH:HAR activity was in the same range either with or without asolectin (Table 3.3).

Complex I of *Y. lipolytica* has been successfully imbedded into proteoliposomes formed of asolectin and by using sodium-cholate for the solubilisation of lipids and Bio Beads for the removal of detergent (Kashani-Poor *et al.,* 2001a; S. Droese *et al. in prep).*

	w/o asolectin (U/mg)		with asolectin (U/mg)	
	NADH:HAR	NADH:DBQ	NADH:HAR	NADH:DBQ
parental	49 (±10)	0.2 (±0.1)	50 (±6)	2.8 (±0.3)
H226M	43 (±6)	0.3 (±0.2)	40 (±2)	3.2 (±0.7)

Table 3.3 Asolectin reactivation of purified parental and H226M mutant complex I

Asolectin to protein ratio is 1200:1 mol/mol (~1:1 mg/mg). Asolectin was added and left on ice for 10-20 min. The results are average from 3 individual measurements, SD is given in brackets.

The redox coupled proton translocation of isolated complex I from the parental strain and strain H226M was analysed after reconstitution into liposomes. NADH:DBQ activities were measured in the presence and in the absence of the protonophore FCCP, that dissipates a proton-motive-force generated during the pumping of protons

into the lumen of the proteoliposomes. The 'theoretical' specific activity (U/mg th.) assumes that all the protein was incorporated and contributed to the activity. This could be regarded as the minimal specific NADH:DBQ activity. And finally, the coupling factor of the proteoliposomes was expressed as the ratio of the activities in the presence and absence of FCCP. One of the possible ways to observe qualitative proton pumping into the lumen of proteoliposomes is quenching of the dye ACMA (9-amino-6-chloro-2-methoxyacridine). After addition of the substrates the quench of ACMA fluorescence indicates proton translocation to the lumen of the proteoliposomes. This ACMA dye fluorescence quench was observed in reconstituted parental and H226M mutant complex I.
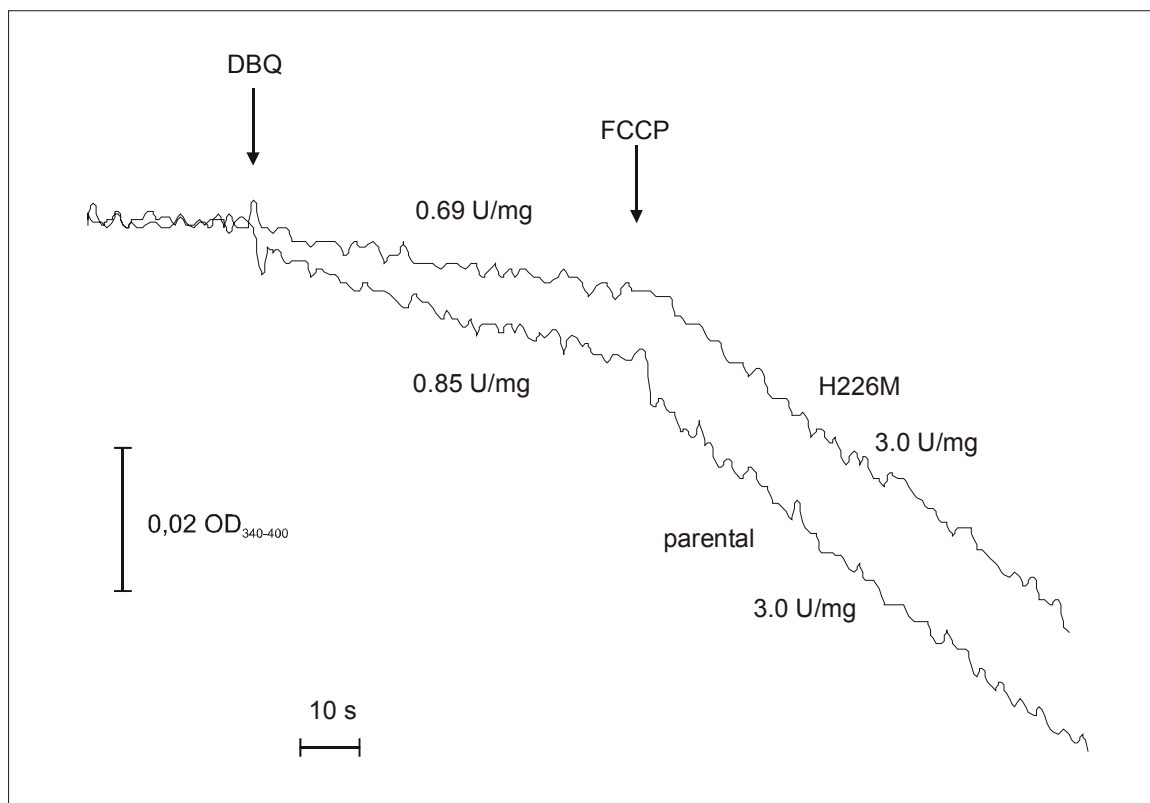

Figure 3.9 Determination of coupling factor of proteoliposomes

Measurements of NADH:DBQ complex I activity in proteoliposomes. $OD_{340-400}$ was followed.

| Strain | NADH:DBQ activity (U/mg th) proteoliposomes | | NADH:HAR activity (U/mg) | | coupling factor |
	- FCCP	+ FCCP	purified complex I	Proteo-liposomes	
parental	0.85 – 1.8	1.8 – 3.0	39 - 59	11 - 20	2.0 – 3.5
H226M	0.69 - 0.92	2.3 – 3.0	37 - 49	14 - 23	2.5 – 4.3

Table 3.4 Sodium-cholate mediated reconstitution of complex I

Proteoliposomes were prepared as described in 2.3.13. The 'theoretical' specific activity (U/mg th.) assumes that all the protein was incorporated and contributed to the activity. And finally, the coupling factor of the proteoliposomes was expressed as the ratio of the activities in the presence and absence of FCCP.

As shown in Figure 3.10, after addition of the ACMA dye fluorescence signal reached a maximum and after addition of DBQ fluorescence signal was slightly lowered due to absorption of emitted light by DBQ. With the addition of NADH the reaction was started and protons were translocated into the proteoliposomes. Due to a change of pH in the proteoliposomes, the ACMA dye is protonated and cannot leave the proteoliposomes in this protonated state. Upon this accumulation of ACMA dye we observe a quenching effect which results in a decrease in fluorescence. The fluorescence comes to steady state when equilibrium is reached between protons translocated into proteoliposomes and protons leaking out of the not perfectly sealed proteoliposomes. This steady state level was sensitive to the complex I specific inhibitor DQA. After addition of DQA the reaction was inhibited and no more protons were translocated into proteoliposomes. The fluorescence signal went back to the same level as it was before adding NADH. In addition, nigericin was added after DQA, which catalyses an electroneutral K^+/H^+ exchange across lipid bilayers. If DQA had not completely inhibited the reaction there would be a further rise of fluorescence signal, what clearly was not the case.

Figure 3.10 ACMA quenching measurements on proteoliposomes for the parental strain and mutant H226M

The reconstitutions followed the 'standard' protocol 2.3.13. All measurements were done in the presence of 50 mM KCl and 5 μM valinomycin with the same volume (20 μl) of proteoliposome solution. 0.5 μM ACMA, 60 μM DBQ and 100 μM NADH were added subsequently. Ionophores/inhibitors were added as indicated (1 μM DQA and 12.5 μM nigericin see Appendix for structure and function of used ionophores).

The same effect was observed if we 'unsealed' proteoliposomes instead of inhibiting the reaction, this was done with uncouplers such as FCCP (Figure 3.11A). FCCP transports protons through membranes and prevents formation of a pH gradient, therefore, ACMA quenching does not occur. Another control is if we add inhibitor, in this case DQA, to the reaction before it starts, so there is no complex I activity; we found that there is no ACMA quenching indicating absence of proton translocation into the proteoliposomes (Figure 3.11B). As can be seen in Figure 3.10, proton translocation could be observed both in the parental strain and in mutant H226M. However these measurements are only qualitative and one can only detect if protons are being translocated or not. However, no conclusion about H^+/e^- stoichiometries can be derived.
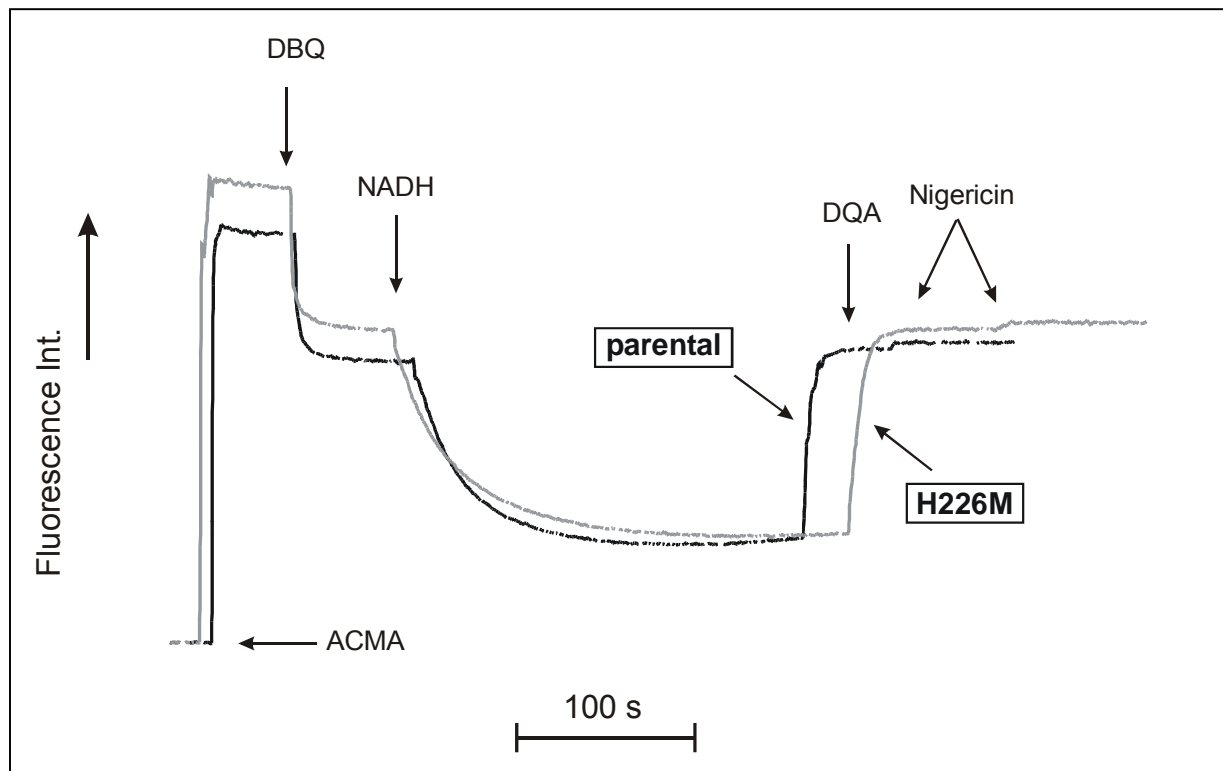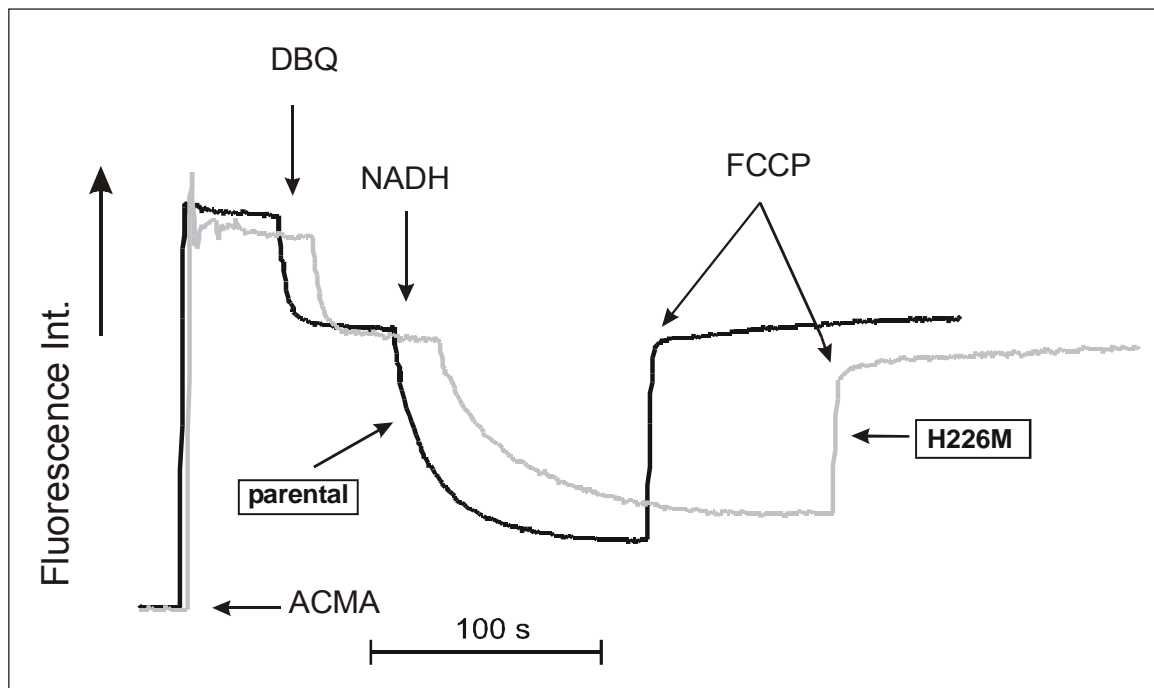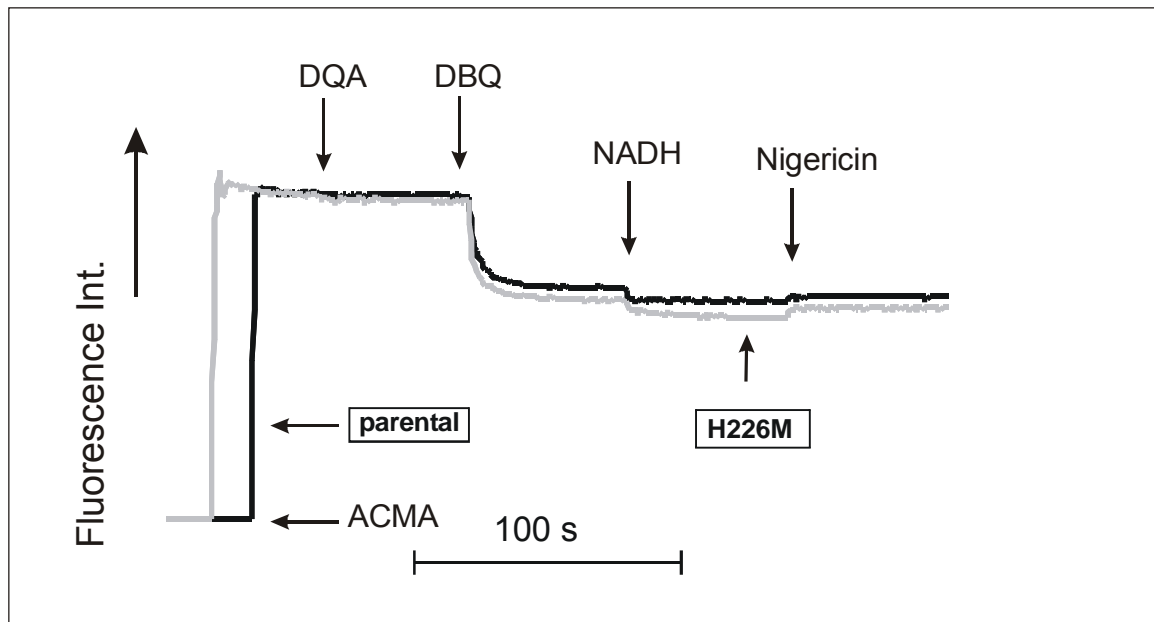
Figure 3.11 ACMA quenching measurements on proteoliposomes for the parental strain and mutant H226M

The reconstitutions followed the 'standard' protocol 2.3.13. All measurements were done in the presence of 50 mM KCl and 5 µM valinomycin with the same volume (20 µl) of proteoliposome solution. 0.5 µM ACMA, 60 µM DBQ and 100 µM NADH were added subsequently. Ionophores/inhibitors were added as indicated 1 µM DQA and 12.5 µM nigericin. A) FCCP control; B) control demonstrating that no proton gradient was built when complex I was inhibited by DQA.

3.2.4 Mutations of Arginine 141 Have Moderate Effects on Activity, but Drastically Reduce Iron-Sulphur Cluster N2 Content

Arg-141 is invariant in all known 49-kDa subunit sequences of complex I and in the large subunits of [NiFe] hydrogenases (Figure 4.1). In the hydrogenase structure it is found in close vicinity to the proximal iron-sulphur cluster (Volbeda *et al.,* 1995). This residue has been changed to alanine, lysine and methionine. In all Arg-141 mutants complex I was assembled (not shown) and complex I content in mitochondrial membranes tended to be even slightly higher than in the parental strain (Table 3.5).

Strain	Complex I		K_M (μM)	I_{50}	
	content (%)	activity (%)		DQA (nM)	rotenone(nM)
Parental	100	100	11	13	600
R141A[1]	130	17	10	21	570
R141K	136	45	13	55	1500
R141M	111	40	11	11	500

Table 3.5 Activity tests, K_M for DBQ and I$_{50}$ for DQA and rotenone measured on mitochondrial membranes of R141 mutants

Complex I content, activity, and inhibitor sensitivity in mitochondrial membranes of site-directed *Y. lipolytica* mutants in the 49-kDa subunit are compared to the plasmid complemented *nucm::URA3* deletion strain (parental). Complex I content is given as specific NADH:HAR oxidoreductase activity in mitochondrial membranes (100% = 1.0 μmol min^{-1}mg^{-1}), dNADH:DBQ oxidoreductase activity was normalised for complex I content (100% = 0.3 μmol min^{-1}mg^{-1}). I_{50}, concentration needed for 50 % inhibition of the inhibitor-sensitive fraction of the dNADH:DBQ oxidoreductase activity.

Mitochondrial membranes from mutant R141A exhibited a dNADH:DBQ activity that was some 80 % reduced, while the two more conservative exchanges R141K and R141M reduced activity only by about 50 %. For 4 different batches of mitochondrial membranes from mutant R141K ubiquinone oxidoreductase activity varied quite substantially between 30 % and 70 % of wild-type activity; the value given in Table 3.5 is the average of all measured values. The K_M value for DBQ was not changed in any of the three mutants, but mutation R141K resulted in a clear 4-5 fold higher I_{50} for

---

[1] Data from Dr. Kashani-Poor

DQA and a 2-3 fold higher I_{50} for rotenone. Of the two other mutations only R141A seemed to have a subtle effect on DQA sensitivity.
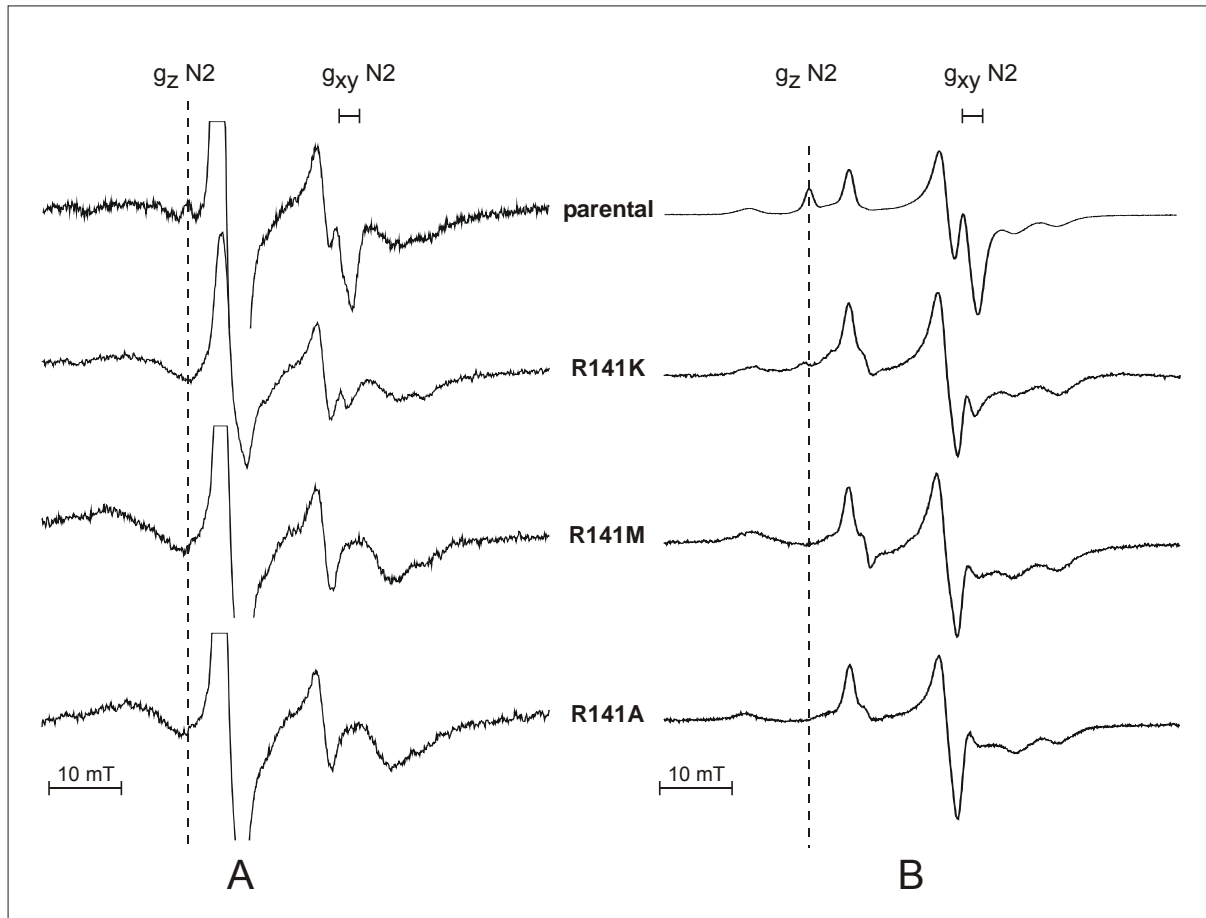
Figure 3.12 EPR spectra of R141 mutants in the 49-kDa subunit. A) mitochondrial membranes. B) purified complex I.

A) EPR spectra of R141 mutants from mitochondrial membranes. The EPR spectra of mitochondrial membranes from *Y. lipolytica* were recorded at a temperature of 12 K, a microwave frequence of 9.48 GHz, a microwave power of 2 mW, and modulation amplitude of 0.8 mT. Membranes were reduced with NADH. The line represents the g_z signal of cluster N2. B) EPR spectra of purified complex I from R141 mutants. EPR spectra of complex I from *Y. lipolytica* reduced with NADH were recorded at a temperature of 12 K, a microwave frequency of 9.48 GHz, a microwave power of 2 mW, and a modulation amplitude of 0.8 mT. Under these condtitions spectra show contributions from clusters N1, N2, N3 and N4 (Djafarzadeh *et al.,* 2000). The dashed lines indicate the position of the g_z signal of cluster N2. Only in the R141K mutant a cluster N2 gz signal was observable and was shifted to lower field values.

In stark contrast to these rather normal functional properties, EPR spectroscopy revealed drastic effects specifically on iron-sulphur cluster N2 (Figure 3.12): In membranes and purified complex I from mutants R141M and R141A, cluster N2 signals were undetectable. Again no altered paramagnetic species were detected in a spectroscopic search under various conditions (not shown). A small amount of cluster N2 in the order of 5 % compared to wild-type level was detectable when mutant R141K was analysed; the very weak g_z signal seemed to be shifted towards lower field values.

To address the question whether cluster N2 was in fact missing in the mutant membranes or whether the cluster had become just undetectable under standard EPR conditions, the possibility that the mutations had turned the spin $S = \frac{1}{2}$ of the ground state of cluster N2 to $S = 3/2$ was considered. EPR signals from Fe_4S_4 clusters with $S = 3/2$ ground states should appear in the $g = 4.0\text{-}5.5$ region, but are very difficult to observe, particularly in the event of significant cluster heterogeneity (Conover *et al.,* 1990; Duderstadt *et al.,* 1999).

The EPR spectra from parental and mutant isolated complex I samples were recorded over a wide field range at low temperature (4.3 K) and high microwave power (63 mW) as shown in Figure 3.13. No indications for novel paramagnetic species could be observed. However, the existence of a $S = 3/2$ spin could not be ruled out completely due to low complex I concentrations and baseline problems in the relevant field region.
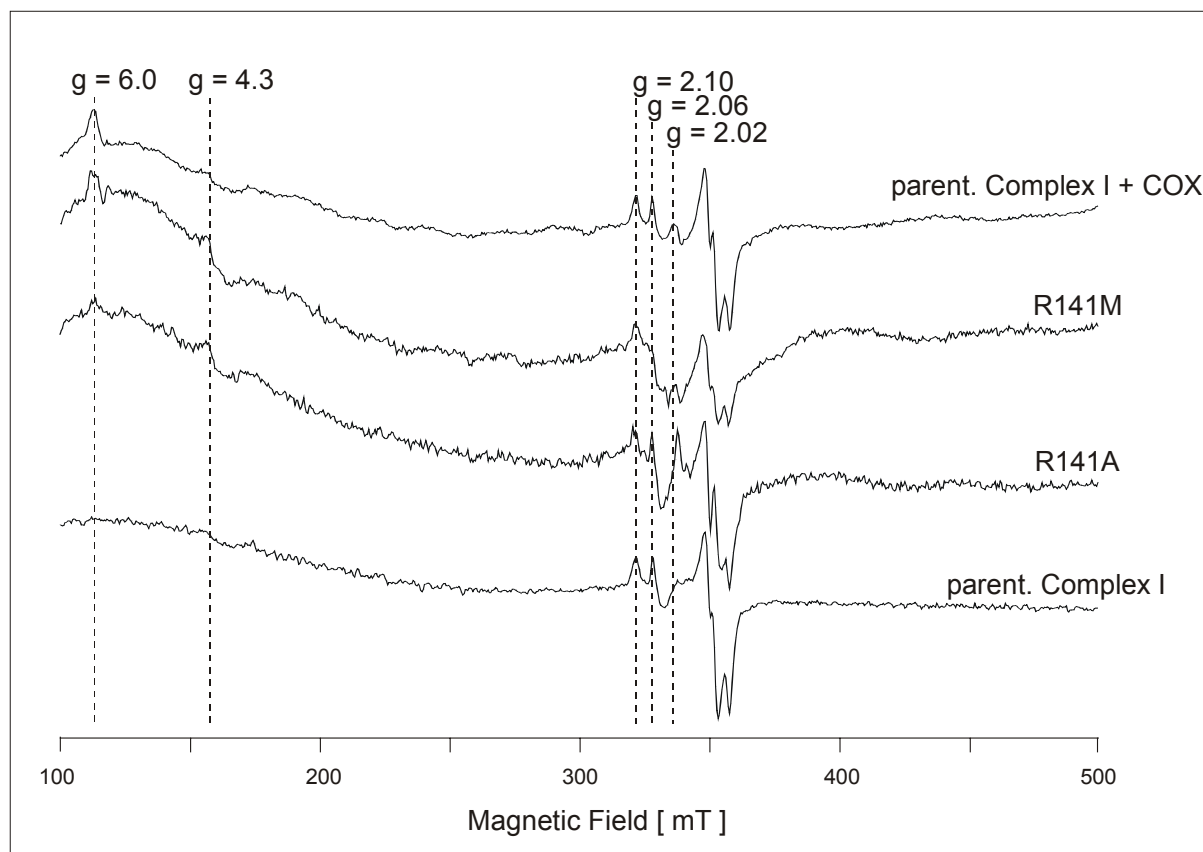
Figure 3.13 Wide-range EPR spectra of isolated complex I from parental and mutant enzyme preparations

To detect possible EPR signals originating from S=3/2 spin states two parental enzyme preparations, one highly pure (bottom) and another containing a small amount of cytochrome oxidase as a contaminant (top) were compared to mutant preparations R141A and R141M (same samples as in Figure 3.12). EPR signals from an S=3/2 state which should appear in the low field region between g = 4 and g = 5.5 could not be identified. The signals at g = 6 in the mutant samples were attributed to the high spin heme of cytochrome oxidase. At g = 4.3 signals from adventitious high-spin Fe(III) were detectable. In the region around g = 2 the g_z-signals of cluster N4 (g_z = 2.10), N5 (g_z = 2.06) and N1 (g_z = 2.02) could be identified. In this field range the EPR signals from cluster N2 are power saturated completely. All samples had protein concentrations between 5–10 mg/ml and were reduced by NADH. EPR conditions: microwave frequency 9.47 GHz, modulation amplitude 1 mT, microwave power 63 mW, temperature 4.3 K.

3.2.5 Mutations of Histidine 91 and Histidine 95 Result in Complete Loss of Catalytic Activity

Residues His-91 and His-95 are strictly conserved in all complex I 49 kDa subunit sequences but not in [NiFe] hydrogenases (Figure 4.1). However, conservation of the structural fold between homologous subunits predicts both residues to be close enough to iron-sulphur cluster N2 to be candidate ligands. His-91 and His-95 were changed into alanine, methionine and arginine. All His-91 and His-95 mutants contained normal or, in the case of H91M and H91R, only slightly reduced amounts of complex I (Table 3.6) that was assembled normally (Figure 3.14). In mitochondrial membranes from all six mutant strains dNADH:DBQ activity was below the detection level of 5 %. However, EPR spectra of all iron-sulphur clusters, including cluster N2 were indistinguishable from those of the parental strain (Figure 3.15). This was also true for complex I from mutant H95A that was purified as a representative of this group of mutations.

Strain	Complex I	
	content (%)	activity (%)
Parental	100	100
H91A	117	<5
H91M	76	<5
H91R	75	<5
H95A	132	<5
H95M	116	<5
H95R	98	<5

Table 3.6 Activity tests measured on mitochondrial membranes from H91 and H95 mutants

Complex I content is given as specific NADH:HAR oxidoreductase activity in mitochondrial membranes (100% = 1.0 μmol min^{-1}mg^{-1}), dNADH:DBQ oxidoreductase activity was normalised for complex I content (100% = 0.3 μmol min^{-1} mg^{-1}).
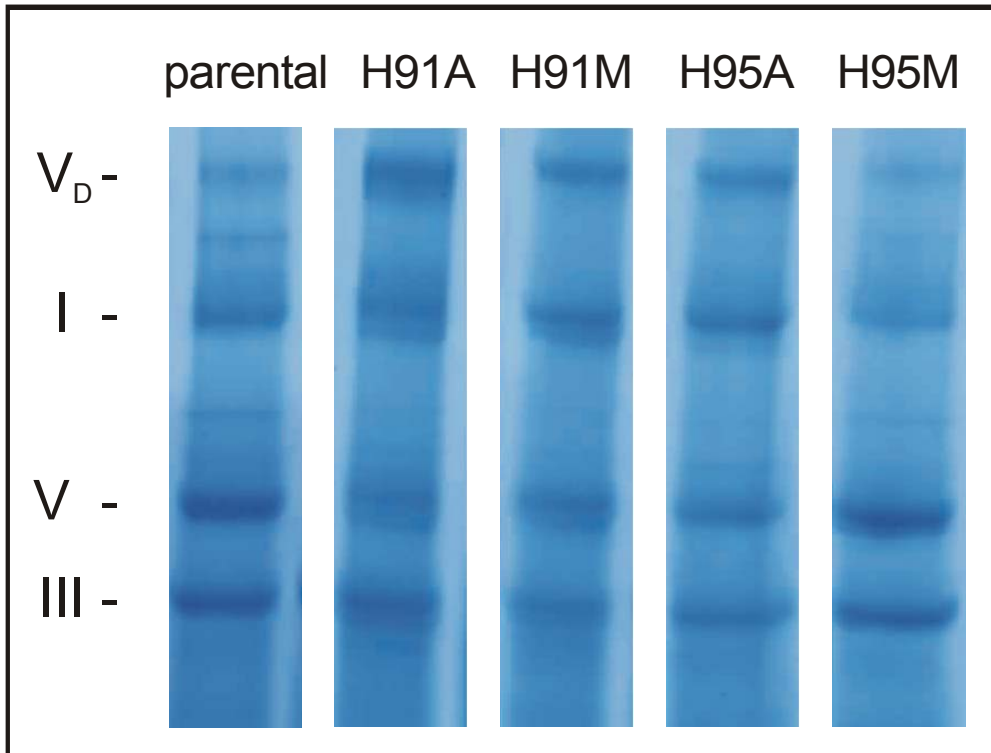
Figure 3.14 1.6 mm Blue Native Gel (4/4 to 13% gradient) from isolated mitochondrial membranes

Isolated mitochondrial membranes from parental strain and from mutants H91A, H91M, H95A and H95M. Roman numbers show individual complexes of the respiratory chain. V_D is complex V dimer that occurs at lower detergent concentrations. All mutants have assembled complex I.
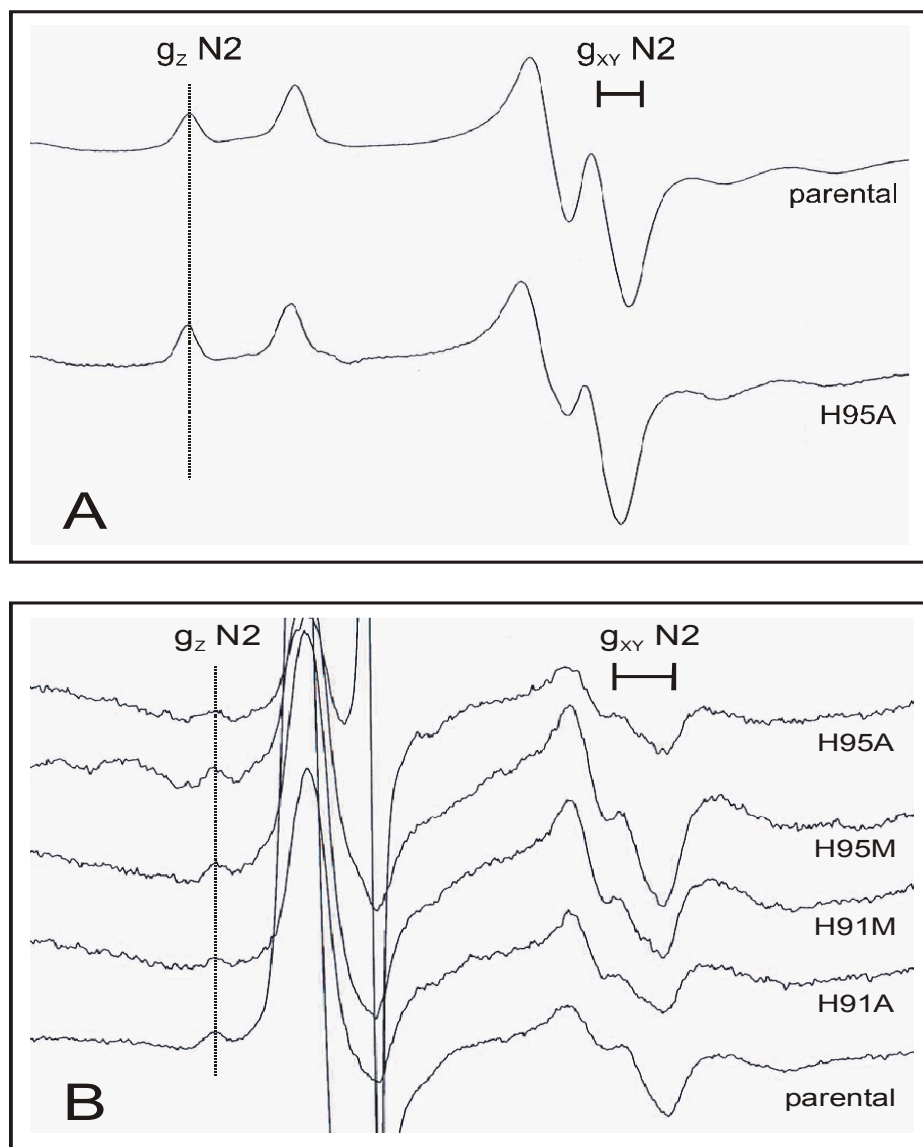
Figure 3.15 EPR spectra of H91 and H95 mutants in the 49-kDa subunit. A) Spectra of purified complex I from parental strain and mutant H95A. B) Spectra of mitochondrial membranes.

A) EPR spectra of purified complex I from parental strain and mutant H95A. EPR spectra of complex I reduced with NADH were recorded at a temperature of 12 K, a microwave frequency of 9.48 GHz, a microwave power of 2 mW, and a modulation amplitude of 0.8 mT. Under these conditions spectra show contributions from clusters N1, N2, N3 and N4 (Djafarzadeh *et al.,* 2000). The dashed lines indicate the position of the g_z signal of cluster N2. B) EPR spectra of H91 and H95 mutants from mitochondrial membranes. The EPR spectra of mitochondrial membranes were recorded at a temperature of 12 K, a microwave frequence of 9.48 GHz, a microwave power of 2 mW, and modulation amplitude of 0.8 mT. Membranes were reduced with NADH. The line represents the g_z signal of cluster N2.

3.2.6 Mutations of Arginine 466 Change Functional Properties of Complex I

The C-terminal arginine R466 is also strictly conserved among complex I from various species. In [NiFe] hydrogenases it corresponds to a strictly conserved histidine that is ligand to a Mg^{2+} site and resides about 9 Å from the [NiFe] site and 14 Å from the proximal iron-sulphur cluster. R466 was changed into alanine, methionine, histidine and glutamate. Assembled complex I was found in membranes from all Arg-466 mutants (not shown) but, with the exception of mutant R466H, content was significantly reduced by 30-50 %.

Strain	Complex I		K_M (μM)	I_{50}	
	content (%)	activity (%)		DQA (nM)	rotenone(nM)
Parental	100	100	11	13	600
R466A	53	75	11	35	750
R466M	73	9	-	-	-
R466H	99	85	25	36	900
R466E	50	53	9	20	700

Table 3.7 Activity tests, K_M for DBQ and I_{50} for DQA and rotenone measured on mitochondrial membranes of R466 mutants

Complex I content, activity, and inhibitor sensitivity in mitochondrial membranes of site-directed *Y. lipolytica* mutants in the 49-kDa subunit are compared to the plasmid complemented *nucm::URA3* deletion strain (parental). Complex I content is given as specific NADH:HAR oxidoreductase activity in mitochondrial membranes (100% = 1.0 μmol $min^{-1}mg^{-1}$), dNADH:DBQ oxidoreductase activity was normalised for complex I content (100% = 0.3 μmol $min^{-1}mg^{-1}$). I_{50}, concentration needed for 50 % inhibition of the inhibitor-sensitive fraction of the dNADH:DBQ oxidoreductase activity

As a strictly aerobic organism, *Y. lipolytica* does not regulate expression levels for complex I. Hence diminished content usually indicates structural destabilization of the complex. In fact, reduced stability made it difficult to isolate sufficient amounts of protein for EPR spectra of purified complex I from these mutants. Still, specific ubiquinone reductase activity was strongly reduced only in membranes from R466M, while the other mutants showed around 80 % (R466A/ R466H) or about 50 %

(R466E) of wild-type activity (see Table 3.7). Steady-state kinetics revealed a 2-3fold increase in the K_M for DBQ for mutant R466H, while this parameter was unaltered in mutants R466A and R466E. These three mutations also exhibited a small, but significant hyposensitivity toward DQA. The normally assembled and most active mutant in this set, R466H, also gave rise to EPR spectra of mitochondrial membranes that were indistinguishable from a parental spectrum (Figure 3.1). With spectra from mitochondrial membranes only, a detailed analysis of the spectral signature of mutants R466A, R466M and R466E was not possible. However, it seemed clear that iron-sulphur cluster N2 was drastically reduced in all of these three mutants, but even in membranes from R466A a trace amount of cluster N2 was detectable in the g_{xy} region.
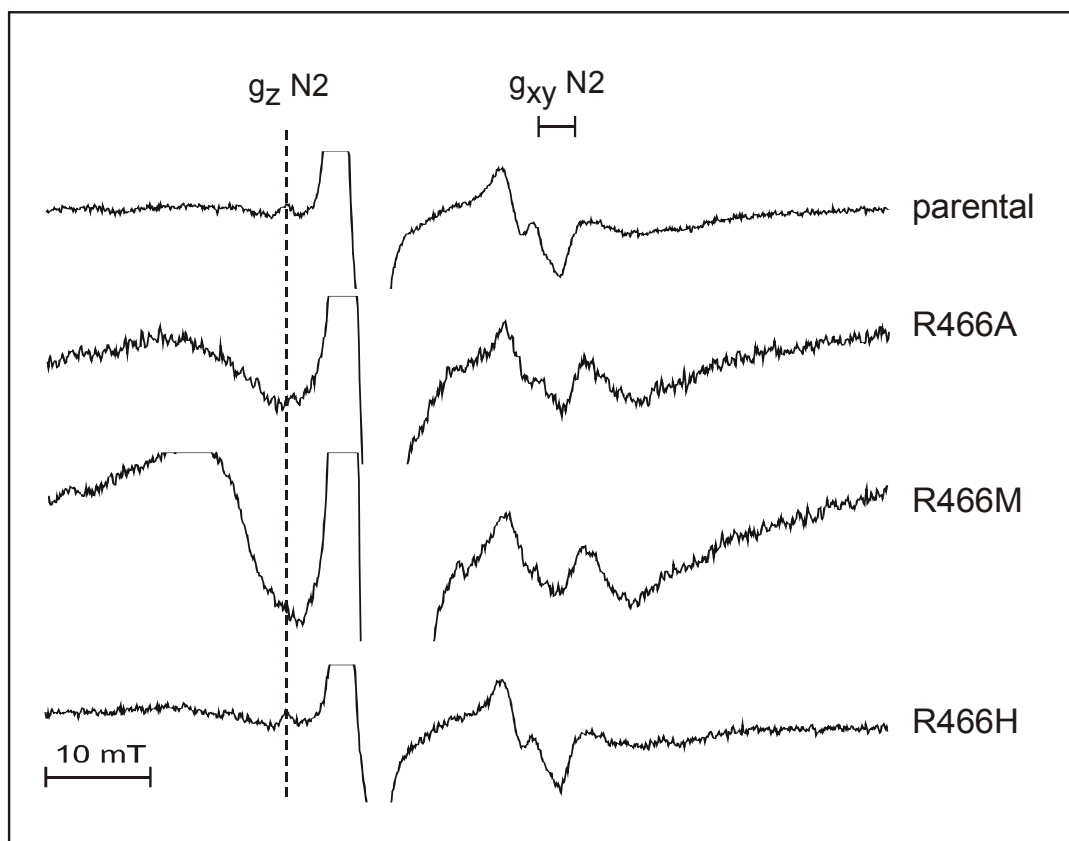

Figure 3.16 EPR spectra of mitochondrial membranes from R466 mutants

Samples were reduced with NADH.The dashed line represents the gz signal of cluster N2. Only mutant R466H shows a similar spectrum as the parental strain. However, the concentration of complex I was very low in mutants R466A, R466M and R466E.

3.2.7 Mutagenesis of Serine 146

Mutations of residues aspartate 143, valine 460 and glutamate 463 in *Y. lipoytica* that correspond to three of four cysteines that ligate the [NiFe] centre in [NiFe] hydrogenases had already been investigated (Kashani-Poor *et al.,* 2001b). The fourth residue, Ser-146 unlike the other three residues from this series is not strictly conserved and has not been studied yet. Inhibitor resistance found in mutants D458A in *Y. lipolytica* (Kashani-Poor *et al.,* 2001b), V407M in *Rh. capsulatus* (Darrouzet *et al.,* 1998) and the corresponding V460M in *Y. lipolytica* raised the question if Ser-146, since it resides in the same domain as resistance mutants according to the [NiFe] hydrogenase structural model, would have any influence on catalytic properties or inhibitor sensitivity.

Strain	Complex I		K_M (μM)	I_{50}	
	content (%)	activity (%)		DQA (nM)	rotenone(nM)
Parental	100	100	11	13	600
S146A	107	110	10	10	300
S146C	100	100	12	**80**	**1500**

Table 3.8 Activity tests, K_M for DBQ and I_{50} for DQA and rotenone measured on mitochondrial membranes of S146 mutants

Complex I content, activity, and inhibitor sensitivity in mitochondrial membranes of site-directed *Y. lipolytica* mutants in the 49-kDa subunit are compared to the plasmid complemented *nucm::URA3* deletion strain (parental). Complex I content is given as specific NADH:HAR oxidoreductase activity in mitochondrial membranes (100% = 1.0 μmol min^{-1}mg^{-1}), dNADH:DBQ oxidoreductase activity was normalized for complex I content (100% = 0.3 μmol min^{-1}mg^{-1}). I_{50}, concentration needed for 50 % inhibition of the inhibitor-sensitive fraction of the dNADH:DBQ oxidoreductase activity

Ser-146 was mutated into Ala, Cys, Val and Asp. Complex I content and dNADH:DBQ activity were parental in both mutants S146A and S146C. K_M values were also parental (see Table 3.8). Mutant S146A showed moderate hypersensitivity toward rotenone, whereas I_{50} for DQA was parental. Mutant S146C exhibited an about six fold higher I_{50} value towards DQA and was 2.5fold less sensitive towards rotenone (Figure 3.17).
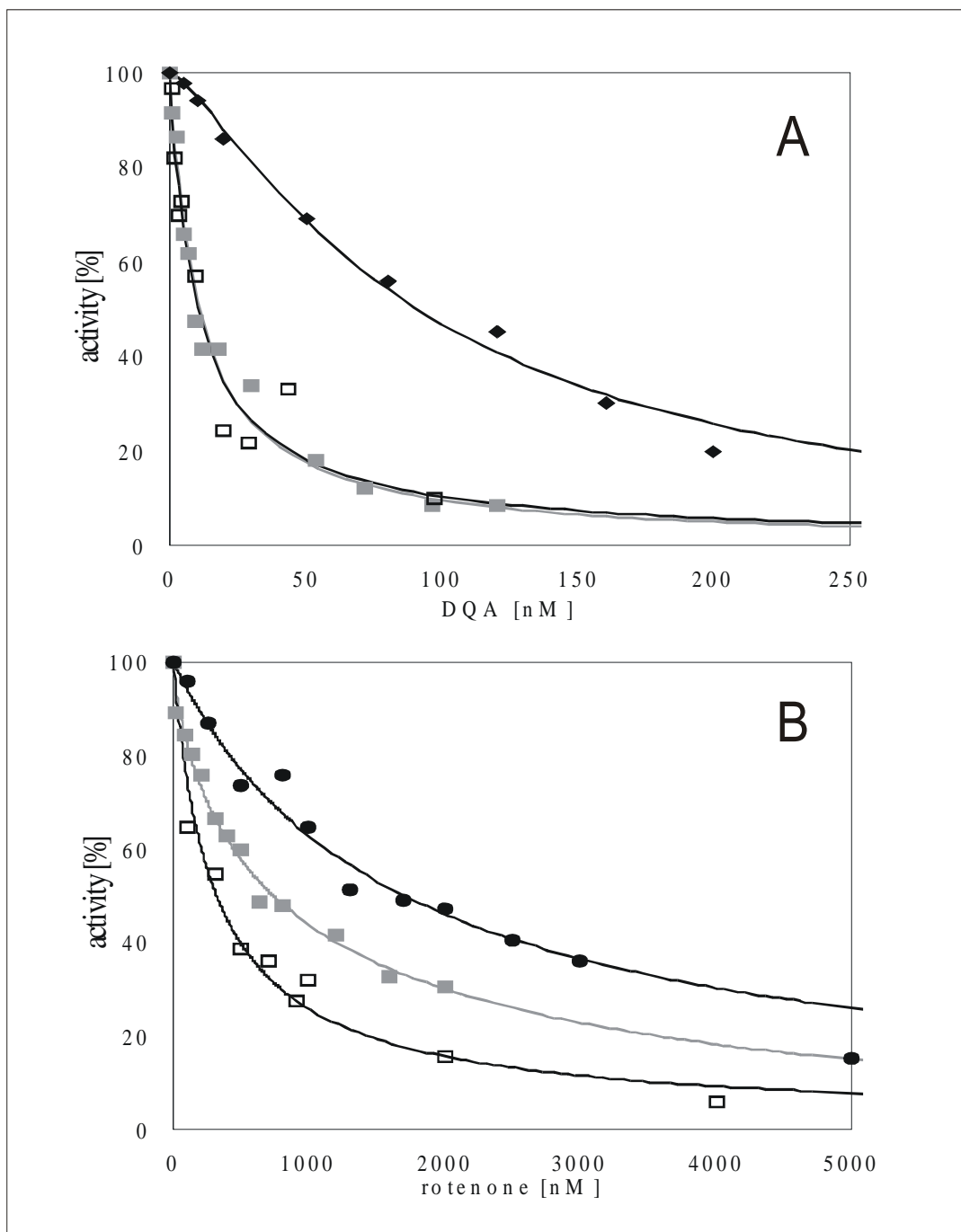
Figure 3.17 DQA and rotenone inhibition in mutants S146A and S146C

The diagram shows DQA (n-decyl-quinazoline amine) (A) and rotenone (B) inhibition of dNADH:DBQ oxidoreductase activity in mitochondrial membranes from (■)parental strain (plasmid complemented strain), (□) mutant S146A and (•) mutant S146C. Mutant S146C showed significant resistance (~ 6fold higher I_{50}) toward DQA and minor resistance (2-3fold higher I_{50}) towards rotenone. Mutant S146A showed moderate hypersensitivity toward rotenone. I_{50} values are listed in Table 3.8.

3.3 Remodelling of Human Pathogenic 49-kDa Mutations in *Y. lipolytica*

As mentioned in the introduction three human pathogenic mutations in 49-kDa subunit of complex I were remodelled in *Y. lipolytica*, namely R231Q, P232Q and S416P. Residues Arg-231 and Pro-232 according to structural model reside very close to [NiFe] active centre of [NiFe] hydrogenases. Arg-231, Pro-232 and Ser-416 are marked grey in Figure 4.1A.

	Strain	Complex I		K_M (μM)	I_{50}	
		content (%)	activity (%)		DQA (nM)	Rotenone(nM)
	Parental	100	100	11	13	600
human pathogenic mutations	R231Q	84	101	16	17	900
	P232Q	38	17	-	-	-
	S416P	90	111	17	17	1100
	R231E	112	74	29	20	850
	P232G	67	56	-	-	-
	S416A	109	86	39	19	1500

Table 3.9 Activity tests, K_M for DBQ and I_{50} for DQA and rotenone measured on mitochondrial membranes

Complex I content, activity, and inhibitor sensitivity in mitochondrial membranes of site-directed *Y. lipolytica* mutants in the 49-kDa subunit are compared to the plasmid complemented *nucm::URA3* deletion strain (parental). Complex I content is given as specific NADH:HAR oxidoreductase activity in mitochondrial membranes (100% = 1.0 μmol min^{-1}mg^{-1}), dNADH:DBQ oxidoreductase activity was normalised for complex I content (100% = 0.3 μmol min^{-1}mg^{-1}). I_{50}, concentration needed for 50 % inhibition of the inhibitor-sensitive fraction of the dNADH:DBQ oxidoreductase activity.

Mutant R231Q had regular complex I content according to NADH:HAR activity. Mutant R231Q was fully assembled as seen in BN-PAGE (Figure 3.18). dNADH:DBQ activity was the same as in the parental strain (Table 3.9). No significant differences were observed in the K_M for DBQ and I_{50} for DQA and rotenone. Purified complex I

from mutant R231Q had wild-type EPR spectra and could be reactivated by the addition of asolectin (data not shown). Also, proteoliposomes containing R231Q mutant complex I showed no difference in proton translocation to the parental strain in ACMA dye measurements (data not shown). In stark contrast mutant P232Q had very low NADH:HAR activity, less than 40 % of the wild type and in BN-PAGE (Figure 3.18) the complex I band was completely absent. dNADH:DBQ activity was very low, less than 20 % (Table 3.9) of the parental activity. Mutant S416P had regular complex I content and the enzyme was assembled normally as judged from BN-PAGE (Figure 3.18). dNADH:DBQ activity was parental (Table 3.9).
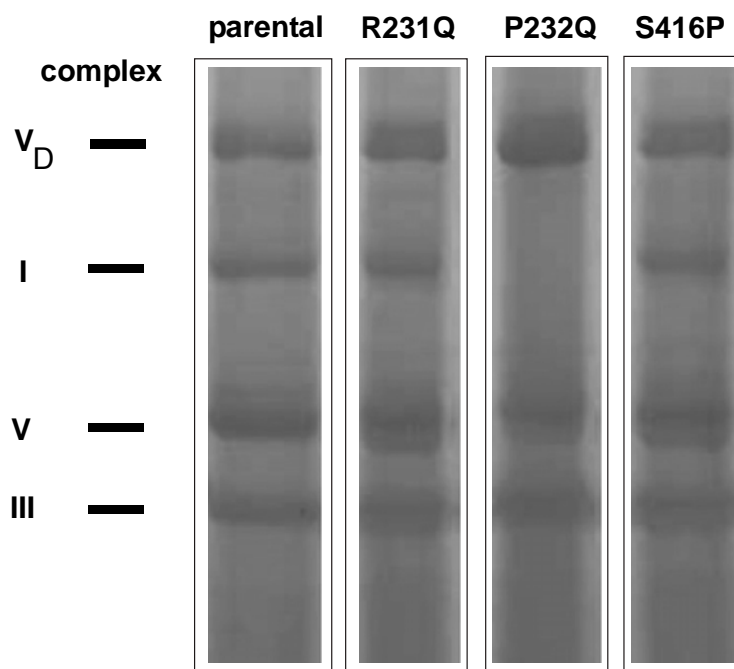
Figure 3.18 1.6 mm Blue Native Gel (4/4 to 13% gradient) from isolated mitochondrial membranes

Isolated mitochondrial membranes from parental strain and from mutants R231Q, P232Q, S416P. Roman numbers show individual complexes of the respiratory chain. V_D is complex V dimer that occurs at lower detergent concentrations. Mutant R231Q and S416P have assembled complex I whereas mutant P231Q shows no assembled complex I.

In summary mutants R231Q and S416P showed no effect on dNADH:DBQ activity and complex I assembly; mutant R231Q could also be reactivated after purification and exhibited proton pumping. From these results it was unclear why these mutations

are pathogenic in humans. One possible explanation was that the mutations made complex I less stable. To explore this possibility, dNADH:DBQ activities were checked after incubation for 10 min at different temperatures. As can be derived from Figure 3.19 there was no difference in temperatures stability between mutants and parental mitochondrial membranes.
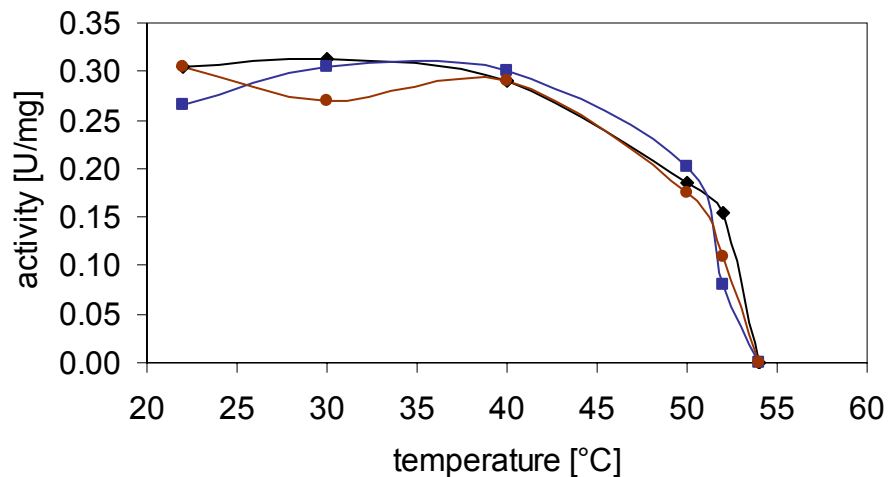
Figure 3.19 Temperature stability of mutants R231Q and S416P

dNADH:DBQ activities measured after incubation for 10 min at different temperatures, normalised to NADH:HAR oxidoreductase activities. (♦) parental; (■) R231Q; (●) S416P.

Since mutants R231Q and S416P did not show appreciable differences to the parental strain, more drastic mutations were introduced such as R231E and S416A. Mutant P232Q had no assembled complex I, so the more conservative mutation P232G was introduced. In mutant R231E there was no effect on dNADH:DBQ activity and complex I assembly. The K_M value was more than 2 fold higher. I_{50} values for DQA and rotenone were just slightly higher. Complex I from mutant P232G in contrast to human pathogenic mutation P232Q was assembled as judged by BN-PAGE. However, NADH:HAR activity was about one third and the NADH:DBQ activity about 50 % lower than in the parental strain. Mutant S416A had regular complex I content and dNADH:DBQ activity was only slightly reduced. The K_M value was more than 3fold higher. I_{50} value for DQA was just slightly higher and for rotenone 2fold higher compared to the parental values (see Table 3.9).

3.4 Mitochondrially Targeted eYFP in *Yarrowia lipolytica*

Some human mutations e.g. R231Q in the 49-kDa subunit have been reported to have a negative effect on the complexity of the mitochondrial network. One goal of the present work was to explore whether similar effects can also be observed in *Y. lipolytica*. To be able to visualise mitochondria in the yeast *Y. lipolytica,* eYFP was chosen because GFP had already been successfully expressed in mitochondria in other related yeasts such as *S. cerevisiae*.

3.4.1 Strategy

To import eYFP into *Y. lipolytica* mitochondria it is necessary to have a mitochondrial targeting signal. Two different approaches, free eYFP and eYFP fused with a mitochondrial protein, were tried.
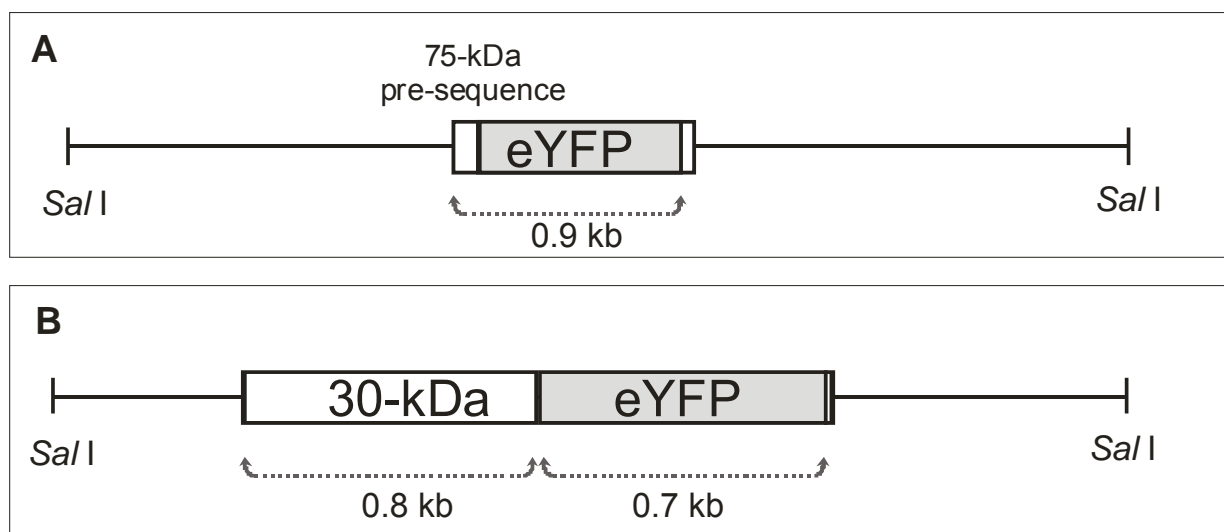
Figure 3.20 Strategies for expression of eYFP in *Y. lipolytica* mitochondria

For detailed sequence see Appendix. A) 75-kDa subunit pre-sequence is used as a targeting signal for import into mitochondria of *Y. lipolytica*. B) fusion of the complex I 30-kDa subunit with eYFP.

The first strategy was to import free eYFP into mitochondria by fusing the mitochondrial import signal of the 75-kDa subunit with eYFP. The 7.7 kb product of the inverse anchor PCR with primers 75NdeInc and 75NdeIc with vector pSK/*NUAM* (9.7 kb) as template was self ligated and amplified in *E. coli*. The newly generated

plasmid (called pLG1) was digested with *Nde* I and its ends dephophorylated to prevent self-ligation. The 0.7 kb product of anchor PCR with primers EYFPc and EYFPnc with pEYFP as template was digested with *Nde* I. The two products were ligated and the resulting plasmid was called pYFP. The *Sal* I fragment of pYFP as shown in Figure 3.20A was subcloned into pUB26 and the new plasmid (called pUB26y) was transferred into strain PIPO. CLSM experiments revealed no fluorescence from this strain. The reason for this was not investigated further.

The second strategy was to fuse eYFP with a mitochondrial protein. The 30-kDa subunit of complex I was chosen because of its small size and also because a His-Tag had already been successfully attached to its C-terminus (Kashani-Poor *et al.,* 2001a). In plasmid pINA240/30-Htag2 *Nde* I site was generated between the C-terminal end of the 30-kDa subunit gene and the his-tag with inverse anchor PCR using primers 30kNdeInc and 30kHtgnc2. The resulting plasmid was restricted with *Nde* I and the above described 0.7 kb PCR product from the EYFP gene was subcloned into this *Nde* I site. The *Sal* I fragment (Figure 3.20B) from the resulting plasmid containing the 30-kDa subunit gene fused in frame with EYFP was subcloned into pUB26. This construct was called pEYFP30. Plasmid pEYFP30 was transferred into strains PIPO and ∆nugm GH1. CLSM on these straines revealed clear signs of fluorescence (Figure 3.21).
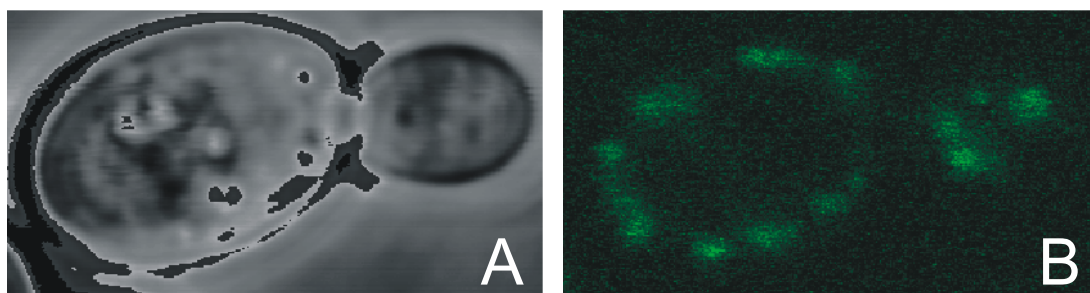
Figure 3.21 *Y. lipolytica* **cells from strain PIPO complemented with plasmid pYFP30 A) Phase Contrast Microscopy and B) CLSM**

The cells were harvested from an overnight culture in YPD medium in the presence of hygromycin B, washed twice with PBS buffer and fixed in 1 % agarose gel. The cells were excited at 475 nm and the emission peak at 508 nm was detected. Only the middle slice from a series of 10 optical sections is shown.
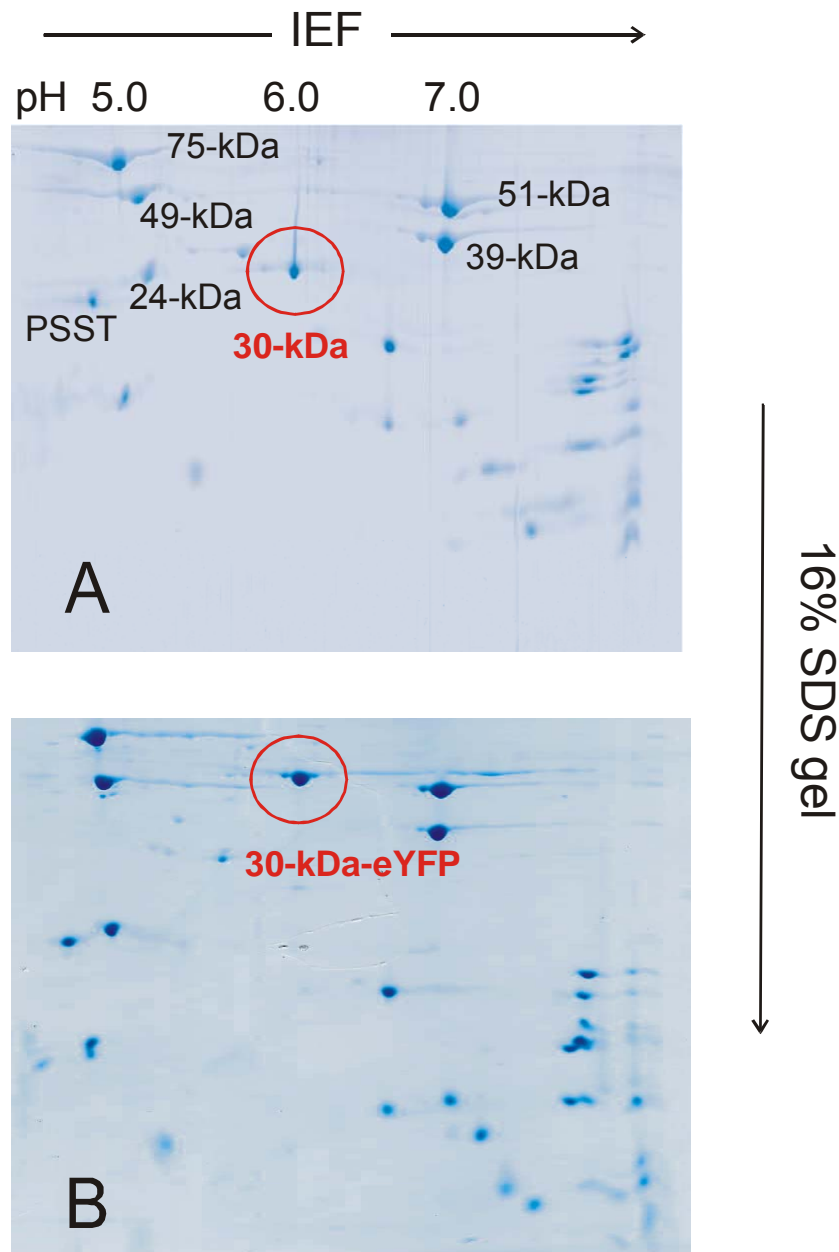
Figure 3.22 Two dimensional isoelectric focusing A) PIPO[1] B) Δnugm GH1 complemented with pEYFP30 plasmid

For IEF-separation of Complex I samples (400 µg/ml) in the first dimension the IPGphor system (Amersham Pharmacia Biotech) and 13 cm immobilised pH gradient (IPG) strips (pH 3-10) were used. The second dimension was 16 % SDS PAGE. A) PIPO, 30-kDa subunit is circled in red. B) complex I from strain Δnugm GH1 complemented with pEYFP30 plasmid. As expected the 30-kDa subunit band does not occur and a new band (circled in red) of about 53-kDa that presents the 30-kDa subunit fused with eYFP is observed.

---

[1] From Albina Abdrakhmanova unpublished data

Complex I from strain Δnugm GH1 complemented with plasmid pEYFP30 was purified and complex I subunits were separated by IEF (Isoelectric Focusing, pH 3-10). Subsequently a second dimension 16% SDS gel was carried out. The SDS gels are shown in Figure 3.22. The wild-type 30-kDa (in Figure 3.22A) and also the new generated subunit (in Figure 3.22B) that presents the 30-kDa subunit fused with eYFP (~ 53 kDa) are circled in red.

In the next step, the normal or the R231Q mutant version of the *NUCM* gene were subcloned as 3.1 kb *Nhe* I fragments into pEYF30, resulting in constructs pEYFP30-*NUCM*-WT and pEYFP30-*NUCM*-R231Q which were transformed into strain Δnucm. In both the normal (in figures marked as EYFP) and the R321Q mutant (in figures marked as EYFP/R231Q) strains there were clear signs of fluorescence (Figure 3.23). As can be derived from CLSM pictures, *Y. lipolytica* cells take a spherical to ovoid shape and the mitochondria are arranged in groups at the periphery of the cells, very close to the cell wall.
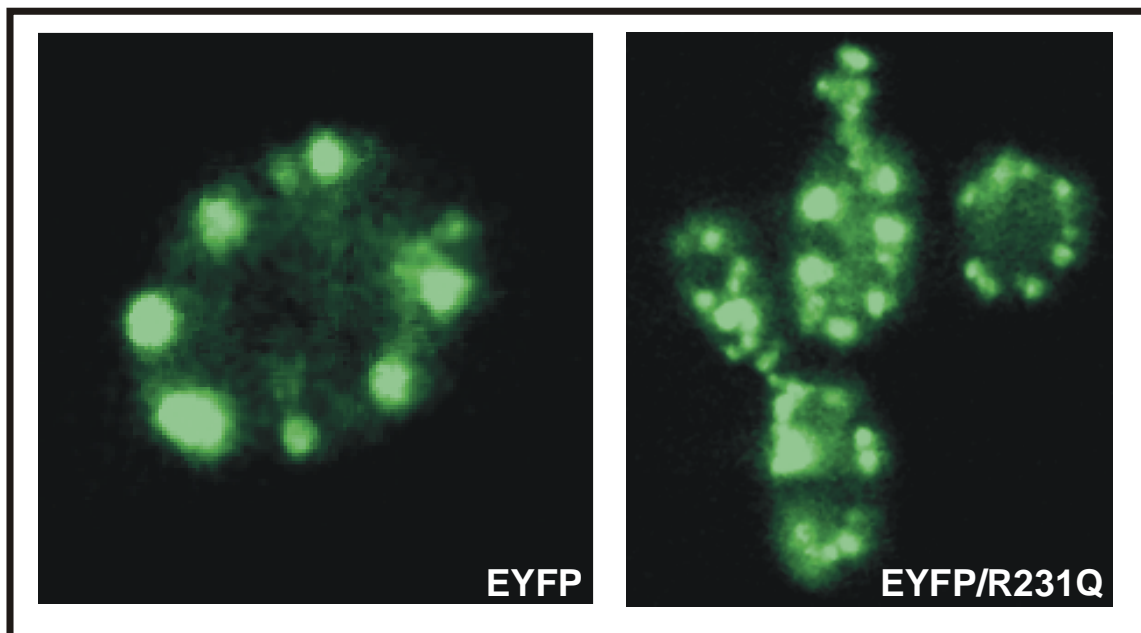
Figure 3.23 CLSM of the EYFP and the EYFP/R231Q mutant strain

EYFP (Δnucm strain complemented with plasmid pEYFP30-*NUCM*), EYFP/R231Q (Δnucm strain complemented with mutated (R213Q) plasmid pEYFP30-*NUCM*). The cells were harvested from an overnight culture in YPD medium in the presence of hygromycin B, washed twice with PBS buffer and fixed in 1 % agarose gel. The cells were excited at 475 nm and the emission peak at 508 nm was detected. Only the middle slice from a series of 10 optical sections is shown.

There was no obvious difference between the normal and the R231Q mutant strains in CLSM pictures. To check for expression of the eYFP fusion construct a Western Blot with Anti-GFP antibody was run (Figure 3.24). In both the normal and the R231Q mutant strains not only a band corresponding to fully assembled complex I but also subcomplexes of complex I were detected. These subcomplexes might not just be breakdown products of complex I but may represent assembly intermediates. They might also indicate interferance of the fusion of the 30-kDa subunit with eYFP with assembly of complex I.
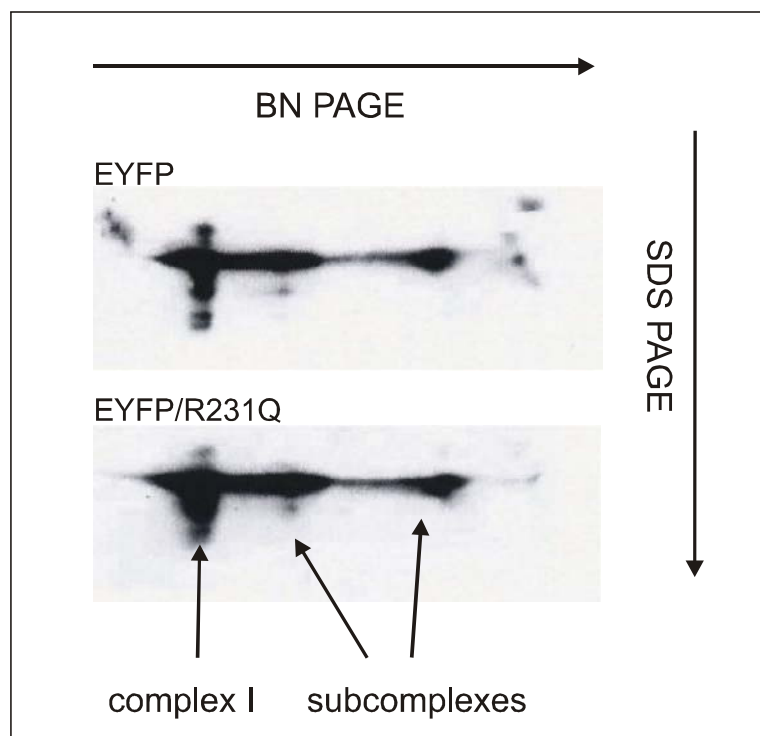
Figure 3.24 Western Blot of EYFP and EYFP/R231Q mutant with an anti-GFP[1] antiserum

Western Blot of two dimensionl BN-PAGE with mitochondrial membranes detected with a polyclonal rabbit anti-GFP primary and a peroxidase conjugated swine anti-rabbit polyclonal secondary antibody.

---

[1] Western Blot was carried out by Dr. Leo Nijtmans in Nijmegen, The Netherlands

4 DISCUSSION

4.1 Ligands of Iron-Sulphur Cluster N2

In the PSST subunit of complex I from different organism there are four conserved cysteines (*Y. lipolytica* nomenclature: Cys-85, -86, -150 and -180) that could ligate iron-sulphur cluster N2. However, according to the homology of the PSST subunits and the small subunits of [NiFe] hydrogenases only three conserved cysteines correspond to the ligands of the proximal iron-sulphur cluster. In addition two cysteines namely Cys-85 and Cys-86 are direct neighbours and it is energetically not favoured that both cysteines serve as ligands of cluster N2 although this was recently proposed by Friedrich (Flemming *et al.,* 2003). Up to now all attempts to find the missing fourth ligand in the PSST subunit have failed (Ahlers *et al.,* 2000b; Garofano *et al.,* 2003). According to the hypothesis that subunits PSST and 49-kDa are direct neighbours and that cluster N2 resides on the interface between these two subunits, one could speculate that the missing fourth ligand resides in the 49-kDa subunit (Kashani-Poor *et al.,* 2001b).

His-228 in the [NiFe] hydrogenase from *D. gigas* forms a hydrogen bond to the proximal iron-sulphur cluster (Volbeda *et al.,* 1995). This His-228 corresponds to a highly conserved histidine in complex I (*Y.l.* His-226 see Figure 4.1). Assuming that during evolution the protein fold of the large subunit of [NiFe] hydrogenases has been maintained in the 49-kDa subunit of complex I, His-226 would be in a distance less than 5 Å from cluster N2. Thus it could also serve as fourth ligand to this cluster (Figure 4.2). In mutant H226R complex I was not assembled and in H226A there was no EPR visible cluster N2 and at the same time complex I activity was abolished. Therefore, one could assume that His-226 plays a prominent role in the catalytic process of quinone reduction and maybe in proton pumping.

Not only His-226 showed such remarkable effects on the catalytic process and on the properties of cluster N2 but also residue Arg-141 if mutated into alanine followed a very similar pattern. R141A showed also abolished complex I activity and no EPR visible cluster N2 (Kashani-Poor *et al.,* 2001b). These results further support the

74

hypothesis that cluster N2 resides on the interface between subunits PSST and 49-kDa.

```
Alignment A
               H91 H95                              H120                    R141
Yl-NUCM   NFGPQHPAAHGVLRLILELSGEEIIRSDPHVGLLHRGTEKLIEYKTYMQALPYFDRLDYVS 146
Nc.NUCM   NFGPQHPAAHGVLRLILELKGEEIVRADPHVGLLHRGTEKLCEYRTYLQALPYFDRLDYVS 111
Bt-49kDa  NFGPQHPAAHGVLRLVMELSGEMVRKCDPHIGLLHRGTEKLIEYKTYLQALPYFDRLDYVS 159
Rc-NouD   NFGPQHPAAHGVLRMVLELDGEIVERADPHIGLLHRGTEKLMESRTYLQNTPYFDRLDYVA  74
Ec-NuoCD  NLGPNHPSAHGAFRIVLQLDGEEIVDCVPDIGYHHRGAEKMGERQSWHSYIPYTDRIEYLG  73


            H226             S416              R466
Yl-NUCM   ARLHAAYVRPGGV 235  VVSDGSERPY 423   DLVFGEVDR 466
Nc.NUCM   ARLHAAYVRPGGV 200  VVSDGSERPY 318   DLVFGEVDR 431
Bt-49kDa  ARMHAAYVRPGGV 248  LVSDGSSRPY 436   DIVFGEVDR 479
Rc-NouD   ARLHANYVFPGGV 162  LVADGTNKPY 350   DVVFGEIDR 394
Ec-NuoCD  FRMHPAWFRIGGV 161  LTSDGSTMSY 349   DFVMSDVDR 393
```

```
Alignment B
               H91 H95                          H120
Yl-NUCM   FTINFGPQHPAAHGVLRLILELSGEEIIRSDPHVGLLHRGTEKLIEYKTYMQALPYF 140
Mb-EchE   TVIPFGPQHPVLPEPVSLKLEIDDNVVVGVLPSLGYVHRGLETFINTKDFNQTTYVC  59
Df-HydB   GPIVVDPIT-RIEGHLRIMVEVENGKVKDAWS-SSQLFRGLEIILKGRDPRDAQHFT  68


            R141             H226                      R466
Yl-NUCM   DRLDYVSMMTNEQ 153  GARLHAAYVRPGGVS 236  AVAIIGTMDLVFGEVDR 466
Mb-EchE   ERICGICSALHGI  72  GNRVIHSISKVGGVT 156  VPIVVLTIDPCVSCTER 358
Df-HydB   QRACGVCTYVHAL  81  GKNPHTQFTVVGGCS 238  ILRTVHAFDPCIACGVH 549
```

Figure 4.1 Alignments

All alignments were done using the program CLUSTAL W. In alignments A and B the [Ni] ligating cysteines in the hydrogenase sequences are highlighted in blue, histidines in red and arginines in yellow the positions of mutations, human pathogenic are marked in grey. A: Sequences of the 49 kDa subunit from *Y. lipolytica*, *N. crassa*, *Bos taurus*, *P. denitrificans*, *Rh. capsulatus* and *E. coli*. B: 49-kDa subunit of complex I from *Y. lipolytica* aligned with the EchE subunit of the membrane bound [NiFe] hydrogenase from *M. barkeri* and the large subunit of the soluble [NiFe] hydrogenase from *D. fructosovorans*. The epitope recognised by a monoclonal antibody (49.2) against the *Y. lipolytica* 49-kDa subunit is underlined (Zickermann *et al.,* 2003)

4.1.1 Histidine 226

Very specific and striking effects on cluster N2 were observed when residue His-226 was exchanged. When it was substituted by a small hydrophobic alanine residue cluster N2 could not be detected in EPR spectra. On the other hand, the more conservative exchange to methionine (H226M) gave rise to EPR signals that were reduced in intensity and shifted towards lower field values. Other mutations in these positions resulted in dramatic reduction (H226C, H226Q) of cluster N2 as judged by EPR spectroscopy. These results initially seemed to support the already mentioned hypothesis that His-226 could serve as 4th ligand of cluster N2.
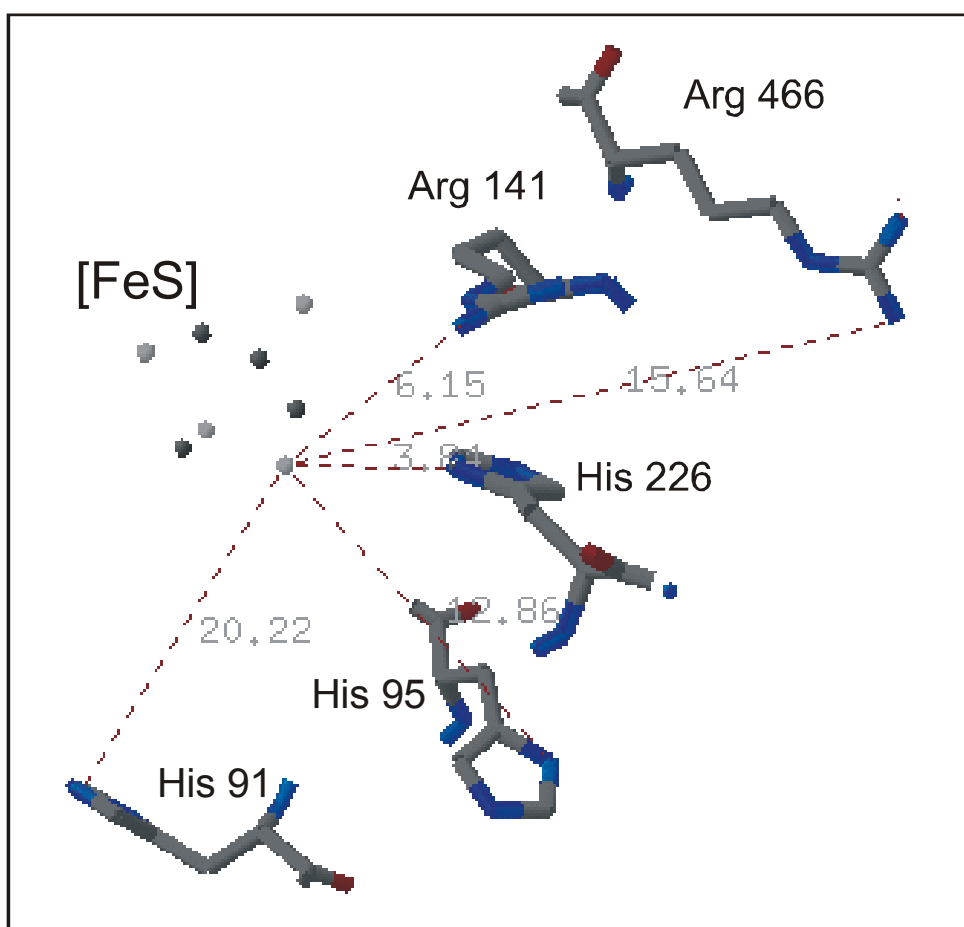

Figure 4.2 Structural model of the 49-kDa subunit based on the [NiFe] hydrogenase from *D. gigas*

Residues from the 49-kDa subunit are placed into the crystal structure of the [NiFe] hydrogenase from *D. gigas*. The approximate distances between [Fe$_4$S$_4$] cluster 'N2' and side chain nitrogen from different residues in Å are shown in grey.

Given the feasibility to purify complex I in milligram amounts, a more detailed EPR analysis was considered as a possibility to investigate the properties of cluster N2. Two specific experiments were adequate to explore the ligand field of cluster N2: First, it would be interesting to detect direct ligands of cluster N2 with ENDOR experiments and second to determine with ESEEM experiments elements that are not direct ligands but interact with cluster N2 (e.g. forming hydrogen bonds). If His-226 would be the ligand of cluster N2 then a specific nitrogen signal should be detectable in ENDOR experiments with parental complex I. On the other hand when His-226 is exchanged to a methionine residue then the nitrogen signal should disapear. In comparison to the ENDOR, the ESEEM experiment would not give information about direct ligands but about the enviroment of the cluster. If His-226 is not a direct ligand but interacts with cluster N2 then in ESEEM experiments a nitrogen modulation should be observed. This nitrogen modulation should not be observed in mutant H226M. In both, parental and H226M, a nitrogen derived modulation was observed in ESEEM measurements and a nitrogen coordination could not be confirmed by ENDOR experiments (Maly, personal communications). From this result we can conclude that His-226 is most likely not the fourth missing ligand of cluster N2.

This result was supported by REFINE (**Re**laxions **Fi**ltered Hyperf**ine**) spectroscopy. REFINE spectroscopy allows the simultanious characterisation of multiple paramagnetic centres within one sample (Maly, *et al.,* 2004 in press). From these measurements it was concluded that the observed nitrogen modulations were due to cluster N1 and not N2.

Although, His-226 is not a direct ligand it seems to play a very prominent role in the catalytic process. Complex I is not well understood mechanistically and there are more assumptions and hypothesis than solid data that could help to determine how this complex enzyme works and how electron transfer is coupled to proton pumping.

It is believed that cluster N2 due to its highest redox midpoint potential (E_m = -139 mV for *Y. lipolytica* Figure 4.3) is the immediate electron donor to ubiquinone (Ingledew and Ohnishi, 1980; Sled *et al.,* 1993). All other iron-sulphur clusters are called 'isopotential' clusters because their redox midpoint potentials are in the same range.

Cluster N1a which also was described to have a pH-dependent midpoint potential, recently was shown to change its redox properties upon pH-linked changes in protein charge and not due to a specific ionisable residue (Zu *et al.,* 2002).
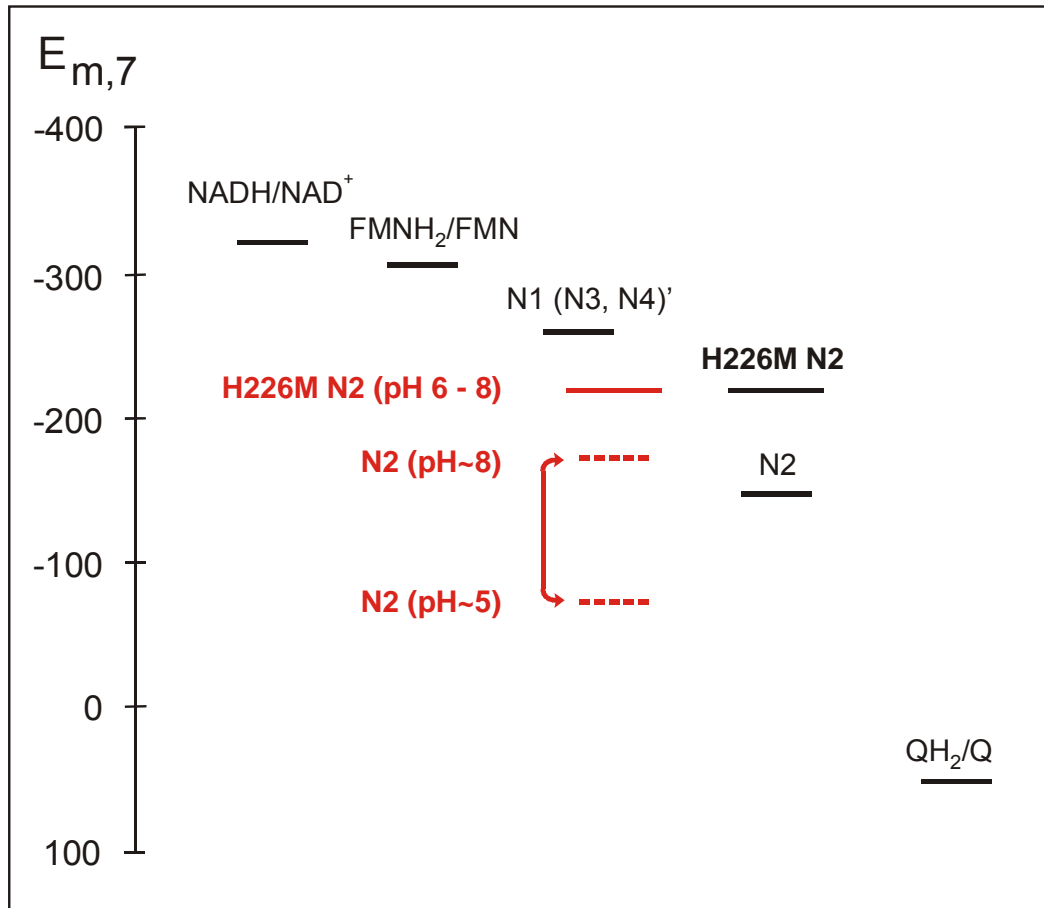
Figure 4.3 Redox midpoint potential (E_m) of complex I prosthetic groups in *Y. lipolytica*

The midpoint potentials of [FeS] cluster N3 and N4 were not determined exactly but were estimated to be similar to that of N1. Clusters N1, N3 and N4 are called 'isopotential' clusters since their redox midpoint potentials are in the same range. The redox midpoint potential of cluster N2 is pH dependent. The range of the redox midpoint potential of cluster N2 is shown in red.

In several mechanistic models, N2 was predicted to function in association with a redox-Bohr group (see Figure 1.3). The group becomes protonated upon reduction of N2 because of the increased basicity and becomes deprotonated again after the cluster is re-oxidised by ubiquinone (Brandt, 1997; Dutton *et al.,* 1998). This would allow the translocation of one proton per one electron. The redox titrations of *Y. lipolytica* mitochondrial membranes also revealed that the redox midpoint potential of

78

cluster N2 is higher than that of the other clusters (e.g. $E_{m,7}(N2)$ = -139 mV, $E_{m,7}(N1)$ = -260 mV) and that it is pH-dependent. But the slope of the pH dependent part of the titration curve did not reflect the expected 60 mV/pH unit. Calculation of the pK-values of reduced and oxidised species revealed values separated only by 1.6 pH-units, with a pK of 7.3 for the reduced state. The close proximity of the pK-values results in the decreased slope of the E_m-pH dependence. The calculated pK_{ox} was less exactly to define than the pK for the reduced form. This was probably due to instability of iron-sulphur clusters below pH ~5.5 which could be deduced from significantly diminished signal intensities. For evaluation of the effects of varying pK_{ox} values on the slope of the pH-dependence and the value of pK_{red} model calculations were performed assuming pK_{ox} in the range of 4.5-6 and fitting the corresponding pK_{red} values. As a result, the pH-dependence was only slightly affected and pK_{red} showed only minor changes ($7 < pK_{red} < 8$) upon variation of pK_{ox}. The still low pK for the reduced form of cluster N2 means that under physiological conditions (pH ~7) the reduced redox centre is not quantitatively in the protonated state which would be a prerequisite for a $1H^+/1e^-$ stoichiometry.

Mutation H226M had no striking impact neither on enzymatic activity of membrane preparations nor on isolated complex I. However as a consequence of the mutation the redox midpoint potential of cluster N2 was dramatically decreased and the pH-dependence of the redox potential was lost. The $E_{m,7}$ value of –218 mV for N2 in the mutant comes closer to the values which are known for the other 'isopotential' clusters (Ohnishi, 1998) N1, N3 and N4 having midpoint potentials in the range of –200 to –270 mV. It is quite obvious that residue His-226 is close enough to influence the electron affinity of cluster N2 by its polar side chain. At low pH the histidine carries a positive charge thereby increases the electron affinity of cluster N2, which means a more positive redox potential. At high pH the histidine is deprotonated and as a consequence the potential is decreased

As pointed out above the proximity of the pK values of the oxidised and reduced forms of cluster N2 and the inadequate slope of its redox-Bohr effect rules out hypothetical mechanisms that directly link proton translocation to electron transfer. In addition, the fact that complex I is active even when the special properties of cluster N2, a high and pH-dependent midpoint potential, are lost such as in mutant H226M also does not support such hypothetical mechanisms. Interestingly, the pH

dependence of the dNADH:DBQ activity of mitochondrial membranes from parental and mutant H226M strains showed very similar behaviour. The highest activity was in the range around pH 7.5 for the parental strain and mutant H226M as well.

ACMA dye measurements in proteoliposomes revealed proton pumping in mutant H226M even though the pH dependence of midpoint redox potential of cluster N2 was lost. However, from our measurements we cannot draw any conclusions about the H^+/e^- stoichiometry. The only possible explanation for this behaviour: Cluster N2 is not involved in proton pumping and its associated redox-Bohr group is only one element of a more complex proton-pumping machinery. Recently this view was supported by the finding that the 49-kDa subunit, and thus cluster N2, is clearly separated from the membrane part of complex I (Figure 1.1) (Zickermann *et al.,* 2003). These results favour an indirect mechanism of proton pumping in complex I, probably accomplished by long range conformational interaction between the peripheral part carrying the catalytic core and the membrane part of the enzyme.

4.1.2 Arginine 141

The EPR spectra of cluster N2 in Arg-141 mutants show a noteworthy parallel pattern to the mutants of residue His-226. In mutant R141A as well as in H226A cluster N2 was not detectable. Similar to mutant H226M, mutant R141K gave also rise to a shifted g_z signal from cluster N2. On the contrary the g_z signal was even more dramatically reduced than in the H226M mutant. The intensity of the g_z signal was less than 5 % in R141K in contrast to about 65 % in the H226M mutant. Mutant R141M showed even more striking results, because there was no observable cluster N2 either in membranes or in purified complex I. This remarkable parallel effect from mutants of both residues Arg-141 and His-226 could not be observed if we consider the activity of complex I. The g_z signal intensities from His-226 mutants corresponds more or less to complex I activity. In contrast, the g_z signal intensities in mutants of Arg-141 do not correspond to the complex I activity. This effect is clearly observable in mutants R141M and R141K. Mutant R141M did not give rise to any of N2 signal whatsoever, but complex I activity was only half reduced. In mutant R141K the DQA sensitive activity varied from 30-55 % whereas in mutant R141M it was stable at about 40 %. These rates were not due to increased reactivity towards the artificial substrate decylubiquinone because inhibitor insensitive rates were not found to be increased in mutant membranes neither in dNADH-oxidase nor in dNADH:DBQ

oxidoreductase activity tests. The most obvious explanation would be that cluster N2 that is believed to be the immediate electron donor to ubiquinone was still present in the mutant enzymes, but could not be detected anymore with standard EPR spectroscopy. The mutation could have changed the redox potential of the cluster to very negative values that prevented reduction of cluster by NADH or NADH/dithionite. However this scenario is most unlikely because in this case the midpoint potential would be below -450 mV, corresponding to a shift of at least 300 mV. To date there is no known mutation that causes such a shift in the midpoint potential of an iron-sulphur cluster. On the other hand the mutation could have changed the magnetic properties of cluster N2 making it undetectable by standard EPR methods. The possibility that the tetranuclear cluster had turned into a Fe_3S_4 cluster in the mutant could be ruled out because samples were analysed in the oxidised and as well as in the reduced state. The EPR signals typical for this type of cluster, which is paramagnetic in the oxidised state could not be detected. The reduced samples were scanned at many different settings (temperature, microwave power and field range) and no new paramagnetic species could be detected. The possibility that the spin of the ground state of the cluster had been changed into S=3/2 could also be ruled out because this would have been observed in the range g = 4.5–6. From this extensive EPR spectroscopic analysis of the mutants it can be concluded that iron-sulphur cluster N2 was mostly (R141K) or completely (R141M) absent.

The view that there is activity even when cluster N2 is not detectable in EPR spectra questions the prominent role that has been ascribed to this cluster. Is it possible that the catalytic core is still functional even in the absence of cluster N2? The exact electron transfer pathway in complex I is not known. Electrons are taken from NADH and transferred via FMN and numerous iron-sulphur clusters to the ubiquinone. As already mentioned it is believed that the last step in this chain is cluster N2. Typically the distances between redox-active clusters are around 5 Å (Volbeda *et al.,* 1995; Montet *et al.,* 1997). If one cluster is missing in the chain the distance rises to about 10 Å. According to electron transfer theory the maximal rates of electron transfer can be calculated using the "Moser-Dutton-ruler" (see also 8.3 for details) (Page *et al.,* 1999). In the case of 5 Å the electron transfer rate would be more than 10^{11} s^{-1}. If one cluster is missing the electron transfer rate would drop about 3 orders of magnitude to around 10^8 s^{-1}. Comparison of these estimates with the steady-state turnover

number of complex I of about 10^2 s^{-1} illustrates that removal of iron-sulphur cluster N2 not necessarily limits steady state turnover, because electron transfer is still predicted to be much faster. Similar results were measured involving very different redox centres of *E. coli* DNA photolyase (Byrdin *et al.,* 2003). Unfortunately on this time range no similar methods are available so far to investigate electron transfer within complex I.

Since His-226 is not the 4th ligand of cluster N2 and since no nitrogen modulation was found in the N2 signal in ESEEM and ENDOR experiments one can rule out Arg-141 as the 4th ligand of cluster N2. Even though Arg-141 is not the ligand of cluster N2 it is in close proximity to it so that it can exert such striking influence on cluster N2 and also on catalytic activity. These results clearly demonstrate a specific significance of Arg-141 for the local environment of cluster N2 and also provide strong support to the structural model of the ubiquinone reducing catalytic core of complex I (Kashani-Poor *et al.,* 2001b).

4.1.3 Histidine 91, 95 and Arginine 466

Mutations of His-91 and His-95 did not provide any information on the ligation or properties of iron-sulphur cluster N2. However, these two residues seem to play a central functional role. Virtually complete loss of catalytic activity was observed in all mutants without affecting iron-sulphur cluster N2 or reducing stability of the complex. According to our structural model based on crystal structures of [NiFe] hydrogenase both residues reside on the interface between the PSST and 49-kDa subunits. Therefore, both residues might be important for proton delivery to the catalytic core. It is also possible that these two residues build hydrogen bonds with residues from the PSST subunit.

Mutation of the C-terminal residue Arg-466 also did not provide any information about the ligation of cluster N2. This residue seems to have marked effects on stability of complex I. Complex I content was lowered in strains carrying non conservative mutation. In the case of mutant R466M even the activity of complex I was abolished. All mutants also showed hypersensitivity towards DQA. All these data indicate that Arg-466 plays an important role in complex I. This residue is probably not directly included in the catalytic process but may somehow influence the catalytic core. As already mentioned the yeast *Y. lipolytica* does not have regulatory mechanisms for

protein expression of the complex I subunits in other words lower enzyme content in mitochondria is most likely the result of degradation that can be either due to instability, misfolding, or assembly problems. Purification of complex I could not be achieved for the Arg-466 mutants and therefore EPR spectra of purified enzyme could not be collected. Only mitochondrial membranes from R466H gave EPR spectra similar to the parental strain and signal from cluster N2 could be detected clearly. However, in all Arg-466 mutants traces of g_{xy} signal could be observed. Residues His-91 and -95 are very close to the epitope recognised by monoclonal antibody (49.2) against the 49-kDa subunit (underlined in Figure 4.1B) (Zickermann *et al.,* 2003). These results support previously stated that catalytic core of complex I is clearly separated from membrane part of complex I suggesting an indirect mechanism of proton translocation by redox-driven conformational energy transfer (Zickermann *et al.,* 2003).

4.2 Serine 146

The hypothesis that the ubiquinone reducing active site of complex I has evolved from the [NiFe] active site of [NiFe] hydrogenases has been discussed previously (Kashani-Poor *et al.,* 2001b). In complex I, three residues that correspond to three cysteines that ligate the [NiFe] centre in [NiFe] hydrogenases have already been mutated and investigated. In contrast to these three residues (Asp-143, Val-460 and Glu-463) that are conserved among complex I from different species, serine 146 which aligns with the remaining cysteine ligand of the hydrogenase [NiFe] site is not conserved. Therefore we were interested to see whether this residue has influence on complex I activity since according to our [NiFe] hydrogenase model it resides directly in the catalytic core of complex I. While there was no change in complex I activity, as expected the mutations had influence on inhibitor sensitivity. This was observed especially in mutant S146C. These results also support previous findings that specific inhibitors of complex I exemplified by DQA and rotenone bind in the same pocket of complex I which probably constitutes the ubiquinone binding site itself.

4.3 Remodelling of Human Pathogenic 49-kDa Mutations in *Y. lipolytica*[1]

In the present work three mutations identified in patients affected with cardiomyopathy and encephalomyopathy (Loeffen *et al.,* 2001) that are located in the gene coding for the 49-kDa subunit of complex I were remodelled in *Y. lipolytica*. In humans all three mutations, R231Q, P232Q and S416P were lethal at very young age. Arg-231 is strictly conserved among complex I from different species and according to our [NiFe] hydrogenase structural model it resides in His228 Loop of the proposed catalytic core of complex I, for the proposed structural model see (Kerscher *et al.,* 2001). Pro-232 is also well conserved, however in *E. coli* it is replaced by isoleucine. This proline also resides in His228 Loop of the proposed catalytic core of complex I. The serine residue is also conserved, however in *Rh. capsulatus* it is replaced by alanine (see Figure 4.1A). Ser-416 is located in Pro475 Loop of the proposed catalytic core of complex I. According to Loeffen *et al.* (2001) mutations R228Q and P229Q (corresponding to R231 and P232 in *Y. lipolytica*) in human the 49-kDa subunit are proposed to cause replacement of an α-helix by a β-sheet. In *Y. lipolytica* the R231Q and S416P mutants had he same properties as the parental strain. However, the P232Q mutant showed no assembly of complex I, probably due to changes in secondary structure and improper folding of this subunit. The attempt to create other mutations at these positions gave slightly different results. The R231E and S416A mutants had higher K_m values for DBQ. This result indicates some influence of these residues on the catalytic properties of complex I. Even if these residues are not directly involved in the catalytic process, they reside in the catalytic core of complex I. The properties of the P232G mutant have changed in comparison to P232Q. The P232G mutant showed assembled complex I, however the expression was one third lower than in the parental strain, which indicates instability of complex I and complex I activity was reduced by almost 50 %. At this point we cannot draw any conclusions about the reason why in humans these mutations were lethal at very young age, it is very likely that the R228 and S413 residues in mammalian complex I have structural importance for the 49-kDa subunit. In the case of mutant P232Q the

---

[1] *Y. lipolytica* nomenclature used for numbering

probable cause was misfolding of the 49-kDa subunit preventing assembly of complex I. Another possibility that should be explained in the future could be higher production of ROS.

4.4 Mitochondrially Targeted eYFP in *Yarrowia lipolytica*

Mutation R228Q caused the fragmentation of mitochondrial network (personal communications) in patients and it would be interesting to see if the same effect occurs in *Y. lipolytica* mitochondria. Since *Y. lipolytica* mitochondria are much smaller than those of mammalian cells, the normally used mitochondrial targeted fluorescence indicators such as rhodamin 123, mitotracker red CMRXos or mitotracker green FM gave no good resolution. It was hoped that the use of a mitochondrially expressed eYFP variant of GFP would produce good enough resolution. The eYFP was successfully expressed as a C-terminal fusion with the 30-kDa subunit of complex I. It was also interesting to see where in the cells the mitochondria reside. The mitochondria in *Y. lipolytica* cells did not reside close to nucleus or dispersed through the cytoplasm but surprisingly are found close to the cell wall. Differences in the mitochondrial network between parental and mutant strains are currently being investigated, however preliminary results do not point to any detectable differences.

5 SUMMARY AND OUTLOOK

5.1 Summary

5.1.1 Ligands of Iron-Sulphur Cluster N2

In this work the ubiquinone reducing catalytic core of NADH:ubiquinone oxidoreductase (complex I) from *Y. lipolytica* was studied by a series of point mutations replacing conserved histidines or arginines in the 49-kDa subunit.

Although the missing 4th ligand of cluster N2 could not be found in the 49-kDa subunit of complex I, it was clearly demonstrated that iron-sulphur cluster N2 resides directly on the interface between the PSST and 49-kDa subunits. The results presented in this work show that residues in the 49-kDa subunit have strong influence on this redox centre and also on catalytic activity. The strong influence of Arg-141 and His-226 residues in 49-kDa subunit on this cluster can be deducted from complete loss of N2 signals in EPR spectra such as in case of mutants H226A and R141A. In the case of mutant H226M the EPR signal from cluster N2 was shifted and cluster N2 even lost the pH dependence of its redox midpoint potential and became more similar to the other so called 'isopotential' clusters. Specifically in the case of mutants R141M and R141K the characteristic signature of cluster N2 became undetectable in EPR spectra. However, specific dNADH:DBQ oxidoreductase activity that could be inhibited with the specific complex I inhibitors DQA and rotenone was not absolutely abolished but rather reduced. These reductions in complex I activity did not correspond to similar reductions in the specific EPR signal of cluster N2 as it was observed in the His-226 mutant series. No indications could be found that these mutations had modified the magnetic properties of cluster N2, resulting in different EPR spectra. From these observations it could be concluded that both mutants R141K and R141M virtually or entirely lack iron-sulphur cluster N2. The rates in complex I activity could be reconciled with electron transfer theory: After removal of a single redox centre in a chain, electron transfer rates are predicted to be still much faster than steady-state turnover of complex I. These results from mutants R141K, R141M and also the result from mutant H226M that protons are being pumped even if the redox midpoint potential of cluster N2 is not pH dependent questions the

prominent role in the catalytic mechanism of complex I that has been ascribed to cluster N2.

Histidine 91 and 95 were found to be absolutely essential for activity of complex I since in both mutants complex I was fully assembled and artificial NADH:HAR activity was parental whereas complex I specific dNADH:DBQ activity was abolished. The signal from cluster N2 in EPR spectra was parental for all His-91 and -95 mutants.

Mutations at the C-terminal arginine 466 affected ubiquinone affinity and inhibitor sensitivity but also destabilised complex I.

All these results provide further support for a high degree of structural conservation between the 49-kDa subunit of complex I and the large subunit of water soluble [NiFe] hydrogenases.

5.2 Remodelling of Human Pathogenic 49-kDa Mutations in *Y. lipolytica*

Y. lipolytica has been proven a good system for studying complex I properties and thus also for studying defects that occur in humans. In this work pathogenic mutations in the 49-kDa subunit of complex I were recreated and studied. The P232Q mutant showed non-assembly of complex I and this is probably the cause why this mutation was lethal in patients. The mutants R231Q and S416P were parental for the content, artificial and also specific complex I activity, K_m for DBQ and IC_{50} for DQA. From these results we can conclude that these two residues Arg-228 and Ser-413 in mammalian cells have specific structural importance for the 49-kDa subunit even if they are not directly involved in catalytic process.

5.3 OUTLOOK

5.3.1 Sub Mitochondrial Particles

Since we do not know how the proton pump of complex I functions and since it is also still unknown if the well established $4H^+/2e^-$ stoichiometry is also true for *Y. lipolytica* complex I it would be essential to make submitochondrial particles and carry out proton pumping experiments. It is also very important to clarify the role of cluster N2 in proton pumping. Further studies on mutant strains would also help to clarify the role of cluster N2 in proton pumping.

Also it would be very interesting to see which residues are active in proton transport either delivering scalar protons to the catalytic core or by forming part of a conformational proton pump.

6 ZUSAMMENFASSUNG

Die mitochondriale Atmungskette besteht aus vier Multiproteinkomplexen (Komplex I, NADH:Ubichinon Oxidoreduktase; Komplex II, Succinat:Ubichinon Oxidoreduktase; Komplex III, Ubichinol:Cytochrom c Oxidoreduktase auch bc_1 Komplex genannt; Komplex IV, Cytochrom c:O_2 Oxidoreductase, auch Cytochrom c Oxidase genannt). Die Elektronen der Reduktionsäquivalente NADH und $FADH_2$, die hauptsächlich in der Glykolyse, der Fettsäureoxidation und dem Citratcyclus gebildet werden, geben ihre Elektronen an die Atmungskette ab, wobei molekularer Sauerstoff als terminaler Akzeptor dient. Die durch diesen Elektronentransport freiwerdende Energie wird in der Form eines Protonengradients gespeichert. Der so aufgebaute elektrochemische Gradient wird zur Synthese von ATP genutzt. Die Kopplung des Elektronentransports durch die Atmungskettenkomplexe und der ATP Synthese durch die ATP-Synthase wird „oxidative Phosphorylierung" genannt. Dieses Prinzip der Energieumwandlung wurde von P. Mitchell als chemiosmotische-Hypothese vorgeschlagen (Mitchell, 1961).

Komplex I ist der größte und am wenigsten untersuchte transmembrane Proteinkomplex der Atmungskette. Elektonenmikroskopische Untersuchungen am Komplex I aus verschiedenen Organismen haben einen L-förmige Struktur für sowohl prokaryotischen also auch eukaryotischen Komplex I gezeigt (*Y. lipolytica,* Djafarzadeh *et al.,* 2000; *N. crassa,* Guenebaut *et al.,* 1997; *E. coli,* Guenebaut *et al.,* 1998; *Bos taurus* Herz, Grigorieff, 1998)). Der Komplex I aus Säugetieren besteht aus 46 Untereinheiten (Carroll *et al.,* 2003; Skehel *et al.,* 1998). Der prokaryotische Komplex I besteht aus 14, den so genanten „zentralen", Untereinheiten (in *E. coli* 13, da die 49-kDa und die 30-kDa Untereinheit fusioniert sind). Alle diese 14 prokaryotischen Untereinheiten sind auch bei Säugetieren vorhanden, 7 von ihnen werden von mitochondrialer DNA kodiert.

In den letzten Jahren wurde *Yarrowia lipolytica,* eine obligat aerobe Hefe, als Modellsystem etabliert. Die Atmungskette der Hefe *S. cerevisiae* beinhaltet keinen Komplex I. *Y. lipolytica* hat dagegen einen stabilen Komplex I der sich gut reinigen lässt und dem Komplex aus *N. crassa* sehr ähnelt. All dies macht diese Hefe zu

einem hervorragenden Modellsystem für strukturelle und funktionelle Untersuchungen an Komplex I (Kerscher *et al.,* 2002).

Aufgrund der Ergebnisse einer zielgerichteten Mutagenese in *Y. lipolytica* wurde vorgeschlagen, dass das katalytische Zentrum des Komplex I während der Evolution aus dem aktiven Zentrum der [NiFe] Hydrogenase entstanden ist und sich wahrscheinlich an der Grenzfläche zwischen den PSST und 49-kDa Untereinheiten befindet (Kashani-Poor *et al.,* 2001b; Garofano *et al.,* 2003). Die 49-kDa Untereinheit ist homolog zu der großen und die PSST zu der kleinen Untereinheit der bakteriellen wasserlöslichen [NiFe] Hydrogenasen (Böhm *et al.,* 1990; Albracht, 1994). Die Kristallstruktur dieser wasserlöslichen [NiFe] Hydrogenasen wurde aufgelöst (Volbeda *et al.,* 1995; Montet *et al.,* 1997). Es wurde auch vorgeschlagen, dass das proximale Eisen-Schwefel Zentrum aus diesen wasserlöslichen [NiFe] Hydrogenasen sich zum Eisen-Schwefel Zentrum N2 entwickelte. In allen bekannten Sequenzen der PSST Untereinheit findet man 4 konservierte Cysteinreste, aber nur 3 von diesen können als Liganden des Zentrums N2 dienen. Da zwei Cysteine direkt benachbart sind, können beide aus energetischen Gründen nicht gleichzeitig Liganden des N2 Zentrums sein. Laut Flemming *et al.,* (2003) wird diese Ansicht nicht geteilt.

Nach unserem Strukturmodell befindet sich das Eisen-Schwefel Zentrum N2 an der Grenzfläche zwischen der PSST und der 49-kDa Untereinheit und es wäre durchaus möglich, dass ein Rest der 49-kDa Untereinheit als 4ter Ligand des Zentrums N2 dient. Um diese Hypothese zu testen wurden Histidine und Arginine, die in Komplex I-Sequenzen aus verschiedenen Organismen oder in Komplex I und [NiFe] Hydrogenasen konserviert sind, mutagenisiert. Histidin 226 ist in allen bis jetzt bekannten Komplex I Sequenzen konserviert und entspricht einem hoch konservierten Histidin aus wasserlöslichen [NiFe] Hydrogenasen. In [NiFe] Hydrogenasen bildet dieser Histidinrest eine Wasserstoffbrücke zu dem proximalen Eisen-Schwefel Zentrum. His-226 wurde in Alanin und in die potentiellen Eisen-Schwefel Cluster Liganden Glutamin, Cystein und Methionin ummutiert. Alle Mutanten dieses Restes hatten einen assemblierten Komplex I. Die Mutante H226A hatte um 80 % reduzierte Komplex I Aktivität. Die Mutanten H226C und H226Q hatten noch ca. 50 % Komplex I Aktivität. Die Aktivität der Mutante H226M war nur um 20 % reduziert. Zur genaueren Ansicht der proteinchemischen Daten siehe Table 3.1. EPR Spektren sowohl aus mitochondrialen Membranen als auch aus isoliertem

Komplex I zeigten einen Einfluss auf das Signal des Zentrums N2, wobei die Signale der anderen Eisen-Schwefeln Zentren unverändert blieben. Das EPR Spektrum der Mutante H226A zeigte kein N2 Signal. Die EPR Signale der übrigen Eisen-Schwefeln Zentren waren unverändert. EPR Spektren, die unter vielen verschiedenen Bedingungen aufgenommen wurden (Temperatur, Mikrowellen-Stärke und Feldbereich) ergaben keine Hinweise auf neue paramagnetische Spezies. Die Schlussfolgerung aus diesen Experimenten ist, dass Cluster N2 in der Mutante H226A nicht nur in seinen Eigenschaften verändert ist, sondern tatsächlich fehlt. Ähnliche Ergebnisse wurden auch in den EPR Spektren der Mutanten H226Q und H226C beobachtet, wobei die Intensität des N2 Zentrums in diesen Fällen zwar deutlich geringer war als im wildtypischen Enzym (Figure 3.4) aber nicht völlig fehlte. Interessanterweise war in den Spektren aus Mutante H226M nicht nur das N2 Signal geringer, sondern auch noch zu kleineren magnetischen Feldstärken verschoben.

Arginin 141 ist in allen bis jetzt bekannten Komplex I Sequenzen konserviert und entspricht einem hoch konservierten Arginin aus wasserlöslichen [NiFe] Hydrogenasen. Im Hydrogenase-Strukturmodell befindet sich dieser Rest sehr nah am Zentrum N2. Der Arg-141 Rest wurde in Alanin, Lysin und Methionin ummutiert. Alle Arg-141 Mutanten hatten einen assemblierten Komplex I. Die Mutante R141A hatte keine hemmbare Komplex I Aktivität, wobei die Mutanten R141K und R141M eine um ca. 50% (unterschiedlich für verschiedene Präparationen insbesondere bei Mutante R141K) reduzierte Aktivität zeigten. Es wurde ein signifikanter Unterschied zwischen EPR Spektren und Aktivitäten beobachtet. Die Komplex I Aktivität war in der Mutante R141M vermindert, wobei das EPR Signal für das Zentrum N2 weder in mitochondrialen Membranen noch im isolierten Enzym nicht detektiert werden konnte. In der Mutante R141K wurde in isoliertem Enzym weniger als 5 % der wildtypischen N2 Intensität beobachtet, und außerdem scheint das g_z Signal des Zentrums N2 verschoben zu sein. Eine wahrscheinliche Interpretation für dieses erstaunliche Ergebnis von Elektronentransport trotz fehlendem Eisen-Schwefel Cluster N2 könnte man anhand der Elektronentransport-Theorie ableiten. Der 'Dutton-Moser-Ruler' gibt die Abhängigkeit zwischen der Reaktionsrate und dem Abstand von benachbarten Redox-Zentren an (Page *et al.,* 1999). Normalerweise beträgt der Abstand zwischen benachbarten Redox-Zentren, in unserem Fall Eisen-Schwefel-Cluster, in einem Protein um 5 Å (Volbeda *et al.,* 1995; Montet *et al.,* 1997).

Die Reaktionsrate beträgt 10^{11} s^{-1} bei 5 Å Abstand. Falls eines der Redox-Zentren fehlt, würde der Abstand ca. 10 Å betragen und die Rate wäre entsprechend um 2-3 Größenordnungen geringer (10^8-10^9 s^{-1}). Im Vergleich zur Wechselzahl von Kompex I, die um 10^2 s^{-1} beträgt, sollte ein Ausfallen von einem der Redox-Zentren keinen gravierenden Effekt auf die Wechselzahl ausüben.

Histidin 91 und 95 sind hoch konserviert in Komplex I Sequenzen aus verschiedenen Organismen aber sind nicht konserviert in [NiFe] Hydrogenasen. Wenn man annimmt, dass die Proteinfaltung während der Evolution erhalten blieb, liegn diese beiden Histidinreste in der Nähe von Zentrum N2. His-91 und -95 wurden in Alanin, Methionin und Arginin ummutiert. Alle Mutanten dieser beiden Histidine 91 und 95 hatten einen assemblierten Komplex I, aber keine von ihnen zeigte Komplex I Aktivität, auch nicht bei einer sehr konservativen Mutation (Histidin zu Arginin). Die EPR Spektren von mitochondrialen Membranen der His-91 und His-95 Mutanten und auch von isoliertem Enzym der Mutante H95A waren wildtypisch.

Der C-terminale Argininrest 466 ist hoch konserviert in Komplex I und entspricht in wasserlöslichen [NiFe] Hydrogenasen einem hoch konservierten Histidinrest, der dem Mg^{2+} Zentrum als Ligand dient. Der Argininrest wurde in Alanin, Methionin, Histidin und Glutamat ummutiert. Alle Arg-466 Mutanten außer R466H hatten einen stark reduzierten Gehalt (30-50 %) an Komplex I. Normalerweise deutet dies auf strukturelle Instabilität hin. Dadurch war es auch nicht möglich, Komplex I zu isolieren um ein EPR Spektrum aufzunehmen. Die Komplex I Aktivität war im Fall von R466M stark reduziert auf 20 % der wildtypischen Aktivität, während die Mutanten R466A und R466H eine Aktivität von 80 % und R466E von 50 % hatten (Table 3.7).

Einer der wichtigsten Ansätze in dieser Arbeit war zu testen, ob einer dieser untersuchten Reste als 4ter Ligand des Eisen-Schwefel Zentrums N2 dienen könnte. His-91 und His-95 kann man mit sehr großer Sicherheit als 4ten Ligand ausschließen, da nach dem Austausch des Histidinrestes gegen ein Alanin das EPR Spektrum wildtypisch blieb. Arg-466 kann man ebenso ausschließen, denn sogar bei so einem geringen Gehalt an Komplex I wie in den Mutanten R466A und R466M konnte man typische Merkmale des N2 Zentrums in der g_{xy} Region des EPR Spektrums erkennen. Spezifische und außergewöhnlich parallele Effekte auf das Zentrum N2 ergaben die Mutationen von Arg-141 und His-226 (siehe Figure 3.4 und

Figure 3.12). Bei Umtausch in einen Alaninrest, der klein und hydrophob ist, konnte kein N2 Signal im EPR nachgewiesen werden. Bei einem konservativen Umtausch (R141K und H226M) wurde die Intensität des EPR Signals für das Zentrum N2 geringer und zu einer niedrigeren Feldregion verschoben. Andere Mutationen zeigten drastische Effekte auf das Zentrum N2, in H226C und H226Q wurde das Signal sehr stark reduziert und im Fall von R141M verschwand es ganz. Resultierend aus diesen Ergebnissen könnte man schließen, dass einer der beiden Resten der 4te Ligand des Zentrums N2 wäre. Das ähnliche Verhalten des Zentrums N2 bei Mutationen der beiden Reste R141 und H226 deutet jedoch mehr auf eine Änderung in der nahen Umgebung des Zentrums N2 und nicht auf einem Ligandenumtausch. Im Vergleich zu R466, wo globale Destabilisierung eintritt, wirkt der Umtausch von H226 und R141 mehr auf lokaler Ebene, insbesondere auf das Zentrum N2. Obwohl der 4te Ligand in dieser Arbeit nicht identifiziert werden konnte, spielen die beiden Reste R141 und H226 eine wichtige Rolle im katalytischen Prozess. Dies ist besonderes anschaulich in der Mutante H226M, wo das Redox-Mittelpunktspotential von N2 um mehr als 70 mV positiver ist (Figure 3.6). Auch die Abhängigkeit vom pH-Wert war nicht mehr vorhanden (Figure 3.7). Aber das Maximum der Enzymaktivität in Abhängigkeit von pH Wert war in der Mutante H226M wildtypisch. Das isolierte Enzym aus H226M konnte auch in Anwesenheit von Asolectin reaktiviert werden. Die Proteoliposomen der Mutante H226M konnten Protonen gleichermaßen wie der Wildtyp pumpen. Aus diesen Experimenten konnte man jedoch nur qualitative Schlüsse ziehen. Die genauere H^+/e^- Stöchiometrie konnte man dabei nicht feststellen.

Dem Zentrum N2 wird eine wichtige Rolle zugeschrieben, es soll die Protonenpumpe von Komplex I mit der Reduktion von Ubichinon koppeln. Nach den hier präsentierten Ergebnissen wird die Rolle des Zentrums N2 in Frage gestellt. Denn die Mutante R141M hatte eine stark ausgeprägte, mit Komplex I spezifischen Inhibitoren hemmbare Aktivität, jedoch wurde kein N2 Signal in der EPR Spektroskopie detektiert. Noch dazu pumpt die Mutante H226M Protonen gleichermaßen wie der Wildtyp, wobei keine pH Abhängigkeit des Mittelpunktspotentials zu beobachten war. Dabei stellt sich auch die Frage auf welche Weise die Protonenpumpe in Komplex I funktioniert: Ist es eine Redox-Pumpe, eine mechanische Pumpe (Konformationsänderung) oder sogar eine Kombination aus beiden Typen? Außerdem ist die Rolle vom Cluster N2 in der Protontranslokation zu klären. Dafür

sind weitere Untersuchungen an dem wildtypischen Komplex I und an den Mutanten H226M, R141M und R141K geplant.

Neben dem großen akademischen Interesse am Mechanismus von Komplex I spielt dieses sehr wenig verstandene und komplizierte Enzym wegen seines Zusammenhangs mit einer Vielzahl von Krankheiten eine wichtige Rolle in der Humanmedizin (Robinson, 1998; Loeffen *et al.,* 2000; Gluck *et al.,* 1994). Außerdem wird Komplex I als eine der Hauptquellen der ROS (Reactive Oxygen Species) diskutiert (Wallace, 1999; Sherer *et al.,* 2003). In dieser Arbeit wurden drei Mutationen (R231Q, P232Q und S416P, *Y. lipolytica* Nummerierung), die für Menschen pathogen sind, in der 49-kDa Untereinheit reproduziert. Die Mutanten R231Q und S416P zeigten keinen Einfluss auf die Enzymaktivität oder auf den K_m für DBQ und v_{max} für DBQ. In der Mutante P232Q wurde Komplex I nicht assembliert. In dieser Mutante ist wahrscheinlich die nicht richtige Proteinfaltung für das Krankheitsbild verantwortlich. Aus den Untersuchungen an Mutanten R231Q oder S416P kann man abschließend nicht sagen, warum diese Mutationen pathogen sind. Drastischere Mutationen an diesen beiden Positionen, R231E und S416A ergaben jedoch Effekte auf das katalytische Zentrum, der K_m Werte für DBQ waren im Fall von R231E mehr als 2fach und in S416A mehr als 3fach höher (Table 3.9). Dies ist im Einklang mit dem [NiFe] Hydrogenase Strukturmodell und auch ein Hinweis auf räumliche Nähe dieser Reste zum Chinon-Reduktionszentrum.

Die Untersuchungen an lebenden Zellen haben gezeigt, dass Mitochondrien nicht einzelne isolierte Organellen darstellen, sondern in Form eines zusammenhängenden Netzwerks organisiert sind. Die Mutation R231Q verursacht bei Menschen eine Fragmentierung des mitochondrialen Netzwerk. Um zu überprüfen, ob dies auch in der Hefe vorkommt, wurde eYFP (eine Variante von GFP, Green Fluorescent Protein) mitochondrial exprimiert. Das Gen für die 30-kDa Untereinheit wurde C-terminal mit dem eYFP-Gen fusioniert. Es wurde beobachtet, dass die Mitochondrien sich in der Nähe der Zellwand befinden. In vorläufigen Untersuchungen der Mutante R231Q wurden keine Unterschiede im Vergleich zum Wildtyp beobachtet. Aber dies muss noch genauer in Kooperation mit Prof. Smeitink von NCMD (Die Niederlande) untersucht werden.

7 REFERENCES

1. Current protocols in molecular biology. Ausubel, F. M., Brent, R., Kingston, R. E., Moore, D. D., Seidman, J. G., Smith, J. A., and Struhl, K. 2000. New York. Ref Type: Serial (Book,Monograph)

2. Ahlers, P., A.Garofano, S.Kerscher, and U.Brandt. 2000a. Application of the Obligate Aerobic Yeast *Yarrowia lipolytica* as a Eucaryotic Model to Analyze Leigh Syndrome Mutations in the ComplexI Core Subunits PSST and TYKY . *Biochim. Biophys. Acta - Bioenerg.* 1459:258-265.

3. Ahlers, P., K.Zwicker, S.Kerscher, and U.Brandt. 2000b. Function of conserved acidic residues in the PSST-homologue of complex I (NADH:ubiquinone oxidoreductase) from *Yarrowia lipolytica. J. Biol. Chem.* 275:23577-23582.

4. Albracht, S.P.J. 1994. Nickel hydrogenases: in search of the active site. *Biochim. Biophys. Acta* 1188:167-204.

5. Albracht, S.P.J. and R.Hedderich. 2000. Learning from hydrogenases: location of a proton pump and of a second FMN in bovine NADH-ubiquinone oxidoreductase (ComplexI). *FEBS Lett.* 24275:1-6.

6. Andrews, S.C., B.C.Berks, J.McClay, A.Ambler, M.A.Quail, P.Golby, and J.R.Guest. 1997. A 12-cistron *Escherichia coli* oeron (hyf) encoding a putative proton-translocating formate hydrogenlyase system. *Microbiology* 143:3633-3647.

7. Betarbet, R., T.B.Sherer, G.MacKenzie, M.Garcia-Osuna, A.Panov, and J.T.Greenamyre. 2000. Chronic systemic pesticide exposure reproduces features of Parkinson's disease. *Nature neuroscience* 3:1301-1306.

8. Böhm, R., M.Sauter, and A.Böck. 1990. Nucleotide sequence and expression of an operon in Escherichia coli coding for formate hydrogenlyase components. *Mol. Microbiol.* 4:231-243.

9. Böttcher, B., D.Scheide, M.Hesterberg, L.Nagel-Steger, and T.Friedrich. 2002. A Novel, Enzymatically Active Conformation of the *Escherichia coli* NADH: Ubiquinone Oxidoreductase (Complex I). *J. Biol. Chem.* 277:17970-17977.

10. Bourgeron, T., P.Rustin, D.Chretien, M.Birch-Machin, M.Bourgeois, E.Viegas-Pequignot, A.Munnich, and A.Rotig. 1995. Mutation of a nuclear succinate dehydrogenase gene results in mitochondrial respiratory chain deficiency. *Nature Genetics* 11:144-149.

11. Brandt, U. 1997. Proton-translocation by membrane-bound NADH:Ubiquinone-oxidoreductase (complex I) through redox-gated ligand conduction. *Biochim. Biophys. Acta* 1318:79-91.

96

12. Brandt, U. and J.G.Okun. 1997. Role of deprotonation events in ubihydroquinone:cytochrome *c* oxidoreductase from bovine heart and yeast mitochondria. *Biochem.* 36:11234-11240.

13. Byrdin, M., A.P.Eker, M.H.Vos, and K.Brettel. 2003. Dissection of the triple tryptophan electron transfer chain in *Escherichia coli* DNA photolyase: Trp382 is the primary donor in photoactivation. *Proc. Natl. Acad. Sci. USA* 100:8678-8681.

14. Carroll, J., I.M.Fearnley, R.J.Shannon, J.Hirst, and J.E.Walker. 2003. Analysis of the subunit composition of complex I from bovine heart mitochondria. *Molecular & Cellular Proteomics* 2:117-126.

15. Chen, D.-C., J.-M.Beckerich, and C.Gaillardin. 1997. One-step tranformation of the dimorphic yeast *Yarrowia lipolytica. Appl. Biochem. Biotechnol.* 48:232-235.

16. Conover, R.C., A.T.Kowal, W.G.Fu, J.B.Park, S.Aono, M.W.Adams, and M.K.Johnson. 1990. Spectroscopic characterization of the novel iron-sulfur cluster in Pyrococcus furiosus ferredoxin. *J. Biol. Chem.* 265:8533-8541.

17. Cormack, B.P., R.H.Valdivia, and S.Falkow. 1996. FACS-optimized mutants of the green fluorescent protein (GFP). *Gene* 173:33-38.

18. Darrouzet, E., J.P.Issartel, J.Lunardi, and A.Dupuis. 1998. The 49-kDa subunit of NADH-ubiquinone oxidoreductase (Complex I) is involved in the binding of piericidin and rotenone, two quinone-related inhibitors. *FEBS Lett.* 431:34-38.

19. de Vries, S. and C.A.M.Marres. 1987. The mitochondrial respiratory chain of yeast. Structure and biosynthesis and the role in cellular metabolism. *Biochim. Biophys. Acta* 895:205-239.

20. Djafarzadeh, R., S.Kerscher, K.Zwicker, M.Radermacher, M.Lindahl, H.Schägger, and U.Brandt. 2000. Biophysical and structural characterization of proton-translocating NADH-dehydrogenase (complex I) from the strictly aerobic yeast *Yarrowia lipolytica. Biochim. Biophys. Acta - Bioenerg.* 1459:230-238.

21. Dröse, S., K.Zwicker, and U.Brandt. 2002. Full recovery of the NADH:ubiquinone activity of complex I (NADH:ubiquinone oxidoreductase) from *Yarrowia lipolytica* by the addition of phospholipids. *Biochim. Biophys. Acta - Bioenerg.* 1556:65-72.

22. Du, C.Y., M.Fang, Y.C.Li, L.Li, and X.D.Wang. 2000. Smac, a mitochondrial protein that promotes cytochrome c-dependent caspase activation by eliminating IAP inhibition. *Cell* 102:33-42.

23. Duarte, M., H.Populo, A.Videira, T.Friedrich, and U.Schulte. 2002. Disruption of iron-sulphur cluster N2 from NADH:ubiquinone oxidoreductase by site-directed mutagenesis. *Biochem J* 364:833-839.

24. Duderstadt, R.E., P.S.Brereton, M.W.Adams, and M.K.Johnson. 1999. A pure S = 3/2 [Fe4S4]+ cluster in the A33Y variant of Pyrococcus furiosus ferredoxin. *FEBS Lett.* 454:21-26.

25. Dupuis, A., M.Chevallet, E.Darrouzet, H.Duborjal, J.Lunardi, and J.P.Issartel. 1998. The Complex I from *Rhodobacter capsulatus. Biochim. Biophys. Acta* 1364:147-165.

26. Dutton, P.L. 1978. Redox potentiometry: Determination of midpoint potentials of oxidation-reduction components of biological electron-transfer systems. *Methods Enzymol.* LIV:411-435.

27. Dutton, P.L., C.C.Moser, V.D.Sled, F.Daldal, and T.Ohnishi. 1998. A reductant-induced oxidation mechanism for Complex I. *Biochim. Biophys. Acta* 1364:245-257.

28. Finel, M. 1998. Organization and evolution of structural elements within complex I. *Biochim. Biophys. Acta* 1364:112-121.

29. Finel, M., A.S.Majander, J.Tyynelä, A.M.P.de Jong, S.P.J.Albracht, and M.K.F.Wikström. 1994. Isolation and characterisation of subcomplexes of the mitochondrial NADH:ubiquinone oxidoreductase (complex I). *Eur. J. Biochem.* 226:237-242.

30. Finel, M., J.M.Skehel, S.P.J.Albracht, I.M.Fearnley, and J.E.Walker. 1992. Resolution of NADH:ubiquinone oxidoreductase from bovine heart mitochondria into two subcomplexes, one of which contains the redox centers of the enzyme. *Biochem.* 31:11425-11434.

31. Flemming, D., A.Schlitt, V.Spehr, T.Bischof, and T.Friedrich. 2003. Iron-sulfur cluster N2 of the Escherichia coli NADH:ubiquinone oxidoreductase (complex I) is located on subunit NuoB. *J. Biol. Chem.* 278:47602-47609.

32. Friedrich, T. and D.Scheide. 2000. The respiratory complex I of bacteria, archaea and eukarya and its module common with membrane-bound multisubunit hydrogenases. *FEBS Lett.* 479:1-5.

33. Galante, Y.M. and Y.Hatefi. 1979. Purification and molecular and enzymatic properties of mitochondrial NADH dehydrogenase. *Arch. Biochem. Biophys.* 192:559-568.

34. Garofano, A., K.Zwicker, S.Kerscher, P.Okun, and U.Brandt. 2003. Two aspartic acid residues in the PSST-homologous NUKM subunit of complex I from *Yarrowia lipolytica* are essential for catalytic activity. *J. Biol. Chem.* 278:42435-42440.

35. Gavrikova, E.V., V.G.Grivennikova, V.D.Sled, T.Ohnishi, and A.D.Vinogradov. 1995. Kinetics of the mitochondrial three-subunit NADH dehydrogenase interaction with hexammineruthenium(III). *Biochim. Biophys. Acta* 1230:23-30.

36. Gluck, M.R., M.J.Krueger, R.R.Ramsay, S.O.Sablin, T.P.Singer, and W.J.Nicklas. 1994. Characterization of the inhibitory mechanism of 1-methyl-4-

phenylpyridinium and 4-phenylpyridine analogs in inner membrane preparations. *J. Biol. Chem.* 269:3167-3174.

37. Green, D.R. and J.C.Reed. 1998. Mitochondria and apoptosis. *Science* 281:1309-1312.

38. Grigorieff, N. 1998. Three-dimensional structure of bovine NADH:Ubiquinone oxidoreductase (Complex I) at 22 Å in ice. *J. Mol. Biol.* 277:1033-1046.

39. Guenebaut, V., A.Schlitt, H.Weiss, K.Leonard, and T.Friedrich. 1998. Consistent structure between bacterial and mitochondrial NADH:ubiquinone oxidoreductase (complex I). *J. Mol. Biol.* 276:105-112.

40. Guenebaut, V., R.Vincentelli, D.Mills, H.Weiss, and K.Leonard. 1997. Three-dimensional structure of NADH-dehydrogenase from Neurospora crassa by electron microscopy and conical tilt reconstruction. *J. Mol. Biol.* 265:409-418.

41. Helenius, A. and K.Simons. 1972. The binding of detergents to lipophilic and hydrophilic proteins. *J. Biol. Chem.* 247:3656-3661.

42. Hunte, C., J.Koepke, C.Lange, and H.Michel. 2000. Structure at 2.3 angstrom resolution of the cytochrome bc(1) complex from the yeast Saccharomyces cerevisiae co-crystallized with an antibody Fv fragment. *Structure* 8:669-684.

43. Ingledew, W.J. and T.Ohnishi. 1980. An analysis of some thermodynamic properties of iron-sulfur centres in site I of mitochondria. *Biochem. J.* 186:111-117.

44. Iwata, S., J.W.Lee, K.Okada, J.K.Lee, M.Iwata, B.Rasmussen, T.A.Link, S.Ramaswamy, and B.K.Jap. 1998. Complete structure of the 11-subunit bovine mitochondrial cytochrome bc_1 complex. *Science* 281:64-71.

45. Iwata, S., C.Ostermeier, B.Ludwig, and H.Michel. 1995. Structure at 2.8 Å resolution of cytochrome *c* oxidase from *Paracoccus denitrificans*. *Nature* 376:660-669.

46. Kashani-Poor, N., S.Kerscher, V.Zickermann, and U.Brandt. 2001a. Efficient large scale purification of his-tagged proton translocating NADH:ubiquinone oxidoreductase (complex I) from the strictly aerobic yeast *Yarrowia lipolytica*. *Biochim. Biophys. Acta - Bioenerg.* 1504:363-370.

47. Kashani-Poor, N., K.Zwicker, S.Kerscher, and U.Brandt. 2001b. A central functional role for the 49-kDa subunit within the catalytic core of mitochondrial complex I. *J. Biol. Chem.* 276:24082-24087.

48. Kerscher, S. 2000. Diversity and origin of alternative NADH:ubiquinone oxidoreductases. *Biochim. Biophys. Acta - Bioenerg.* 1459:274-283.

49. Kerscher, S., S.Dröse, K.Zwicker, V.Zickermann, and U.Brandt. 2002. *Yarrowia lipolytica*, a yeast genetic system to study mitochondrial complex I. *Biochim. Biophys. Acta - Bioenerg.* 1555:83-91.

50. Kerscher, S., N.Kashani-Poor, K.Zwicker, V.Zickermann, and U.Brandt. 2001. Exploring the catalytic core of complex I by *Yarrowia lipolytica* yeast genetics. *J. Bioenerg. Biomembr.* 33:187-196.

51. Kerscher, S., J.G.Okun, and U.Brandt. 1999. A single external enzyme confers alternative NADH:ubiquinone oxidoreductase activity in *Yarrowia lipolytica*. *J. Cell Sci.* 112:2347-2354.

52. Kroemer, G. and J.C.Reed. 2000. Mitochondrial control of cell death. *Nature Medicine* 6:513-519.

53. Künkel, A., J.A.Vorholt, R.K.Thauer, and R.Hedderich. 1998. An *Escherichia coli* hydrogenase-3-type hydrogenase in methanogenic archaea. *Eur. J. Biochem.* 252:467-476.

54. Leif, H., V.D.Sled, T.Ohnishi, H.Weiss, and T.Friedrich. 1995. Isolation and characterization of the proton-translocating NADH:ubiquinone oxidoreductase from *Escherichia coli. Eur. J. Biochem.* 230:538-548.

55. Loeffen, J., O.Elpeleg, J.Smeitink, R.Smeets, S.Stöckler-Ipsiroglu, H.Mandel, R.Sengers, F.Trijbels, and L.Van den Heuvel. 2001. Mutations in the Complex I *NDUFS2* Gene of Patients with Cardiomyopathy and Encephalomyopathy. *Ann. Neurol.* 49:195-201.

56. Loeffen, J., J.Smeitink, R.Triepels, R.Smeets, M.Schuelke, R.Sengers, F.Trijbels, B.Hamel, R.Mullaart, and L.Van den Heuvel. 1998. The first nuclear-encoded complex I mutation in a patient with Leigh syndrome. *Am. J. Hum. Genet.* 63:1598-1608.

57. Loeffen, J.L.C.M., J.A.M.Smeitink, J.M.F.Trijbels, A.J.M.Janssen, R.H.Triepels, L.P.Sengers, and L.P.Van den Heuvel. 2000. Isolated complex I deficiency in children: Clinical, biochemical and genetic aspects. *Human Mutation* 15:123-134.

58. Lowry, O.H., N.R.Rosebrough, A.L.Farr, and R.J.Randall. 1951. Protein measurement with the folin phenol reagent. *J. Biol. Chem.* 193:265-275.

59. Magnitsky, S., L.Toulokhonova, T.Yano, V.D.Sled, C.Hagerhall, V.G.Grivennikova, D.S.Burbaev, A.D.Vinogradov, and T.Ohnishi. 2002. EPR characterization of ubisemiquinones and iron-sulfur cluster N2, central components of the energy coupling in the NADH- ubiquinone oxidoreductase (complex I) in situ. *J. Bioenerg. Biomembr.* 34:193-208.

60. Mathiesen, C. and C.Hägerhäll. 2002. Transmembrane topology of the NuoL, M and N subunits of NADH:quinone oxidoreductase and their homologues among membrane-bound hydrogenases and bona fide antiporters . *Biochim. Biophys. Acta* 1556:121-132.

61. Mitchell, P. 1961. Coupling of phosphorylation to electron and hydrogen transfer by a chemi-osmotic type of mechanism. *Nature* 191:144-148.

62. Montet, Y., P.Amara, A.Volbeda, X.Vernede, E.C.Hatchikian, M.J.Field, M.Frey, and J.C.Fontecilla-Camps. 1997. Gas access to the active site of Ni-Fe hydrogenases probed by X-ray crystallography and molecular dynamics. *Nature Struct. Biol.* 4:523-526.

63. Morin, J.G. and J.W.Hastings. 1971. Energy transfer in a bioluminescent system. *Journal of Cellular Physiology* 77:313-318.

64. Moser, C.C., C.C.Page, R.Farid, and P.L.Dutton. 1995. Biological Electron-Transfer. *J. Bioenerg. Biomembr.* 27:263-274.

65. Ohnishi, T. 1998. Iron-sulfur clusters semiquinones in Complex I. *Biochim. Biophys. Acta* 1364:186-206.

66. Okun, J.G., P.Lümmen, and U.Brandt. 1999. Three classes of inhibitors share a common binding domain in mitochondrial complex I (NADH:ubiquinone oxidoreductase). *J. Biol. Chem.* 274:2625-2630.

67. Ormo, M., A.B.Cubitt, K.Kallio, L.A.Gross, R.Y.Tsien, and S.J.Remington. 1996. Crystal structure of the Aequorea victoria green fluorescent protein. *Science* 273:1392-1395.

68. Ostermeier, C., A.Harrenga, U.Ermler, and H.Michel. 1997. Structure at 2.7 A resolution of the Paracoccus denitrificans two- subunit cytochrome c oxidase complexed with an antibody FV fragment. *Proc. Natl. Acad. Sci. USA* 94:10547-10553.

69. Page, C.C., C.C.Moser, X.Chen, and P.L.Dutton. 1999. Natural engineering principles of electron tunnelling in biological oxidation-reduction. *Nature* 402:47-52.

70. Pilkington, S.J., J.M.Skehel, R.B.Gennis, and J.E.Walker. 1991. Relationship between mitochondrial NADH-ubiquinone reductase and a bacterial NAD-reducing hydrogenase. *Biochem.* 30:2166-2175.

71. Rasmussen, T., D.Scheide, B.Brors, L.Kintscher, H.Weiss, and T.Friedrich. 2001. Identification of two tetranuclear FeS clusters on the ferredoxin-type subunit of NADH:ubiquinone oxidoreductase (complex I). *Biochem.* 40:6124-6131.

72. Rasmusson, A.G., V.Heiser, E.Zabaleta, A.Brennicke, and L.Grohmann. 1998. Physiological, biochemical and molecular aspects of mitochondrial complex I in plants. *Biochim. Biophys. Acta* 1364:101-111.

73. Rich, P.R. and N.Fisher. 1999. Quinone-binding sites in membrane proteins: structure, function and applied aspects. *Biochem. Soc. Trans.* 27:561-565.

74. Rigaud, J.-L., B.Pitard, and R.M.Levy. 1995. Reconstitution of membrane proteins into liposomes: application to energy-transducing membrane proteins. *Biochim. Biophys. Acta* 1231:223-246.

75.	Robinson, B.H. 1998. Human Complex I deficiency: Clinical spectrum and involvement of oxygen free radicals in the pathogenicity of the defect. *Biochim. Biophys. Acta* 1364:271-286.

76.	Sambrook, J., E.F.Fritsch, and T.Maniatis. 1989. Molecular cloning. A Laboratory Manual. Cold Spring Harbor Laboratory Press, Cold Spring Harbor, NY.

77.	Sazanov, L.A. 2002. Structural characterisation of complex I from *E. coli. Biochim. Biophys. Acta - Bioenerg.* 1555:201.

78.	Sazanov, L.A., S.Y.Peak-Chew, I.M.Fearnley, and J.E.Walker. 2000. Resolution of the Membrane Domain of Bovine complex I into Subcomplexes: Implications for the Structural Organization of the Enzyme. *Biochem.* 39:7229-7235.

79.	Schägger, H. 2003. Blue Native Electrophoresis. *In* Membrane Protein Purification and Crystallization: A Practical Guide. C.Hunte, G.von Jagow, and H.Schägger, editors. Academic Press, San Diego. 105-130.

80.	Schägger, H. and K.Pfeiffer. 2000. Supercomplexes in the respiratory chains of yeast and mammalian mitochondria. *EMBO J.* 19:1777-1783.

81.	Schägger, H. and G.von Jagow. 1987. Tricine-sodium dodecyl sulfate polyacrylamide gel electrophoresis for the separation of proteins in the range from 1-100 kDalton. *Anal. Biochem.* 166:368-379.

82.	Schägger, H. and G.von Jagow. 1994. Native und denaturierende Elektrophorese von Proteinen: Analytische und präparative Möglichkeiten in der Proteinchemie und der klinischen Diagnostik. *In* Messe-Exponate der Universität Frankfurt. Universität Frankfurt/Main, editor. Universtität Frankfurt, Frankfurt/M.

83.	Schuler, F., T.Yano, S.Di Bernardo, T.Yagi, V.Yankovskaya, T.P.Singer, and J.E.Casida. 1999. NADH-quinone oxidoreductase: PSST subunit couples electron transfer from iron-sulfur cluster N2 to quinone. *Proc. Natl. Acad. Sci. USA* 96:4149-4153.

84.	Sherer, T.B., R.Betarbet, C.M.Testa, B.B.Seo, J.R.Richardson, J.H.Kim, G.W.Miller, T.Yagi, A.Matsuno-Yagi, and J.T.Greenamyre. 2003. Mechanism of toxicity in rotenone models of Parkinson's disease. *Journal of Neuroscience* 23:10756-10764.

85.	Skehel, J.M., I.M.Fearnley, and J.E.Walker. 1998. NADH:ubiquinone oxidoreductase from bovine heart mitochondria: sequence of a novel 17.2-kDa subunit. *FEBS Lett.* 438:301-305.

86.	Sled, V.D., T.Friedrich, H.Leif, H.Weiss, Y.Fukumori, M.W.Calhoun, R.B.Gennis, T.Ohnishi, and S.W.Meinhardt. 1993. Bacterial NADH-quinone oxidoreductases: iron-sulfur clusters and related problems. [Review]. *J. Bioenerg. Biomembr.* 25:347-356.

87. Sled, V.D., N.I.Rudnitzky, Y.Hatefi, and T.Ohnishi. 1994. Thermodynamic analysis of flavin in mitochondrial NADH: ubiquinone oxidoreductase (complex I). *Biochem.* 33:10069-10075.

88. Steuber, J. 2001. The Na+-translocating NADH:quinone oxidoreductase (NDH I) from *Klebsiella pneumoniae* and *Escherichia coli*: Implications for the mechanism of redox-driven cation translocation by complex I. *J. Bioenerg. Biomembr.* 33:197-186.

89. Triepels, R., L.P.Van den Heuvel, J.L.Loeffen, C.A.Buskens, R.J.P.Smeers, M.E.Rubio-Gozalbo, S.M.S.Budde, E.C.M.Mariman, F.A.Wijburg, P.G.Barth, J.M.Trijbels, and J.A.Smeitink. 1999. Leigh Syndrome Associated with a Mutation in the NDUFS7 (PSST) Nuclear Encoded Subunit of Complex I. *Ann. Neurol.* 45:787-790.

90. Volbeda, A., M.H.Charon, C.Piras, E.C.Hatchikian, M.Frey, and J.C.Fontecilla-Camps. 1995. Crystal structure of the nickel-iron hydrogenase from *Desulfovibrio gigas. Nature* 373:580-587.

91. Wallace, D.C. 1999. Mitochondrial diseases in man and mouse. *Science* 283:1482-1488.

92. Wang, J.M., J.P.Silva, C.M.Gustafsson, P.Rustin, and N.G.Larsson. 2001. Increased in vivo apoptosis in cells lacking mitochondrial DNA gene expression. *Proceedings of the National Academy of Sciences of the United States of America* 98:4038-4043.

93. Weiss, H., T.Friedrich, G.Hofhaus, and D.Preis. 1991. The respiratory-chain NADH dehydrogenase (complex I) of mitochondria. *Eur. J. Biochem.* 197:563-576.

94. Wikström, M.K.F. 1984. Two protons are pumped from the mitochondrial matrix per electron transferred between NADH and ubiquinone. *FEBS Lett.* 169:300-304.

95. Yankovskaya, V., R.Horsefield, S.Tornroth, C.Luna-Chavez, C.Leger, B.Byrne, G.Cecchini, and S.Iwata. 2003. Architecture of succinate dehydrogenase and reactive oxygen species generation. *Science* 299:700-704.

96. Zickermann, V., B.Barquera, M.K.F.Wikström, and M.Finel. 1998. Analysis of the pathogenic human mitochondrial mutation ND1/3460, and mutations of strictly conserved residues in its vicinity, using the bacterium *Paracoccus denitrificans. Biochem.* 37:11792-11796.

97. Zickermann, V., M.Bostina, C.Hunte, T.Ruiz, M.Radermacher, and U.Brandt. 2003. Functional implications from an unexpected position of the 49 kDa subunit of complex I. *J. Biol. Chem.* 278:29072-29078.

98. Zu, Y., S.Di Bernardo, T.Yagi, and J.Hirst. 2002. Redox Properties of the [2Fe-2S] Center in the 24 kDa (NQO2) Subunit of NADH:Ubiquinone Oxidoreductase (Complex I). *Biochem.* 41:10056-10069.

8 APPENDIX

8.1 Non-Standard EPR Experiments (ESEEM and ENDOR)

Since it is still unknown which residue is the 4th ligand of cluster N2 it is possible that a nitrogen from the peptide backbone or some nitrogen containing side chain of amino acids such as histidine or arginine could serve as ligand. In x-band cw EPR spectroscopy such stakes cannot be visualised. If nitrogen ligates one of the iron-sulphur clusters in complex I it is possible to detect this using more extensive EPR studies. The proposed experiments were ESEEM and ENDOR. ESEEM stands for **E**lectron **S**pin **E**cho **E**nvelope **M**odulation, (cw) ENDOR for (**c**ontinuous **w**ave) **E**lectron **N**uclear **Do**uble **R**esonance.

8.1.1 Strain KL6×CH3

For non-standard EPR experiments it was necessary to make a *Y. lipolytica* strain that can be grown on minimal media without adding any external nitrogenous compounds except ammonium sulphate. To make this strains KL6 (*nukm::LEU2 Mat*B *ndh2i leu2*-270 *lys11*-23 *xpr2*-322 *ura3*-302) and CH3 (*nucm::URA3, 30Htg , ndh2i, his-1, ura3*-302, *leu2*-270, *xpr2*-322) were mated to yield the diploid strain KL6×CH3. There was no need for DNA analysis since only the diploid strain with both alleles *nucm::ura3* and *nukm::leu2* could grow on SD media without uracil, leucine, lysine or histidine.

8.1.2 ^{15}N-labelled Complex I

The ^{14}N nucleus has spin I = 1 and the quadrupole coupling with weakly coupled nitrogen can have an extensive influence on the hyperfine spectrum. This leads to further splitting of the resonance positions in ESEEM and ENDOR spectra. This effect generally causes peak dispersion, which on the other hand complicates peak detection. This problem can be solved through a global ^{15}N labelling because the ^{15}N nucleus has spin I = ½ and does not show any quadrupole coupling and the resonance positions can be easier detected. Also, the spectra of ^{15}N labelled enzymes directly deliver hyperfine tensors whose values can be entered into the simulations of ^{14}N spectra.

104

To make fully ^{15}N-labelled complex I from *Y. lipolytica* firstly it was necessary to have a protothrophic strain so that the sole nitrogen source would be ^{15}N-labelled ammonium sulphate. Since ^{15}N-labelled ammonium sulphate is very expensive it was necessary to work with the minimally required amount (Figure 8.1). This was determined using small scale (250 ml) cultures.
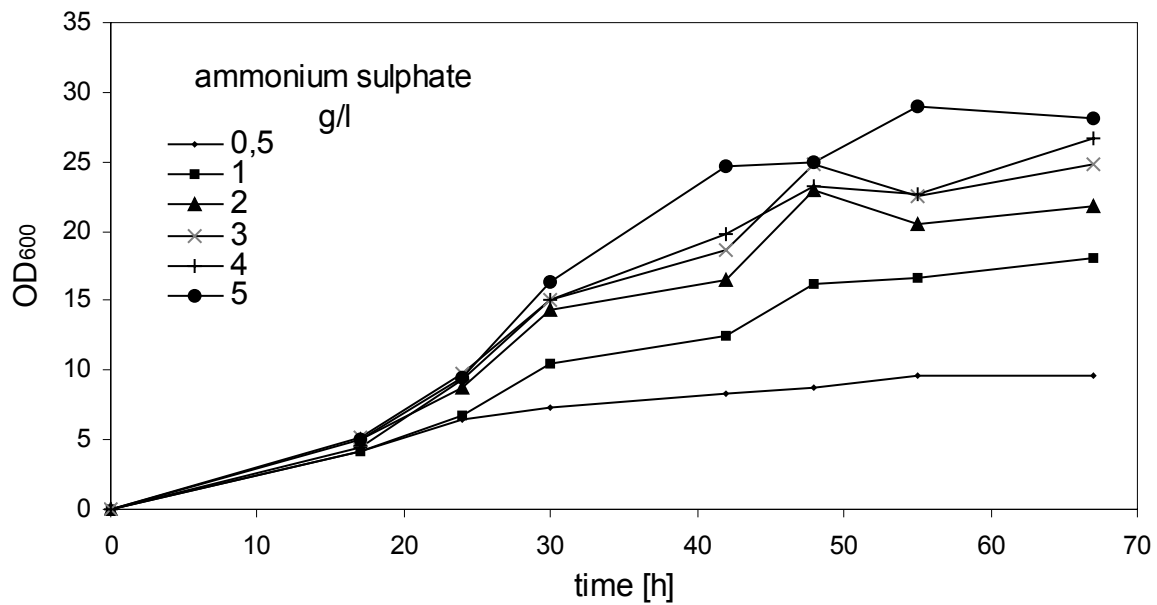

Figure 8.1) *Y. lipolytica* **growth depending on ammonium sulphate concentrations**

Y.lipolytica was grown in flasks in SD medium in the presence of 50 mM NaP$_i$ buffer, pH 6. Different curves present different amounts of ammonium sulphate used.

For a large scale culture (10 l) ^{15}N-ammonium sulphate was added in SD medium at a concentration of 2.5 g/l. About 300 g of wet cells were obtained from a 10 l fermenter. Mitochondrial membranes had very low complex I content at about 50 % according to NADH:HAR activity, whereas dNADH:DBQ activity was parental when normalised for complex I content. Complex I was purified via His-Tag affinity chromatography and EPR experiments were performed in group of the Prof. Prisner, Department of Physical and Theoretical Chemistry at the JWG University of Frankfurt.

| Strain	Complex I	
	content (%)	activity (%)
Parental	100	100
KL6×H3	50	100

Table 8.1 Activity tests measured on mitochondrial membranes from strain KL6×H3

Complex I content is given as specific NADH:HAR oxidoreductase activity in mitochondrial membranes (100% = 1.0 μmol min^{-1}mg^{-1}), dNADH:DBQ oxidoreductase activity was normalized for complex I content (100% = 0.3 μmol min^{-1}mg^{-1}).

8.2 Proton Pumping

8.2.1 ACMA dye

ACMA (9-amino-6-chloro-2-methoxyacridine)
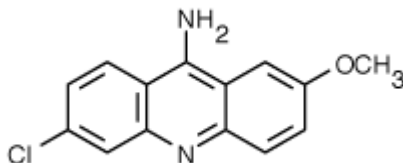
8.2.2 Ionophores used in ACMA Measurements

8.2.2.1 Valinomycin

Valinomycin is mobile carrier that catalyses the electrical movement of K^+ across phospholipid bilayers. This implies that the potassium distribution across the membrane obeys the Nernst equation once equilibrium has been attained.
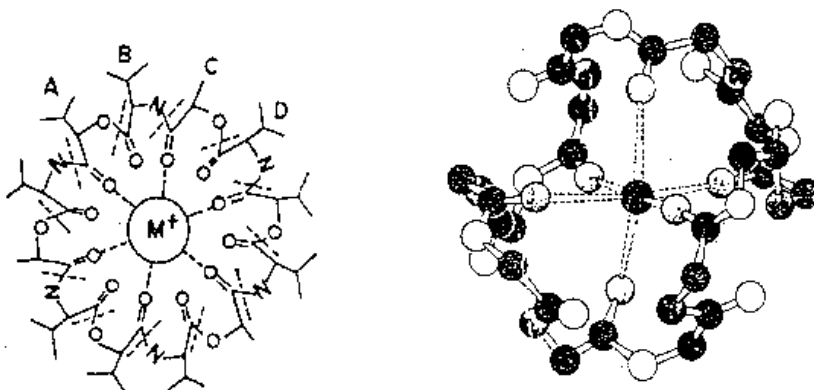

It is a cyclic amide/ester in which the sequence D-hydroxy- isovalerate, L-valine, L-lactate and D-valine is repeated three times (-A-B-C-D- in the Figure above). The ionophore provides a polar interior to accommodate the potassium ion, but presents a non-polar lipophilic exterior to the outside.

8.2.2.2 Nigericin

Nigericin is mobile carrier that resembles valinomycin but contains a carboxyl group and forms a potassium salt. It therefore catalyses an electroneutral potassium/proton exchange across lipid bilayers.

This implies that the potassium distribution will be related to the pH gradient once equilibrium has been attained:
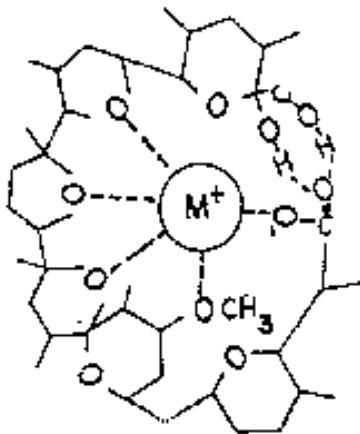
$$[K^+]_{in} / [H^+]_{in} = [K^+]_{out} / [H^+]_{out}$$

In some cases (e.g. valinomycin) the ionophore - ion complex has a net electrical charge, whereas the empty carrier is neutral. Other ionophores (e.g. nigericin) only form electrically neutral complexes. Charge makes an enormous difference to the behaviour of each carrier, since the charged complexes interact with membrane potentials, whereas the neutral complexes are unaffected. We speak of electrical and electroneutral carrier mechanisms to draw attention to this difference.

8.3 Moser-Dutton Ruler: A Formalism to Calculate Electron Tunnelling Rates in Redox Proteins[1].
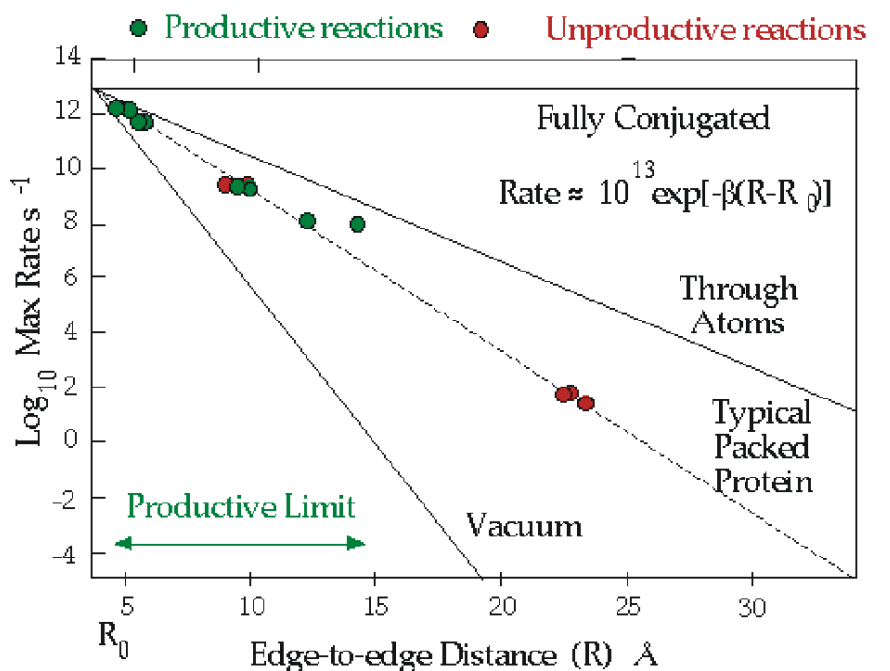
Figure 8.2 Moser-Dutton ruler. Free energy optimised electron transfer rates vs. distance in *Rp. viridis* and *Rb. sphaeroides* reaction centres[2]

---

[1]taken from http://www.life.uiuc.edu
[2] taken from http://www.uphs.upenn.edu/biocbiop/local_pages/dutton_lab/ettheory.html

Research on photochemical reaction centres has been a primary arena for advances in our understanding of the relation between structure and rates of electron transfer in proteins, because the crystallographically defined structures provided for the first time, in the context of an experimental system in which the rates could be accurately measured by picosecond spectroscopy, the spatial parameters and details of the reaction medium (the protein) necessary for understanding these processes.

A major advance in these studies came from an extensive set of experiments from Dutton's lab (Moser *et al.,* 1995), in which several different reactions of the photochemical cycle were measured (and rate constants determined), with a variety of molecular engineering tricks to set up a range of values for ΔG^o for the reactions. These made it possible to determine whether the reactions behaved as expected from Marcus theory, and to derive a general rule (Dutton's Ruler) relating rate of reaction to distance apart of redox centres.

8.4 *NUCM* Gene

8.4.1 *NUCM* Gene encoding 49-kDa subunit, ACC. No. AJ249783

```
                                       Xba I
                             TCTAGAATGTGGTTGGTCGTTTCCTTTTTTGGCGT      35
        TTTTGAAGGGGTTAATCTTGCATCTCATTCACAAAATATGGTGGATTCTGAAGGAGAGAGA      95
        TGTAGGTTCAAATTTGGGGGAAATATAAGCCGAAACCGTAGTAGGGGTGAAGTTGAGGGG     155
        GAGGTCGTTGGGACGCCATAATATACTGTGTTGTAGGATATTCTGTGCTAAAATCAACAC     215
        AAATTAATGGAATAGAGTCCTTTAGAAGTAAATATTCGCAAATTGCGTCCAAAAAATACA     275
        CCCCTACAGAGCCCGCTCACAGTCACCTGAATCAACTCATTAAACGTTGCTAACCAACTT     335
        TATCCACTACTTGGAATAAAACAAAGCAGTCTTCAAACTCCCCCAAAAGATCACTTATTG     395
        AAACTATGAAACTTGCATTACAATAACCGTCCCTTTTTATCCCCTTTTGTATCTTTATAT     455
        CTTCCTGTTAAACCTCTCAAACTCGCAAACGTGATTCCTTTGAGCTTGGGAAGTTTGGC     515
n49knc1TGGTCAGACTTCCACACATAAACCTCCACCCAATGAAAGCCGAGCTATTGAAAGAGGGAG     575
        ATGGTAGAACGATGCAATTGGGCTTTTTCCACGGGACAAGTCGTGAATTATATAGCTACG     635
        GGCCAATTGTCTTAATCTACTGACTTCTTACCACCACAACCACCCCCACAACCTATATAC     695
        ACTCCTTCAACCCTAACCCCCGTTTGCGCCAATCAGCGTTCTCGGAATACTCCCATCTGG     755
        ACTAAACTCTTCACAGCGACCGAACCTCTGTTACACACCAAAAGCACAACCCCTCACACA     815
            49-1
        ATGCTGCGATCTGCTGCTGCCCGAGCCGTCAGGGCTGTGCGCCCCCGGCTGTCTGCTCGA     875
        MetLeuArgSerAlaAlaAlaArgAlaValArgAlaValArgProArgLeuSerAlaArg      20

        TACATGGCCACCACCGCTCTGCCCCAGGACCCCATCCCCTCCGGAGCTCTGGGCCAGAAG     935
        TyrMetAlaThrThrAlaLeuProGlnAspProIleProSerGlyAlaLeuGlyGlnLys      40
                      n49nc2
        GTGCCTCACGTCGATGAGAGCCACCAGGACCTGCTGTTCCGAACCTCTCACATGGTGGAG     995
        ValProHisValAspGluSerHisGlnAspLeuLeuPheArgThrSerHisMetValGlu      60

        GATCTCGAGACCTACGACGAGGACTCCCCTATCAACACGTCGGACGCCAACACCCGAATC    1055
        AspLeuGluThrTyrAspGluAspSerProIleAsnThrSerAspAlaAsnThrArgIle      80
            49-4
        CGAGCCTTCACCATCAACTTTGGTCCCCAGCATCCCGCTGCCCACGGTGTGCTGCGTCTG    1115
        ArgAlaPheThrIleAsnPheGlyProGlnHisProAlaAlaHisGlyValLeuArgLeu     100
                                  A
        ATTCTGGAGCTGTCTGGAGAGGAAATCATTCGATCGGACCCCCACGTCGGTCTGCTGCAC    1175
        IleLeuGluLeuSerGlyGluGluIleIleArgSerAspProHisValGlyLeuLeuHis     120
                                      49-2   G
        CGAGGAACCGAGAAGCTCATTGAGTACAAGACTTACATGCAGGCGCTGCCATACTTTGAT    1235
        ArgGlyThrGluLysLeuIleGluTyrLysThrTyrMetGlnAlaLeuProTyrPheAsp     140

        CGTCTGGATTACGTGTCCATGATGACCAACGAGCAGGTTTTCTCTCTGGCTGTCGAGAAG    1295
        ArgLeuAspTyrValSerMetMetThrAsnGluGlnValPheSerLeuAlaValGluLys     160

        CTGCTCAACGTGGAGGTGCCCCTGCGAGGCAAGTACATCCGAACCATGTTCGGAGAGATC    1355
        LeuLeuAsnValGluValProLeuArgGlyLysTyrIleArgThrMetPheGlyGluIle     180

        ACCCGAGTGCTCAACCATCTCATGTCCGTGTGTTCACACGCCATGGATGTCGGTGCTCTG    1415
        ThrArgValLeuAsnHisLeuMetSerValCysSerHisAlaMetAspValGlyAlaLeu     200

        ACCCCCTTCCTTTGGGGTTTTGAGGAGCGAGAAAAGCTTATGGAGTTCTACGAGCGAGTC    1475
        ThrProPheLeuTrpGlyPheGluGluArgGluLysLeuMetGluPheTyrGluArgVal     220
            49i
        TCTGGAGCCCGTCTGCACGCCGCGTACGTGCGACCTGGAGGAGTCTCCCAGGACCTGCCC    1535
        SerGlyAlaArgLeuHisAlaAlaTyrValArgProGlyGlyValSerGlnAspLeuPro     240
```

```
        GCCGGCCTGCTGGACGATATTTACATGTGGGCTACACAGTTCGGTGACCGTCTGGACGAA   1595
        AlaGlyLeuLeuAspAspIleTyrMetTrpAlaThrGlnPheGlyAspArgLeuAspGlu    260
                    49-3
        ATCGAGGAGCTGCTGACCGATAACCGAATTTGGAAGCTACGAACCGTCAACATTGGAACC   1655
        IleGluGluLeuLeuThrAspAsnArgIleTrpLysLeuArgThrValAsnIleGlyThr    280
                                                              BamHI
        GTGACCGCCCAGGACGCCTTGAACCTTGGTCTTTCCGGCCCCATGCTGCGAGGATCCGGT   1715
        ValThrAlaGlnAspAlaLeuAsnLeuGlyLeuSerGlyProMetLeuArgGlySerGly    300

        ATCCCCTTTGACATTCGAAAGAACGCCCCCTACGACGCATACGACAAGGTCGACTTCGAC   1775
        IleProPheAspIleArgLysAsnAlaProTyrAspAlaTyrAspLysValAspPheAsp    320

        GTCCCCGTCGGCATGAACGGAGATTGTTACGACCGATACCTGATTCGAATGGCCGAGTTC   1835
        ValProValGlyMetAsnGlyAspCysTyrAspArgTyrLeuIleArgMetAlaGluPhe    340

                                 T
        CGACAGTCGCTGCGAATCATCGAGCAGTGCTGCAACGACATGCCTGCCGGCGCCGTTAAG   1895
        ArgGlnSerLeuArgIleIleGluGlnCysCysAsnAspMetProAlaGlyAlaValLys    360
                                                          49i1
        GTGGAGGACTTCAAGATTAACTCGCCTCCTAGAAACCTCATGAAGGAGGATATGGAGGCC   1955
        ValGluAspPheLysIleAsnSerProProArgAsnLeuMetLysGluAspMetGluAla    380

        CTGATCCACCACTTCCTGCTCTACACAAAGGGATACTCTGTTCCTCCCGGAGAGACCTAC   2015
        LeuIleHisHisPheLeuLeuTyrThrLysGlyTyrSerValProProGlyGluThrTyr    400
         49-2.5              G                              C
        ACCGCCATCGAGGCCCCCAAGGGAGAGATGGGTGTCTACGTCGTCTCCGACGGTAGTGAG   2075
        ThrAlaIleGluAlaProLysGlyGluMetGlyValTyrValValSerAspGlySerGlu    420

        CGACCATACAAGTGCAAGATCCGAGCCCCCGGATTTGCCCATCTCGGAGCCTTTGATCAC   2135
        ArgProTyrLysCysLysIleArgAlaProGlyPheAlaHisLeuGlyAlaPheAspHis    440
                           n49kc2
        ATTGCCCGAGGACATTTCCTTCCCGACGCCGTGGCCATTATTGGTACCATGGATCTTGTG   2195
        IleAlaArgGlyHisPheLeuProAspAlaValAlaIleIleGlyThrMetAspLeuVal    460

        TTTGGAGAGGTTGATCGATAGTCATAGAATACATACTAAGCAGAGTCGCATATGCGTGTG   2255
        PheGlyGluValAspArg***                                          466

        CTCGTGGAATGTACTGTAGAGGGTTGTACACTGTATGTGAGAGCAGAGTTGCTATAAGGA   2315
        GAGGTGGTGGATGCGTGACTGTTAGTTGGACTGTGAGTCAGAATGGTCCGTTGAGAGCAA   2375
        TGTGGGTCATGCTAAATCTCTTAATGCTTTCTCTTCTACTATGGTGATGTTACCTCACAG   2435
        ATACAACAATCGAGATACGGGTCGCGAGACGAGTAGATGTGAGACTACAAATACTGTACA   2495
        CTTGTATAACTAATCTACAGGACAGGTGAATGCGAAAGTAAAATGCGATCATCTCTCGGC   2555
        CGTAGATGGTCATATTAGTCACATATAATCTGATGCCGGTAAATTTCACATGTCAAGCAT   2615
n49kc3  GTCCATATGGATCTGTCATCAAGCGAGACAGCCACCAAGACTGGAACCAATGCCGCTGGT   2675
        AGTAATGGACCTTCTGGTACCAGAGCTGTCATCATTTGCTTGAACCACCTCCTTCATATG   2735
        CTCACAAAATCACATGGCTGTGGTTCATCTCACACCAATCCTTTGAGCATATGTCATTCA   2795
  SphI  TGTAGCATGCATAAACATGTCATCAAAGAAACATATTGGGGCGATGGGAACTGATAAGGG   2855
        GGTGGATGAACATCTGATCTATTGGATGAACTCGATATAAATGATCGTTAATTGAACTAC   2915
        TTGTAGTTATTACAAACACTTTTGCAAGTGCTAGATCATGATTACTTGTGTACACCTACT   2975
        GATGCGTGATCAATAGGTAAACCATGATCTGGTGAATACCATTACCTGTCCCCTGGTGTA   3035
        CATAAGCATACTACGGGACAACTTCTGCACAGAGAGAGATC                     3076
```

Used oligonucleotides, silent mutations and some restriction sites are marked with grey, darker grey indicates direction of the primer.

8.4.2 Used oligonuceotides in the *NUCM* gene

direction	name	sequence	binding site
	49-1	5'-TCACACAATGCTGCGATC-3'	809-827
	49-4	5'-TCCGAGCCTTCACCATCAAC-3'	1054-1073
	49-2	5'-ACATGCAGGCGCTGCCATAC-3'	1221-1230
forward	49i2	5'-GCGTACGTGCGACCTGGA-3'	1497-1516
	49-3	5'-AGGAGCTGCTGACCGATAAC-3'	1600-1620
	49-2.5	5'-GAGACCTACACCGCCATCGAG-3'	2007-2027
	n49kc2	5'-ACGCCGTGGCCATTATTG-3'	2160-2175
	n49knc1	5'-ATGTGTGGAAGTCTGACC-3'	534-515
reverse	n49nc2	5'-CCTGGTGGCTCTCATCGACG-3'	963-943
	49i1	5'-GCCTCCATATCCTCC-3'	1954-1940

Table 8.2 Oligonucleotides for sequencing the *NUCM* gene

name	sequence	binding site
49us	5'-GATCACGCATCAGTAGGT-3'	2986-3004
49ds	5'-TGTATGCATTGCGTCCAC-3'	outside of sequenced area

Table 8.3 Oligonucleotides for deletion checking via PCR

8.5 Mitochondrially expressed eYFP

8.5.1 Fusion of the 75-kDa presequence with the eYFP gene[1]

```
GTCGACGGTCTCTCCCAGGACACTCCTCTTCCTCATGTCCATGTTCATTGCTTCCACAAG        60
TGGGAGGCTGGAGAAGAAGAGCCCTCCAAGGAGGAGACCAAGGCTGCTCTTTTGGAGCGG       120
GTGTACAAGCAGATCGACGTGCGACTGGACCCCAACGAGGTTGGAATGCATTGGGTTCGA       180
AAGGTGTCTCCCAAGAAGGACATGTTTTGCATTTCTTTCGAGCTGCCCAAGGAGGTTGCA       240
TGGGCCCCTCAGGTTAACAAGGAGTAAATGTATATATATGTATTATAATGGTAATGACGG       300
CGATGAATTTGCAGAAGTACTCAGGACAGTTCTTTCGTGAGTGGGTGATTTTTCTTGATT       360
TTTTCGATTTCTTGATTTTTTCGATTTCTTGATTTTTTCGATTTTCTTGATTTTCCCATT       420
ATTCGATTTTCCCCATTATTCGATTTTCCCCATTATTCGATTTTTCATTTTTATGCCGAA       480
ATACGAGTATTGTACCACTGGCACCATAAATACAAACCATTCATGACTCCCACAGACCTG       540
GACCAAAGAACATCGTACTTGTATCTGAACTCACGACTTCATTATTGCTTGTACCCGTCC       600
TCATACCTCTCCCTCCGCTCCGTCTCCCTCCACCATTACTAAGCAACAAGGGCCAATTGT       660
GTCGGAGCTTTCTGCTGACCAAAACTCTCCCTCTTGCCAACTTCTCCAATCAAAAGATG       720
ATTTTGCAAGATGTCATTGCCAACACTAGCTTTTAGAGTTGGTCTGGAGGGCTACACAAC       780
ATCCGGTAGCGATGCATCCATGTCCGAAAATTTGTAGTGGATGGCGGTGATATTATTGCG       840
AGAATTTGCCAACCGCAGCTGAATCAGCCAATTGAGGGGTTTTCCGGCTCCACAGCTCTC       900
TGCCACGGCGGAGTTCAACCGACCCCCAAATCTCCGTACTGACATGTACTGTAGGCAGAC       960
CCAAAAATAAGCTCTCCCAAGGTCGTAACTCCCAGCCAATGGTAGTGGACCAATTGTGGT      1020
GCGTCTGTGTGTAGAAGTGGGTGGGTTTAATCCATCTTTTGAGTATTCAATAGAGTGAAC      1080
AGACACATTTCTCAGAAGACACGTCTTAGAAAAGGTGAGTGAAATGAGGACATGTGGAGG      1140
ACAAATTGGAGAGATATCAGCAGAGATGCAGCAGGATGAACACACAGACAGACACAACAG      1200
CAGGAACGACACAGATGGAACGGCAGACAACACATCCAGGGAAGGACACTATCGGCGGAA      1260
GGACACACGCAAAAGGACAGCTGAAAGGGATGGATGACAGCCGAGCCCGACCGAAGACGG      1320
TGGCAAAACGAGATGCGACACAATACAGCTGAATCGACAGTTCGATTGTGTCTGGAAGAT      1380
GGGCCGTACGGAGATCCAAGCAATACACGGGGTTAGCTGTGCCCCTTCAAAGAGCGGCAA      1440
TCGTGCACGAAAAACATAGTCGTGCATCCCCGACAACGGTGGATATGTGGCTGCGTCCGT      1500
GTCACTTTGCCCGTGTCATCCAGTTCAGTTTTCTGCAAAGAATATCTCACATCGTTACCT      1560
CTTATCTCCAAACCATGCCAATCCACCCAGCTACTAACATAGATGCTCTCGAGAAACCTC      1620
                                          MetLeuSerArgAsnLeu       6

AGCAAGTTTGCTCGAGCCGGTCTCATCCGGCCAGCAACCACATCCACACACACCCGACTA      1680
SerLysPheAlaArgAlaGlyLeuIleArgProAlaThrThrSerThrHisThrArgLeu      26

TTCAGCGTCTCCGCCCGACGTCTCGCCGAGATTGAACTCACTATCGATGGTCATATGGTG      1740
PheSerValSerAlaArgArgLeuAlaGluIleGluLeuThrIleAspGlyHis M  V      46

AGCAAGGGCGAGGAGCTGTTCACCGGGGTGGTGCCCATCCTGGTCGAGCTGGACGGCGAC      1800
 S  K  G  E  E  L  F  T  G  V  V  P  I  L  V  E  L  D  G  D      66

GTAAACGGCCACAAGTTCAGCGTGTCCGGCGAGGGCGAGGGCGATGCCACCTACGGCAAG      1860
 V  N  G  H  K  F  S  V  S  G  E  G  E  G  D  A  T  Y  G  K      86

CTGACCCTGAAGTTCATCTGCACCACCGGCAAGCTGCCCGTGCCCTGGCCCACCCTCGTG      1920
 L  T  L  K  F  I  C  T  T  G  K  L  P  V  P  W  P  T  L  V     106

ACCACCTTCGCCTACGGCCTGCAGTGCTTCGCCCGCTACCCCGACCACATGAAGCAGCAC      1980
 T  T  F  G  Y  G  L  Q  C  F  A  R  Y  P  D  H  M  K  Q  H     126

GACTTCTTCAAGTCCGCCATGCCCGAAGGCTACGTCCAGGAGCGCACCATCTTCTTCAAG      2040
 D  F  F  K  S  A  M  P  E  G  Y  V  Q  E  R  T  I  F  F  K     146
```

---

[1] 3 letter code used for 75-kDa subunit, 1 letter code used for eYPP

```
GACGACGGCAACTACAAGACCCGCGCCGAGGTGAAGTTCGAGGGCGACACCCTGGTGAAC        2100
 D   D   G   N   Y   K   T   R   A   E   V   K   F   E   G   D   T   L   V   N     166

CGCATCGAGCTGAAGGGCATCGACTTCAAGGAGGACGGCAACATCCTGGGGCACAAGCTG        2160
 R   I   E   L   K   G   I   D   F   K   E   D   G   N   I   L   G   H   K   L     186

GAGTACAACTACAACAGCCACAACGTCTATATCATGGCCGACAAGCAGAAGAACGGCATC        2220
 E   Y   N   Y   N   S   H   N   V   Y   I   M   A   D   K   Q   K   N   G   I     206

AAGGTGAACTTCAAGATCCGCCACAACATCGAGGACGGCAGCGTGCAGCTCGCCGACCAC        2280
 K   V   N   F   K   I   R   H   N   I   E   D   G   S   V   Q   L   A   D   H     226

TACCAGCAGAACACCCCCATCGGCGACGGCCCCGTGCTGCTGCCCGACAACCACTACCTG        2340
 Y   Q   Q   N   T   P   I   G   D   G   P   V   L   L   P   D   N   H   Y   L     246

AGCTACCAGTCCGCCCTGAGCAAAGACCCCAACGAGAAGCGCGATCACATGGTCCTGCTG        2400
 S   Y   Q   S   A   L   S   K   D   P   N   E   K   R   D   H   M   V   L   L     266

GAGTTCGTGACCGCCGCCGGGATCACTCTCGGCATGGACGAGCTGTACAAGCATATGGCC        2460
 E   F   V   T   A   A   G   I   T   L   G   M   D   E   L   Y   K HisMetAla      286

AAGAGCAGCATTGCATTCAACAAAGACAACAAGAAAAACCAGGCTTTTGCCTAATTAAGT        2520
LysSerSerIleAlaPheAsnLysAspAsnLysLysAsnGlnAlaPheAla***            303

AATCAATTAGATGTTATATGAAAACCCGAGTACAGCATGTACTGGTAGAGGAGTAGGGAT        2580
GATTCGAGGATAGTGGAGCTATTGTGAAGTGACCGGGTGGGTTAACAAAA GTATTGCTT      2640
TGAATTAGTTTGACGATATAGATGTATATGACTACTGTATGTACTTGTAGTTGCGAGCTC      2700
AGAACGAATGAGACAGAGCAGCTCAGCCATTTACAGTACAGTATGTGCTTGCTCATGGGC      2760
AGTTACAAGTTCCTACTTGTAATACGGAGTCTGGTTTTTCAGTTGACATGGATTATACAA      2820
CTTTAAGGCGCTCGAAAAGCGTTGTACCACTTTCTATCCACTAAGATATGTTTGAACCAA      2880
CCAGAGCTATCTACTTGTAGCTACACGGCTGACCACCAAACTCTTGGTCAACTAATGTCA      2040
CCAGCAACAACTGATGAACTCCAAAGGGTGAACCATAGACTCCACGCTGTGGAAGGATAT      3000
GTAAATAAAGACAACCATAAAACAGAACTTCAGACACTTGGCAAGGAAAAGATTACAGC      3060
ACCTAGGATTCTCGTATGGTCTCCCACTACAATACTAACTAGGCTCTCTGGTGCTTGACT      3120
ATGGCTGATCGGACGGGAAGCCGTATTTTCACCAGGATATGGCCGTAACCAAGACTCCGA      3180
TACGGGGAATCGAACCCCGGTCTCCACGGTTCTCAACATGAGAGCGTGATGTGATAGCCC      3240
CTACACTATATCGGAAATGTGCAAGACACGGTGTTTTTGGCGTCACGCATCTGATTCGCC      3300
AAATAAGGTTTAATTAAAAAGTTAACGAATATTAAAATAGTTAGAATAAAAATAATTTGT      3360
CAAGCGTTTGTATCGGCTCAAGAAAAGAAAAATAAGGGAACCGGGGAGTGTGGAATTTTC      3420
AAACTGTTCGGAGAAAAACTATTACGGGTCTATTGCACGAGATTTCTCCCTGTTTTATGG      3480
TCGTTTAGTTGCTGAGATGCATTGGGCAAGAATCACAAAATAAAATGACTCGTGAAATGC      3520
GCACAATGCGACCTTAATGCACGTTTAGCCAGTAGTGTGCATGATAATCCACATACAAAG      3580
TTAAGATCCGATGTTAGCCTACGTGTATTTACTATAGCTGAAATGTCTACCTGTACTCAT      3640
TTAGTGCGAAAAAATTTAACCACCTCTAGCGCCCGGTCTTGTCATGTCTTGGCTCATGTA      3700
CATGAGATGAGAGTGTATGTGATCTGACGGAAGTGGGCACATACACGCTGATAACATTTC      3760
AGGTGCGTTCCTGCGGTTGATATCACAAGCATCTCCGAGCACACGAAAATGAGATGGTAT      3820
GCTGAAGTCTCCACCTTTAGTCGAC                                       3845
```

8.5.2 Oligonucelotides used for fusion of the 75-kDa presequence with the eYFP gene

name	sequence	binding site
EYFPCc	5'-ATATATCATATGGTAAGCAAGGGCGAGG-3'	612-631[a]
EYFPCnc	5'-ATATATCATATGCTTGTACAGCTCGTCCAT-3'	1330-1311[a]
75Nde1c	5'-ATATATCATATGGCCAAGAGCAGCATTGC-3'	1734-1708
75Nde1c	5'-ATATATCATATGACCATCGATAGTGAGTTC-3'	2451-2472

Table 8.4 Oligonucleotides for introducing *Nde* I sites into *NUAM* and eYFP genes

[a] the numbering of the oligonucleotides sequence binding site refers to the original sequence of eYFP gene

name	sequence	binding site
LGseq1	5'-CCAGCAACCACATCCACAC-3'	1650-1669
LG75kseq2	5'-CCACTATCCTCGAATCAT-3'	2696-2676
75kseq1	5'-CCGTGTCATCCAGTTCAG-3'	1511-1529
EYFPseq	5'-CGCACCATCTTCTTCAAGG-3'	2022-2041

Table 8.5 Oligonucleotides for sequencing the fusion between the NUAM ad eYFP gene

8.5.3 Fusion of the 30-kDa with the eYFP gene[1]

```
TATGGTCAGATCAGGTGGTAGTGTGGCAACGCTATCTGTGTGTGGTGTAAAGAGAGTTGT        60
ATCGCCAAGTTGTCTGTTTAGTGCCGGGTAAGTTCACAATTTGGCGTGTTTTGTGCCTGC       120
TGGGAGCTTGCCCAATTCGGCTGACTAAGTTCCACTTGTATGGAGTCTAATGACATGTGA       180
GGACAGGACAGAAATGTGCCTAATACGGTGTTTTACTATCAAAATGCCTGTGGGAAAAAA       240
CATAAATACTTATCTGACCCCCCTAAATTCCATCTCCGACCAACCCCTACCCCATCACCG       300
CTTCATACACCCACTTATTCAATACCTCCCACTTTTTGGTCACGTGCAGGGTTTCTCCCA       360
ACGTCTCGCCCAATCAAACTCGCCAAAATTCAATTGTCAAACCCAACTCTTGTCTGGTGC       420
AAAAGCCTGTAATACTGGTTACGCAGGAGCCGTCGTGACACACAACACACAACTAACACA       480
```

```
ATGCTCTCTCGATTCGCCAGAATTGGCAGCATGGGCATCCGCCCCGTCGCAGCAGCCCGT       540
MetLeuSerArgPheAlaArgIleGlySerMetGlyIleArgProValAlaAlaAlaArg        20
```

```
GCTACCTTTGTGACCTCCGCCCGAGCCGCCCAGGCCGCCCCCTCTTGGGAGAACATCAAG       600
AlaThrPheValThrSerAlaArgAlaAlaGlnAlaAlaProSerTrpGluAsnIleLys        40
```

```
GACATCCGACTCGACCCCAAGGTCCATGTTGACGAGGTTTACGAGCCCATCGTCAACCCC       660
AspIleArgLeuAspProLysValHisValAspGluValTyrGluProIleValAsnPro        60
```

```
GCAGACCGATACCTCCAGCACGTGTCGGACCTCCACCAGTACGCCAAATACATCATGGCT       720
AlaAspArgTyrLeuGlnHisValSerAspLeuHisGlnTyrAlaLysTyrIleMetAla        80
```

```
GCTCTGCCCAAGTACATCCAGGGCTTTTCTGTGTGGAAGGACGAGCTGACTCTGCACGTT       780
AlaLeuProLysTyrIleGlnGlyPheSerValTrpLysAspGluLeuThrLeuHisVal       100
```

```
GCACCAAGCGCTGTCATTCCCGTCACTACCTTCCTGCGAGACAACACCTCGACTCAGTAC       840
AlaProSerAlaValIleProValThrThrPheLeuArgAspAsnThrSerThrGlnTyr       120
```

```
AAGTCCATCATCGATATTACCGCCGTGGACTACCCCTCTCGAGAAAACCGGTTCGAGGTG       900
LysSerIleIleAspIleThrAlaValAspTyrProSerArgGluAsnArgPheGluVal       140
```

```
GTCTACAACTTTCTGTCTGTGCGACACAACTCGCGAATCCGACTTAAGACATACGCTACC       960
ValTyrAsnPheLeuSerValArgHisAsnSerArgIleArgLeuLysThrTyrAlaThr      160
```

```
GAGGTGACCCCCGTCCCCAGTATCACCTGCCTGTACGAGGGCGCCAACTGGTTCGAGCGA      1020
GluValThrProValProSerIleThrCysLeuTyrGluGlyAlaAsnTrpPheGluArg      180
```

```
GAGGCCTACGATATGTACGGAGTCTTCTTTGAGGGCCACCCCGATCTGCGACGAATCATG      1080
GluAlaTyrAspMetTyrGlyValPhePheGluGlyHisProAspLeuArgArgIleMet      200
```

```
ACCGACTACGGTTTTGAGGGCCACCCTCTGCGAAAGGACTTCCCTCTCACCGGATACACT      1140
ThrAspTyrGlyPheGluGlyHisProLeuArgLysAspPheProLeuThrGlyTyrThr      220
```

```
GAGGTCCGATGGGACGAGGAGAAGCGACGAGTGGTTTACGAGCCCCTGGAGCTTACCCAG      1200
GluValArgTrpAspGluGluLysArgArgValValTyrGluProLeuGluLeuThrGln      240
```

```
GCCTTCCGAAACTTCTCTGCCGGCTCCACCGCTTGGGAGCCTGTTGGACCCGGTCGAGAC      1260
AlaPheArgAsnPheSerAlaGlySerThrAlaTrpGluProValGlyProGlyArgAsp      260
```

```
GACCGACCCGACTCTTTCAAGCTCCCCACCCCCAAGCCCGAGGAGAAGGAAGGCGACAAG      1320
AspArgProAspSerPheLysLeuProThrProLysProGluGluLysGluGlyAspLys      280
```

---

[1] 3 letter code used for 30-kDa subunit, 1 letter code used for eYPP, new inroduced amino acid are marked in bold

```
AAGCATATGGTGAGCAAGGGCGAGGAGCTGTTCACCGGGGTGGTGCCCATCCTGGTCGAG    1380
LysHis M  V  S  K  G  E  E  L  F  T  G  V  V  P  I  L  V  E      300

CTGGACGGCGACGTAAACGGCCACAAGTTCAGCGTGTCCGGCGAGGGCGAGGGCGATGCC    1440
 L  D  G  D  V  N  G  H  K  F  S  V  S  G  E  G  E  G  D  A      320

ACCTACGGCAAGCTGACCCTGAAGTTCATCTGCACCACCGGCAAGCTGCCCGTGCCCTGG    1500
 T  Y  G  K  L  T  L  K  F  I  C  T  T  G  K  L  P  V  P  W      340

CCCACCCTCGTGACCACCTTCGCCTACGGCCTGCAGTGCTTCGCCCGCTACCCCGACCAC    1560
 P  T  L  V  T  T  F  G  Y  G  L  Q  C  F  A  R  Y  P  D  H      360

ATGAAGCAGCACGACTTCTTCAAGTCCGCCATGCCCGAAGGCTACGTCCAGGAGCGCACC    1620
 M  K  Q  H  D  F  F  K  S  A  M  P  E  G  Y  V  Q  E  R  T      380

ATCTTCTTCAAGGACGACGGCAACTACAAGACCCGCGCCGAGGTGAAGTTCGAGGGCGAC    1680
 I  F  F  K  D  D  G  N  Y  K  T  R  A  E  V  K  F  E  G  D      400

ACCCTGGTGAACCGCATCGAGCTGAAGGGCATCGACTTCAAGGAGGACGGCAACATCCTG    1740
 T  L  V  N  R  I  E  L  K  G  I  D  F  K  E  D  G  N  I  L      420

GGGCACAAGCTGGAGTACAACTACAACAGCCACAACGTCTATATCATGGCCGACAAGCAG    1800
 G  H  K  L  E  Y  N  Y  N  S  H  N  V  Y  I  M  A  D  K  Q      440

AAGAACGGCATCAAGGTGAACTTCAAGATCCGCCACAACATCGAGGACGGCAGCGTGCAG    1860
 K  N  G  I  K  V  N  F  K  I  R  H  N  I  E  D  G  S  V  Q      460

CTCGCCGACCACTACCAGCAGAACACCCCCATCGGCGACGGCCCCGTGCTGCTGCCCGAC    1920
 L  A  D  H  Y  Q  Q  N  T  P  I  G  D  G  P  V  L  L  P  D      480

AACCACTACCTGAGCTACCAGTCCGCCCTGAGCAAAGACCCCAACGAGAAGCGCGATCAC    1980
 N  H  Y  L  S  Y  Q  S  A  L  S  K  D  P  N  E  K  R  D  H      500

ATGGTCCTGCTGGAGTTCGTGACCGCCGCCGGGATCACTCTCGGCATGGACGAGCTGTAC    2040
 M  V  L  L  E  F  V  T  A  A  G  I  T  L  G  M  D  E  L  Y      520

AAGCATATGGCCGCAGCCCATCATCATCATCATCACTAGATGCTGGTTACATGGGAATGT    2100
 K  HisMetAlaAlaAlaHisHisHisHisHisHis***                        532

AGGGTGAGATTCGGAATGAGTGCTATTGAAAAGTCCAGAGTAGGAAGATGGCTTTTCACG    2160
GAAGTACAACCCGTGATGGCATTGGATGGAGTACTTGTAGTTCAATGGTTGATGCATTAG    2220
GGTACAACCTGGGTCGATTCAGAAGGACGGCTTTTGCATGCAACATCTTCTTTGGCAGAT    2280
CAAAGAGTGGGTTTCATGGGATTCGAGCTCGCAATAAGTAACATGATAAGTAGGTTACTT    2340
AGATTTTAAAGTAATATCAACACTCATCTATCTCCTAACCATTGAGAAGTGTCGTGCACT    2400
TTCCCATTCTAAGGCAAAAGCAACAGTTACGAGTAGTTACATATCTACAAGTACTTGTAG    2460
TGCTTCCAGACTGAGATTACCTACTGTCACCGGCACAGATTGAGAGAGCATAAGTCGACA    2520
CATTGTACATACTGTACAAAGAGAATACTCTTAACTGGGGGCTTATATATAACGGTGACT    1860
ACTATGCATAGATTTGTATCATGAGATCTCTCGAGCTGTATGTTTGCTTCACTTTTAGAA    2580
AAGCGGCTGGCAATCTCTGTCTTCGCACATGCACGTCCTGTTCCAGTCATTCATTGGCTA    2640
TGCTTTCCAGCATTTTTCAGACATTTCTTCATTGCTCGTCAAATTTGTCATTAAATATAC    2700
AGCTCAGTTGTGCACCTTCTACTAGAAAATGGTGCTCTACTTACTTTCTCAGAGAAGCCA    2760
```

8.5.4 Oligonucelotides used for fusion of the 30-kDa with the eYFP gene

name	sequence	binding site
EYFPCc	5'-ATATATCATATGGTAAGCAAGGGCGAGG-3'	612-631[a]
EYFPCnc	5'-ATATATCATATGCTTGTACAGCTCGTCCAT-3'	1330-1311[a]
30kNdeInc	5'-GGCTGCGGCCATATGCTTCTTGTCGCCT TCCTTCTCCTC-3'	2052-2013
30kHtgnc2	5'-GCCGCAGCCCATCATCATCATCATCACTAG-3'	2049-2079

Table 8.6 Oligonucleotides for introducing *Nde* I site into *NUAM* and eYFP genes

[a] the numbering oligonucleotides sequence binding site refers to the original sequence of the eYFP gene

name	sequence	binding site
30c3	5'-GTTGGACCCGGTCGAGAC-3'	1242-1260
30nc1	5'-CTGCCAAAGAAGATGTTG-3'	2218-2199
EYFPseq	5'-CGCACCATCTTCTTCAAGG-3'	2022-2041

Table 8.7 Oligonucleotides for sequencing the fusion between *NUGM* and eYFP genes

8.6 Abbreviations

(mt)DNA	(mitochondrial) Deoxy Ribonucleic Acid
ACC. No.	Accession Number
ACMA	9-amino-6-chloro-2-methoxyacridine
ATP	Adenosine Triphosphate
BN-PAGE	Blue-Native Polyacryl Amide Gel Electrophoresis
bp	base pair
BSA	Bovine Serum Albumin
CF	Connecting Fragment
CLSM	Confocal Laser Scanning Microscopy
CPEO	Chronic Progressive External Ophthalmoplegia
DBQ	n-Decyl-Benzoquinone
DF	Dehydrogenase Fragment
dNADH	deamino Hydronicotineamide Adenine Dinucleotide (reduced form)
DQA	2-decyl-4-quinazolinyl amine
EPR	Electron Paramagnetic Resonance
eYFP	enhanced Yellow Fluorescent Protein
FAD	Flavin Adenine Dinucleotide
$FADH_2$	Flavin Adenine Dinucleotide reduced form
FCCP	Trifluorocarbonylcyanide Phenylhydrazone
FeS	Iron-Sulphur Cluster
FMN	Flavin Mononucleotide
FP	Flavo Protein
GFP	Green Fluorescent Protein
HAR	Hexaammine ruthenuim(III) chloride

kb	kilobase
KSS	Kearns-Sayre syndrome
LHON	Leber's hereditary optic neuropathy
MELAS	Mitochondrial Encephalomyopathy, lactic acidosis and stroke like episodes
MERRF	Myclonic Epilepsy with Ragged Red Fibers
MF	Membrane Fragment
MPP^+	1-methyl-4-phenylpyridium ion
MPTP	N-methyl-4-phenyl-1,2,3,6-tetrahydropyridine
NAD^+	Nicotinamide Adenine Dinucleotide
NADH	Hydronicotineamide Adenine Dinucleotide (NAD^+ reduced form)
NDH-2(i)	external alternative NADH Dehydrogenase (internal)
OXPHOS	Oxidative Phosphorylation
PCR	Polymerase Chain Reaction
PD	Parkinson's Diseas
PMSF	Phenylmethylsulfonyl flouride
Q	Ubiquinone
Q_1	Quinone with 1 isoprenyl side chain
QH_2	Ubihydroquionone (Ubiquinol)
ROS	Reactive Oxygen Species
SDS	dodecylsulphate Na-salt

8.7 List of Figures

8.8 List of Tables

124

Lebenslauf

Persönliche Daten

Vorname: Ljuban

Name: Grgić

Adresse: Niddastr. 82
                    60329 Frankfurt/Main

Geburtsdatum und -ort   03. März 1973 in Osijek, Kroatien

Familienstand   ledig

Schul- und Berufsausbildung

Jul 2000 - Apr 2004   Promotionsstudium am Zentrum der Biologischen Chemie, Institut für Biochemie I des Universitätsklinikums Frankfurt in der Arbeitsgruppe von Prof. Ulrich Brandt im Rahmen des SFB 472 „Molekulare Bioenergetik"

                        Thema der Arbeit: Untersuchungen an 49-kDa Untereinheit von mitochondrialen Komplex I aus Hefe *Yarrowia lipolytica*

Sep 1999 – Mär 2000   Diplomarbeit, Untersuchungen an der Riboflavin-Biosynthese am Lehrstuhl für Organische Chemie und Biochemie (Prof. Bacher), TU München

Nov 1995 – Sep 1999   Hochschulstudium, Chemie (Diplom) an der Technischen Universität München

Jun 1994 – Nov 1995   Chemiestudium an der Naturwissenschaftlich-Mathematischen Fakultät der Universität Zagreb

Okt 1993 – Jun 1994   Deutschkurs für Ausländer an der LMU München

Okt 1991 – Okt 1993   Chemiestudium an der Naturwissenschaftlich-Mathematischen Fakultät der Universität Zagreb, Kroatien

Sep 1987 – Jun 1991   Mittelschule mit Fachabitur in Osijek, Kroatien

Sep 1979 – Jun 1987   Grundschule in Tenja, Kroatien